ISSN: 1863-5598

ZKZ 64717
07-20

Bodo´s Power Systems®

Electronics in Motion and Conversion

July 2020

Identification of PMSM Motor Parameters With a Power Analyzer

CONTENT

![Bodo´s Power Systems®]

The Gallery

Bodo´s Power Systems®

A Media
Katzbek 17a
D-24235 Laboe, Germany
Phone: +49 4343 42 17 90
Fax: +49 4343 42 17 89
info@bodospower.com
www.bodospower.com

Publishing Editor
Bodo Arlt, Dipl.-Ing.
editor@bodospower.com

Junior Editor
Holger Moscheik
Phone + 49 4343 428 5017
holger@bodospower.com

Editor China
Min Xu
Phone: +86 156 18860853
xumin@i2imedia.net

UK Support
June Hulme
Phone: +44 1270 872315
junehulme@geminimarketing.co.uk

US Support
Cody Miller
Phone +1 208 429 6533
cody@eetech.com

Creative Direction & Production
Bianka Gehlert
b.gehlert@t-online.de

Free Subscription to qualified readers
Bodo´s Power Systems
is available for the following
subscription charges:
Annual charge (12 issues)
is 150 € world wide
Single issue is 18 €
subscription@bodospower.com

ASC audit since 09/2006

Printing by:
Brühlsche Universitätsdruckerei GmbH & Co KG; 35396 Gießen, Germany

www.bodospower.com

Our First Virtual Event

We have been very busy over the last few weeks preparing for the digital version of Bodo's traditional podium discussion, which was originally planned to be held during PCIM in Nuremberg. It will now take place virtually on Wednesday, 8th of July and will start with a 30-minute SiC-session at 12pm followed by a 15-minute live Q & A session. At 12.45pm the presentations on GaN will be aired, also followed by a live session in which the experts will answer your questions. Bodo plans to moderate the live sessions, a first for him. Hopefully, this will feel a little bit like coming together.
Visit https://ogy.de/BodosSiC-Podium2020 and https://ogy.de/BodosGaN-Podium2020 for more details.

We realize that 15 minutes for Q & A is not very long and not everybody will be able to make the live virtual event, so we will upload the presentations and all related content along with contact information of the presenters to our website shortly after the end of the event. By the way, going virtual must be a success - it was hard to purchase a webcam at a time when everybody is working from their home office. They were sold out everywhere!

While you are holding your physical issue of the magazine in your hand, you might realize that the size is considerably larger than the one in June - something that you will not necessarily notice on a screen. PCIM Europe, in its digital version, is still attracting industry and that means a lot of work for us, as in past years. After some weeks of confusion, whether the show will take place or not, a postponement, and then the transition into a digital event, the run on magazine spaces in our July issue started. It has resulted in an issue containing articles written by experts from across the industry. It is our opinion that the ones who are working in technology and who have access to all the relevant data, are in the best position to deliver accurate and valuable information in the form of technical articles.

So, we are very grateful for each contribution, especially in tough times like these. Concentrating is not that easy with your kids running through your home office screaming for attention, I know!

Please pay attention to the PCIM show feature which can be found in the centerfold. We created this format to provide companies a platform to promote their virtual stands or to reach the audience in this alternative way. It is important that we stay open minded to alternative event formats. In my opinion it would make sense to continue to move on with both the face-to-face as well as the virtual concept, in parallel to best reach the whole audience, those used to the conventional way of doing shows and the generation that is more attracted into a digital format.

A special thank you goes out to Professor Leo Lorenz for his opener. Also, Bodo's review on the history and the development of PCIM is worth reading. Be sure, he knows what he is talking about since he has been attending PCIM since the eighties, forty years ago. At that time we were still rewinding our audio cassettes with a pencil in case the magnetic tape came out of the housing.

Bodo's Power Systems is the only magazine that spreads technical information on power electronics globally. We have EETech as a partner serving North America efficiently.
If you are using any kind of tablet or smart phone, you will find our content optimized for mobile devices on the updated website www.bodospower.com.
If you speak the language, or just want to have a look, do not miss our Chinese version: www.bodospowerchina.com

My Green Power Tip for the Month:
Optimize the equipment in your home office and help to establish this new way of working together. Business trips and personal meetings can often be avoided by using communication technology.

Best regards

Holger Moscheik

Events

Electronica China 2020
Shanghai, China July 3-5
www.electronica-china.com

SEMICON West 2020
Online July 20
www.semiconwest.org

CWIEME Shanghai 2020
Shanghai, China July 29-31
http://cn.coilwindingexpo.com

PCIM Europe 2020
Online July 7-8
https://pcim.mesago.com

SMTconnect 2020
Online July 28-29
https://smt.mesago.com

Thermal Management 2020
Online August 6-7
www.thermalconference.com

IEEE CPE- POWERENG 2020
Online July 8-10
http://cpe-powereng2020.uninova.pt

SEMI-THERM TMPES 2020
Online July 28-30
www.semitherm.com

World Battery Expo 2020
Guangzhou, China August 16-18
www.battery-expo.com

Partnership Agreement Signed

Foxy Power, Berlin, Germany-based Strategy, Business Development, and Sales company is proud to announce its partnership with IQ evolution. IQ evolution is an Aachen, Germany based manufacturer of 3D-printed liquid cooled heatsinks; enabling thinner, ultra-light

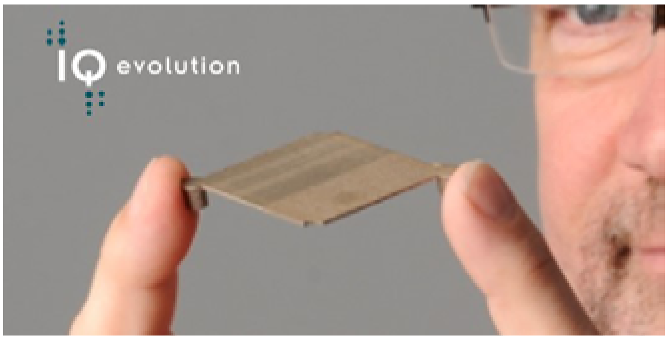

weight, high performant cooling in applications such as EV's, Aviation and others where limited size and volume, highest power density, highest efficiency, and low weight are key. "IQ Evolution nickel based cooler are already established in the high power Laser market", says Dr. Ebert, CEO and Founder of IQ Evolution" and signing Foxy Power as our strategic partner for Business development and Sales will enable us to expand into various power electronic applications." "The stainless steel heatsinks enable a cooling performance greater than 150W/cm² and in collaboration with RWTH Aachen a 20kW converter was demonstrated achieving a world record of 100kW/l or 33kW/kg", adds Christopher Rocneanu, CEO and founder of Foxy Power GmbH. IQ evolution technology starts where conventional liquid cooling technology resigns.

sales@foxypower.com

Chips for Electro-Mobility

In view of the long-term growing market demand for power semiconductors for electric cars, Danfoss A/S and Infineon Technologies AG have signed a multi-year volume agreement. Infineon will supply chipsets of IGBTs and diodes to the Danfoss Silicon Power business unit. The chips are mainly used in power modules for inverters that control the motors in electric vehicles. "The market for electro-mobility is picking up noticeably, and the supply industry is getting ready for this,"

says Claus Petersen, Senior Vice President and General Manager at Danfoss Silicon Power. "For us as a manufacturer of power modules for electric drivetrains, a long-term secure supply of semiconductors is extremely important. With this agreement we can accommodate the high growth expectations of our customers," Petersen concludes. "With electro-mobility, the semiconductor content per car will increase to almost double that of conventional cars. Power semiconductors represent by far the largest part of this additional content," says Peter Schiefer, President of the Automotive Division at Infineon. "The expansion of our manufacturing capacities, for example in Villach, Austria, enables us to establish a long-term cooperation with customers like Danfoss. A reliable and resilient supply chain is crucial for the rapid success of the mobility revolution." Infineon produces the IGBTs and diodes for Danfoss at its plants in Dresden, Germany, and Villach, Austria. Danfoss manufactures its power modules in Flensburg, Germany, and Utica, New York, USA.

www.infineon.com

www.siliconpower.danfoss.com

Radiation Hardened Power Electronics for Mission Critical Applications

Efficient Power Conversion (EPC) Corporation and VPT, Inc., A HEICO company announce the establishment of EPC Space LLC, a joint venture focused on designing and manufacturing radiation hardened (Rad Hard) GaN-on-silicon transistors and ICs packaged, tested, and qualified for satellite and high-reliability applications. EPC Space will provide advanced, high-reliability, power conversion solutions for critical spaceborne environments in applications including power supplies, light detection and ranging (lidar), motor drive, and ion thrusters. These GaN-based components offer superior performance advantages over traditional silicon-based solutions.
Alex Lidow, CEO and Co-Founder of EPC noted, "VPT's global leadership in power conversion solutions for avionics, military, and space applications is the perfect complement to EPC's leadership in GaN-based power conversion devices." Further, Dr. Lidow said, "The joint venture – EPC Space – is taking the superior performance of gallium nitride to the high reliability community offering electrical and radiation performance beyond the capabilities of the aging Rad Hard silicon MOSFET."

Dan Sable, Founder and CEO of VPT, Inc. commented, "EPC's GaN technology enables a new generation of power converters in space operating at higher frequencies, higher efficiencies, and greater power densities than ever achievable before.
We are excited about this venture's ability to provide mission-critical components and services to our high-reliability markets."

www.epc.space

Partnership for Next-generation EV Inverters

ZF Friedrichshafen AG and VisIC Technologies Ltd. announce a partnership to create the next generation of high-performance and high-efficiency electric drivelines for vehicles. The partnership will see the two companies deepen their development efforts, based

on VisIC D3GaN semiconductors technology. The focus of the joint efforts will be on 400-Volt driveline applications, covering the largest segment of the electric vehicle market. “Our partnership with ZF for the development of gallium nitride-based power inverters in electric vehicles illustrates the break-through of gallium nitride technology in the automotive industry,” said Tamara Baksht, CEO of VisIC. ”VisIC’s D3GaN technology was developed for the high reliability standards of the automotive industry and offers the lowest losses per RDS(on). It also simplifies the system solution and enables high-efficiency and affordable power train solutions. It is definitely the next step for the automotive electrical driveline.” ZF’s fast adoption of wide band gap semiconductor technology, such as silicon-carbide and gallium nitride, makes it a leader in the development of the most cost-effective and highly efficient electric drivelines. Through their extended R&D partnership, ZF and VisIC deepens their existing joint efforts in the application of gallium nitride semiconductors for inverters.

www.visic-tech.com

Growing Portfolio of Power Electronics

Sanan IC has signed DMR Technical Sales and Redtree Solutions Ltd. to oversee the company’s growing portfolio of power electronics, RF and optical foundry services. Silicon Valley-based DMR Technical Sales has over two decades of experience in the semiconductor, networking and optical communications markets. With a major focus on the Hyperscale Datacenter and supporting technology customers, DMR has a wide and deep reach into the critical customers and infrastructure providers in this ever-expanding space. The firm, based in San Jose, California, will manage Sanan IC’s large-scale optical solutions, featuring foundry services for customized vertical-cavity surface-emitting lasers (VCSEL) and products for optical device applications. For inquiries, contact David Selby at david@dmrtechsales.com. United Kingdom-based firm Redtree Solutions is the largest Pan-European Representative company in the semiconductor industry, delivering cutting edge technology and architecture to 19 countries and over 500 customers. Featuring a robust portfolio of electronic devices, partners and technical expertise, Redtree provides a unique ecosystem to support Sanan IC’s semiconductor compound foundry services in the European market. Redtree Solutions will also

represent Sanan IC’s advanced SiC and GaN wide bandgap power electronics, VCSEL, FP/DFB laser, and photodiode technologies. For Europe inquiries, contact Jean-Marie Houillon at jmhouillon@redtree-solutions.com.

www.sanan-ic.com

Cooperation on Silicon Carbide Power Solutions

The powertrain business area of Continental Vitesco Technologies and ROHM Semiconductor have recently signed a development part-

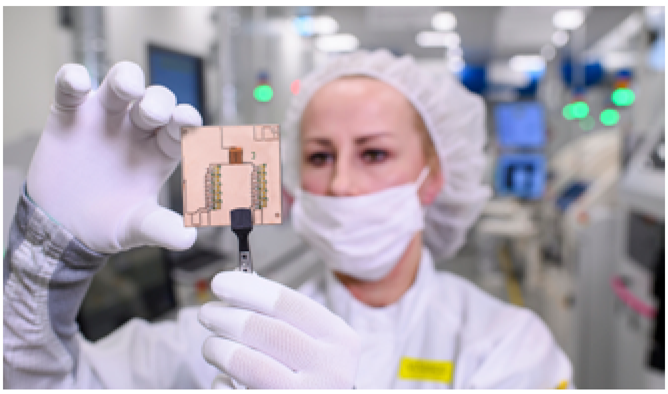

nership, beginning in June 2020. Vitesco Technologies will use SiC components to further increase the efficiency of its power electronics for electric vehicles (EV). Through their higher efficiency SiC semiconductors make better use of the electric energy stored in a vehicle battery. Thus, an EV has a longer range, or the battery cost can be reduced without impacting the range. “We are looking forward to the future cooperation with Vitesco Technologies”, says Dr. Kazuhide Ino, Corporate Officer, Director of Power Device business unit at ROHM Co.,Ltd. “We are the leading company in SiC power semiconductors and have achieved a significant technological lead in this field along with the provision of power solutions combined with gate driver ICs. Together with Vitesco Technologies we want to further improve the energy efficiency of the electronic system in EVs to use the full potential of the SiC technology for a sustainable mobility.”

www.rohm.com


HITACHI
Inspire the Next
Discover Parallel Power
Full SiC 3.3kV Power Module in nHPD²
High Voltage IGBT
The only way to boost your performance.
Hitachi Europe Limited, Power Device Division
email pdd@hitachi-eu.com +44 1628 585151

Silicon Catalyst Ecosystem

Silicon Catalyst and STMicroelectronics jointly announce that ST has joined Silicon Catalyst as both a Strategic and In-Kind Partner. As a Strategic Partner, the collaboration provides STMicroelectronics with early access to review and help select the early-stage silicon start-ups seeking to participate in the Silicon Catalyst Incubator. The initial focus of the In-Kind collaboration will be MEMS sensors and actuators.
“Innovation through silicon is driving advancements in technology. Hardware development is challenging, which is why Silicon Catalyst plays a key role in enabling silicon start-ups to develop their technology and fueling the new cycle of semiconductor innovation,” said Kirk Ouellette, Vice President Strategic Marketing and Strategy Development, STMicroelectronics. “ST has a strong collaborative R&D and industrialization culture, which makes a perfect fit with Silicon Catalyst. As both a Strategic and In-Kind Partner, ST looks forward to providing guidance and resources for start-up partners as well as gaining access to cutting-edge silicon innovation.” Silicon Catalyst has created a unique ecosystem to provide critical support to semiconductor hardware start-ups, including tools and services from a comprehensive network of In-Kind Partners (IKPs) to dramatically reduce the cost of chip development. In its fifth year of operation, Silicon Catalyst has reviewed over 300 early-stage companies and has now admitted a total of 31 start-ups into the incubator.

www.st.com

Head of External Communications

Susanne Kochs is taking over as Head of External Communications at Infineon Technologies. She succeeds Bernd Hops, who took over as Corporate Vice President Communications and Public Affairs & Associations at the start of this year with global responsibility for internal, external and political communications. Susanne Kochs will report to him in her new position. The psychology graduate was previously a member of the Executive Board of Ketchum Germany and at the same time managed the company’s Munich agency. Susanne Kochs has more than 20 years’ experience in corporate and strategic brand communications. In her career she has worked for well-known B2C and B2B companies from many different branches of industry and advised them primarily in integrated campaign development. In addition to Ketchum, she has also held positions at the international communications agencies Edelman and Emanate.

www.infineon.com

UKRI Fast Start Competition Award

Amantys has won funding to develop a technology that will assist in maintaining robustness and resilience in critical energy and transport infrastructure. This was a competitive award under the UK Government’s Fast Start competition. The successful projects are overseen by Innovate UK, part of UK Research and Innovation. The project will extend Amantys’ proprietary semiconductor junction temperature estimation technology, to predict the condition of the power electronics in converter stacks. This is vital for extending lifetime and maximising return on investment.
The funding will help to develop remote, real-time monitoring of the condition of power electronics in converters for off-shore wind turbines, power grids and those in rail traction systems. It will enable early predictive maintenance, reducing the risk of catastrophic failures and maximising up time of the assets in question. Benefits include the reduced cost of asset ownership and operation, overall reduction in carbon emissions and greater resilience, particularly important in times of crisis.
Dr Angus Bryant, Systems Architect at Amantys,commented: “It is great to see this fundamental technology recognised by Innovate UK, and the funding will enable us to move us closer to reducing the total cost of ownership of power converters in mission-ciritcal applications, particularly those at megawatt scale. ” Dr Keith Ferguson, General Manager of Amantys, commented:”We are really pleased that UKRI has recognised t this Amantys technology and its potential societal benefits and we are looking forward to engaging with early adopters in the energy and transport markets to help them add value to their products and services”

www.amantys.com

IWIPP Call for Papers

IWIPP 2021 will be held April 28-30th, 2021, on the campus of Aalborg University, in Aalborg, Denmark. IWIPP is a growing and successful power technology workshop with excellent speakers and networking opportunities. The contents of IWIPP 2021 will include a set of keynote addresses from leading experts, a broad range of technical sessions, as well as a complement of technical tutorial sessions, all of which are included in the registration fee.
The International Workshop on Integrated Power Packaging (IWIPP) brings together industry, academic and government researchers in the field of power electronics components, electrical insulating materials, and packaging technologies to facilitate and promote the development and commercialization of high-density and high-efficiency power converters. Invited presentations and contributed papers will range from core materials technology and components to power converters. Presenters will address important challenges and present solutions to increase reliability and manufacturability while targeting improved performance and reduced system cost.

http://iwipp.org

High Speed Series (VW series)

Si-IGBT + SiC-FWD (SiC Schottky Diode)

MAIN FEATURES

- Optimized for $f_{sw} = 20 \ldots 50$ kHz
- Extremly low recovery losses
- Sufficient short circuit capability
- Low turn-on losses
- Low surge voltage
- Allows downsizing of inverter
  - Smaller filters
  - Higher power output per module

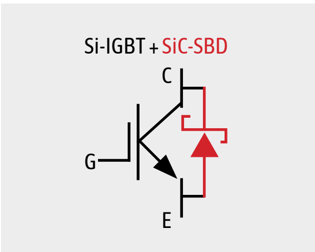

www.fujielectric-europe.com
www.americas.fujielectric.com/semiconductors

Fuji Electric
Innovating Energy Technology

Automotive Electronics Assembly and Packaging Webinar

Indium Corporation's Andy Mackie, PhD, MSc, Senior Product Manager for Semiconductor and Advanced Assembly Materials, will host an automotive electronics webinar as part of Indium Corporation's InSIDER Series on Webex at 8 a.m. and 2:30 p.m. EST on Tuesday, July 28. Over the last decade, the evolution of the automobile has been faster than ever before, and the 2020s promise even more rapid progress. The foreseen changes include the nature of car ownership, how the car is powered, increased safety, and driver automation. Each of these changes is only possible with advances in electronics hardware and systems, electronics assembly, and semiconductor packaging. In "What's Driving: Automotive Electronics Assembly and Packaging", Dr. Mackie will discuss the impact of these changes on electronics assembly and packaging, and the impact of mission profiles on component and system level reliability. A live Q&A session will immediately follow his presentation. Indium Corporation's InSIDER Series is a free program designed to deliver expert technical content, share industry knowledge, and promote professional growth using a virtual platform.

www.indium.com

Expanding Power Device Business

Mitsubishi Electric Corporation announced that it will acquire buildings and land from Sharp Fukuyama Semiconductor Co., Ltd., located in Fukuyama, Hiroshima Prefecture, Japan.

The acquired properties will serve as a new site where Mitsubishi Electric's Power Device Works will process wafers for the manufacture of power semiconductors. New production facilities scheduled to start up in November of next year will enable Mitsubishi Electric to expand its power device business. The demand for power semiconductors needed to control electric power with efficiency is rapidly rising in

parallel with efforts to conserve energy and protect the global environment through carbon-reduction measures, including the ongoing electrification of automobiles worldwide. To meet this growing demand, Mitsubishi Electric conducted a search for potential new manufacturing sites.

As a result, the company has reached an agreement with Sharp Corporation to acquire buildings and land from Sharp Fukuyama Semiconductor.

www.mitsubishielectric.com

APEC 2021: Call for Technical Session Papers

Mark your calendars now for APEC 2021 March 21-25, 2021, and plan to attend the leading event bringing together power electronics professionals from all sectors to exchange knowledge, build valuable connections, and explore new products, solutions, and technology.

Call for Technical Session Papers Now Open

APEC 2021 will address issues of immediate and long-term interest to the practicing power electronic engineer through the presentation of technical content.

Take advantage of the opportunity to present a technical session by submitting a digest explaining:

- The challenge that will be addressed by the paper;
- The major results;
- How this is different from the closest existing literature.

All digests are due by August 14, 2020.

www.apec-conf.org

Global Franchise Agreement

Richardson RFPD announced that it has entered into a global franchise agreement with AVX Corporation. AVX's newest division, AVX RF Solutions, manages and works to expand the already extensive portfolio of leading-edge microwave and RF components. AVX RF Solutions encompasses AVX's RF products along with RF products from two additional AVX brands—American Technical Ceramics and Ethertronics®. The global agreement between Richardson RFPD and AVX covers the products managed by the AVX RF Solutions division, as well as AVX's power film capacitors and SuperCapacitors. The primary product lines covered by the new agreement include antennas, capacitors, couplers, crossovers, filters and inductors. "We are excited about the technology and solutions that AVX represents," said Rafael R. Salmi, Ph.D., Richardson RFPD's president. "These products are an excellent fit for our customers, and we look forward to building on our long-time success working with American Technical Ceramics."

"We believe that our history of developing highly engineered products is a good match for Richardson RFPD's longtime dedication to building teams of specialized engineers," said Alex Schenkel, senior vice president, global sales. "We look forward to mutual successes extending across the automotive, consumer, telecommunications, military, and aerospace market segments."

www.richardsonrfpd.com

SiC DIPIPM™ for a Greener Tomorrow

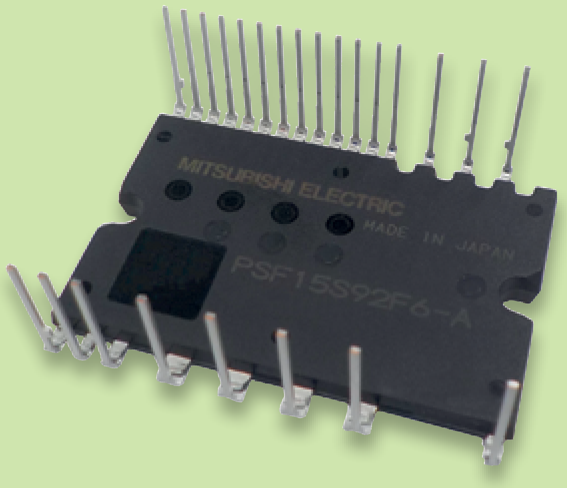

How do we contribute to a „greener“ world and have a positive effect by reducing CO_2 emissions? This question arises daily in newspapers, in social media and in the minds of many people. MITSUBISHI ELECTRIC proposes a solution for one application area which is widely used in our daily lives and which contributes to carbonization. The application is air conditioning for residential homes. Where we are today? Well, the total number of air conditioners in use is approximately 1.6 billion units and of this the number of residential air conditioners is estimated at one billion units. The use of air conditioning in the home consumes more power than that of any other electrical device, at between 5 and 15 times more than that of a refrigerator (depending upon size). During hot summer days, 50% of the total power consumed in the big agglomerations like New-York or Shanghai can be attributed to air conditioning use and today, nine out of ten homes in the USA have air-conditioning. On the other hand, only 8% of homes in Africa, Asia and Latin America are equipped

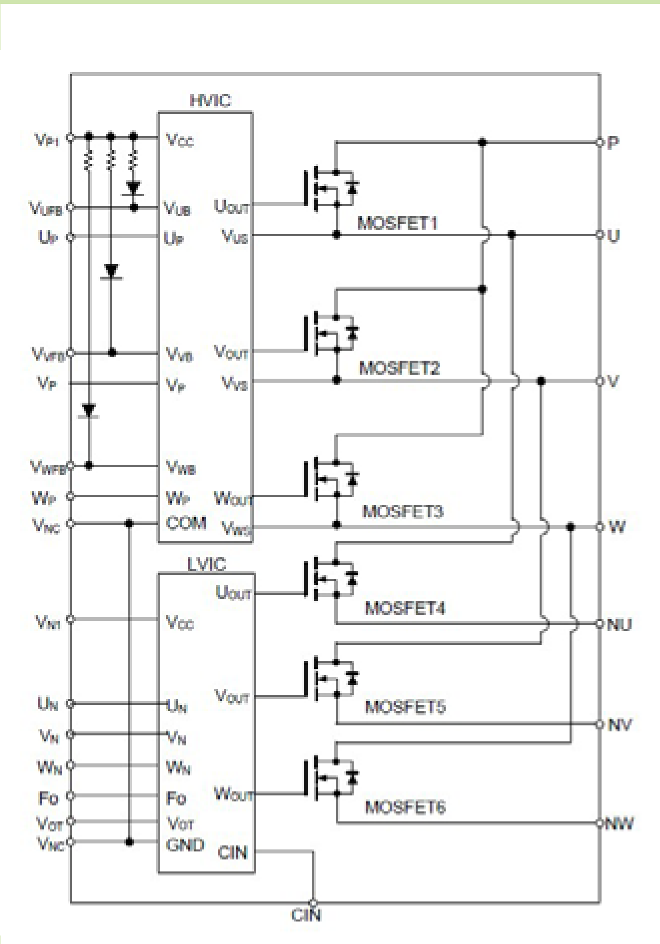

with air conditioning, but this is expected to change significantly over the coming years. According to the International Agency of Energy, IAE, the number of air conditioning units worldwide is expected to increase to 4.6 billion units in 2050 and by then, the power consumed by air-conditioners is expected to be comparable to the total power consumption of China today. This trend can be compared to growth in the use of cell phones and in the case of air conditioning then this upward trend would have a self-acceleration effect – the more installations, the more CO_2 produced, the more CO_2 produced, the more environmental heating, the higher the air temperature, the higher the demand for air-conditioning and so on. How do we avoid this closed loop effect? Simply restricting usage is probably not a good approach because the availability of air conditioning is not simply about luxury. The 2012 study by A. Barreca et al. shows that the utilization of residential air conditioning resulted in 75% reduction in the rate of mortalities caused by high temperatures in the USA after 1960. Consequently, any attempt to restrict air conditioning usage would not be good for humanitarian reasons. Similarly, the same type of argument could be used for the restriction of road traffic. Restriction would avoid carbonization and reduce road deaths due to accidents, but this action would create other issues.

The most realistic solution today is to increase the efficiency of air-conditioners by utilizing power electronics containing power devices developed with the very latest materials. For such a solution SiC can be offered. MITSUBISHI ELECTRIC has launched a power module in its DIPIPM™ family which incorporates MOSFETs based on SiC material.

The module type name is PSF15S92F6-A. This power module is an IPM, an intelligent power module, with a rating of 15A/600V. It includes a temperature sensor, protection against supply under-voltage and protection against short circuit events.The internal structure of PSF15S92F6-A is shown in the block diagram on the left. We can make a direct comparison of efficiency in an air conditioning application for new and current materials by analyzing the power losses of the SiC power module PSF15S92F6-A and the Si power module PSS15S92F6-AG, as both have exactly the same current and voltage rating of 15A/600V. The power loss in the SiC module PSF15S92F6-A is approximately 1/3 of that in the Si module PSS15S92F6-AG. So, by using SiC in future air conditioning designs, we can reduce power consumption by 2/3 and contribute to “a greener tomorrow”, helping society live with peace of mind.

www.mitsubishielectric.com

HIGH PERFORMANCE
SENSING TECHNOLOGY

AOCT TECHNOLOGY

A new technology based on high precision closed-loop technology

Speed up your projects

Reliable in extreme conditions

Continous operation

JPC SERIES

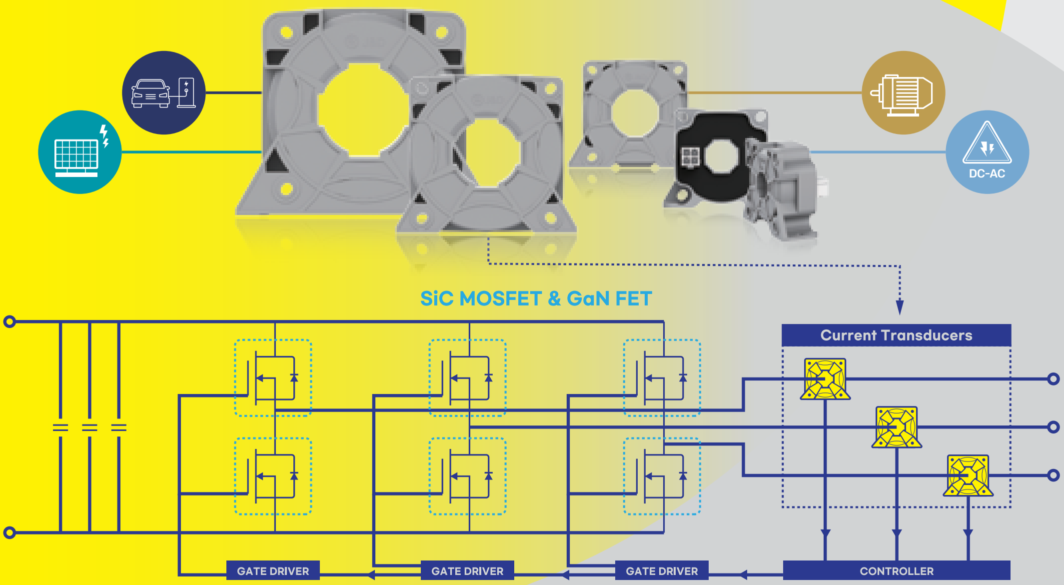

OFFS
Optimized Front-end circuit Fluxgate Sensor

A innovative technology based on the ultra-precise fluxgate technology

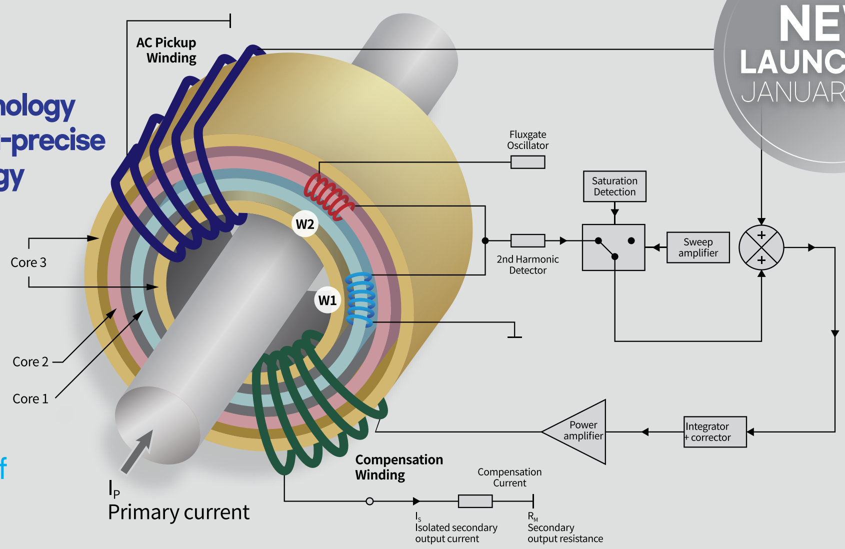

NEW LAUNCHING JANUARY 2021

high bandwidth of up to **300kHz**

CE c US E344623 RoHS3 COMPLIANT

J&D

https://www.hqsensing.com
support@hqsensing.com

Dual-channel Plug-and-play Drivers for MIAA, MIFA and MIDA-type IGBT Modules

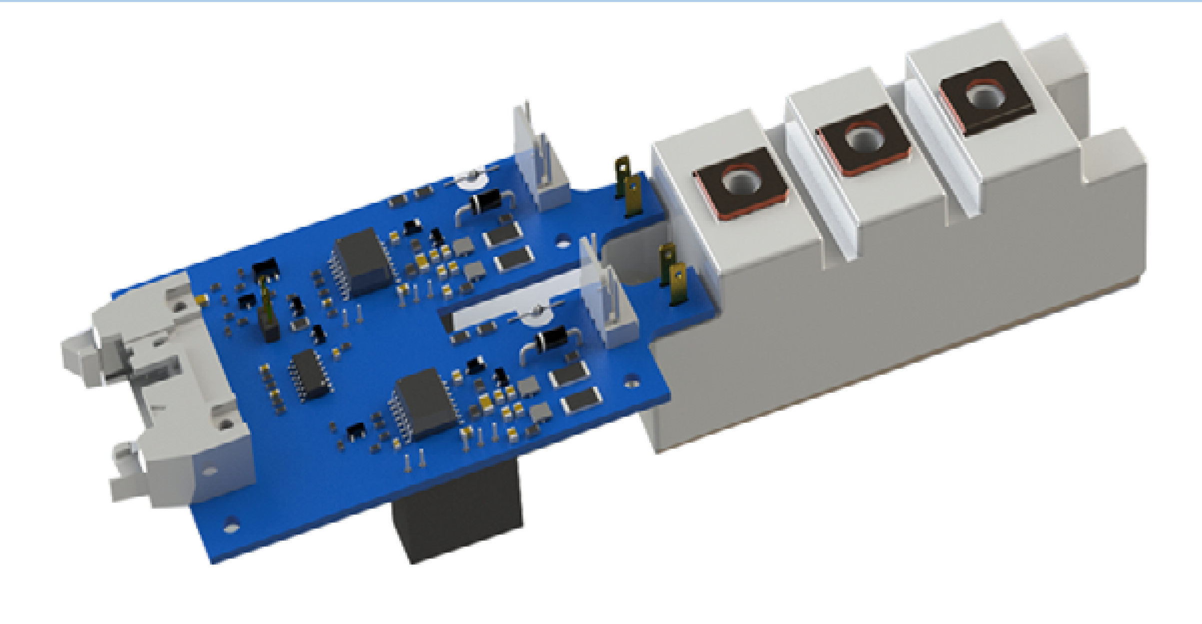

Proton-Electrotex now offers compatible drivers for the entire lineup of its IGBT modules. They are advanced dual-channel plug-and-play IGBT drivers for MIAA, MIFA and MIDA-type IGBT modules with collector current up to 600A and voltage class up to 1700 V.

Depending on application the driver can operate in 2 modes – independent control (direct mode) or half-bridge mode. Features include short-circuit protection with "soft shutdown" of the IGBT module.

Features

- For IGBTs with VCE up to 1700V
- Plug-and-Play solution
- Gate peak current IOUT ±15 A
- Gate output voltage UOUT +15/-9 V
- 15V logic control
- Direct/half-bridge mode
- Isolation testing voltage 4kV AC
- PWM frequency up to 15 kHz
- IGBT short-circuit protection
- Power-supply monitoring (UVLO)

Applications

- Converters for solar and wind energy
- Uninterruptible power supplies (UPS)
- Electric transport
- Frequency converter
- Active rectifiers

More info on our website:

Part number	IGBT type	V_{CES} [V]	V_{isol} [V]	I_{out} [A]	Q_G [uC]	Channels
DI215-17-E-1	MIDA	1700	4000	15	5600	2
DI28-17-E-1	MIAA	1700	4000	8	5600	2
DI28-17-E-2	MIFA	1700	4000	8	5600	2

For more info please contact us by marketing@proton-electrotex.com or phone +7 4862 440456.

www.proton-electrotex.com

Identification of PMSM Motor Parameters with a Power Analyzer

To boost overall efficiency of inverter and motor, it is necessary to measure power and motor parameters simultaneously because it is essential to verify the performance accurately to optimize the control parameters. The power analyzer PW6001 provides a new level of processing performance required to execute most accurate power measurement over a wide bandwidth and simultaneously identify various fundamental control parameters in the pursuit of high-efficiency power conversion with a power analyzer. Focusing on vector controlled PMSM, this article explains the effectiveness of these measurements.

By Hidekazu Masuda and Shozo Yoda, HIOKI EUROPE GmbH

Background

Electric Motor Driven Systems (EMDS) are currently responsible for 53 % of global electricity consumption (IEA 2017) [1]. Herein, the worldwide electric car deployment will grow rapidly in the next one or two decades, and electric vehicles supposedly become the main source of demand growth in the sustainable development scenario. Consequently, the development of more efficient motor drive systems, is one of the important technologies in the strive to reduce the global energy demand. Continuous improvement of motor efficiency of inverter-controlled motors is a key objective and vector control of Permanent Magnet Synchronous Motors (PMSMs) is a commonly adopted technique to realize high-efficiency power conversion.

Accurate solution using innovative power analyzers

In pursuit of overall improved power conversion efficiency, highly accurate power analysis and simultaneous analysis of motor parameters are required to validate optimized control parameters. This can be realized with highly accurate power analyzers deriving various parameters as shown in the evaluation image for motor control efficiency of Figure 1.

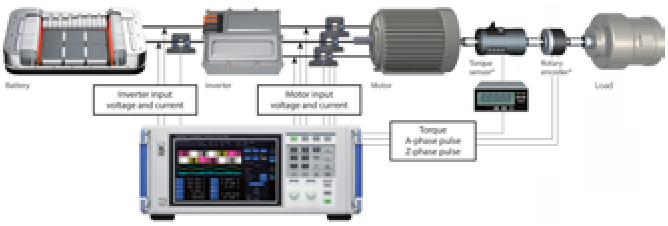

Figure 1: Evaluation system for motor control efficiency with Power Analyzer PW6001

Simultaneous calculation of power and motor efficiency that is regarded as standard nowadays, has been one of many newly introduced features and applications that Hioki has continuously been developing over more than 30 years in pursuit of a more precise power analysis. This was also resulted in the development of a wide range of Hioki high-accuracy current sensors.

When a power analyzer is adopted in a high precision power measurement application at higher frequencies, current sensors are typically used to accurately measure currents, but every current sensor in the world exhibits a gradually increasing phase error at the high-frequency region. This is due to the nature of current transformers and delay of subsequent electronic circuitry. Hioki put its know-how of current sensors into the design and production process to suppress variations of phase delay of individual sensors and the PW6001 has an integrated current sensor phase shift correction function that achieves a more accurate power analysis over a wide bandwidth [Figure 2].

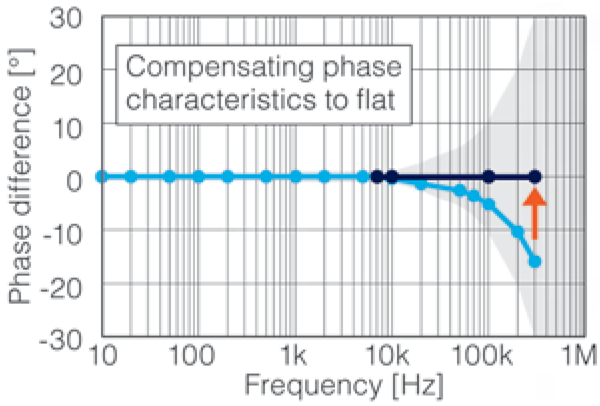

Figure 2: Phase error with and without compensation

In addition, a newly developed "Power Analysis Engine" adds the enhanced high-performance processing power to perform oscilloscope-like waveform analysis, as well as power and motor analysis with leading measurement accuracy, a wide measurement bandwidth, and measurement stability. In regards to motor analysis, although a variety of high-performance control methods have been proposed for PMSMs, accurate identification of motor and control parameters such as *d*-axis inductance *Ld*, and *q*-axis inductance *Lq*, in *d-q* equivalent circuits is essential to optimize motor control parameters. Correct measurement of electrical angle, *d-q* axis voltage and current using a harmonic analysis is the method to identify these parameters.

Measurement principles

In general, power analyzers create folding noise by aliasing, which can be reduced by anti-aliasing filters (AAF). [Figure 3(a)]. However, AAFs limit wide band measurements. The newly developed "Power Analysis Engine" realizes optimal data sampling and analysis with AAF that rejects higher frequency components than Nyquist frequen-

cies from the input wave form [Figure 3(b)]. It also enables accurate harmonic analysis with optimal sampling speed simultaneously with subsequent independent Zero-cross filter and AAF.

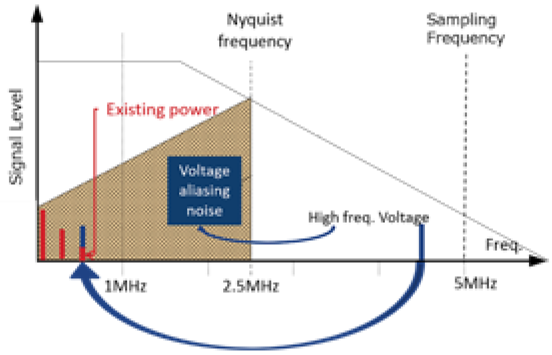

Figure 3(a): Example: 5MHz sampling without AAF

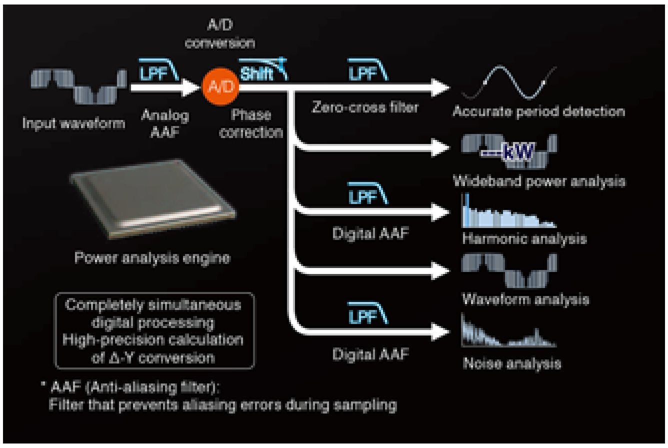

Figure 3(b): Independent AAF and synchronization

Consequently, these configurations of AAF offer 2 MHz bandwidth measurement without aliasing noise and this level of harmonic analysis accuracy enables accurate power and efficiency measurements. In addition, accurate and steady measurement of fundamental frequency components of power parameters realizes to derive motor and control parameters correctly.

Identification of motor and control parameters

In general, PMSM analysis and control are based on the equivalent circuit model for a motor expressed on the *d*- and *q*-axes. Although a variety of high-performance control methods have been proposed for PMSMs, and these control algorithms are based on *d-q* equivalent circuits with motor parameters such as *d*-axis and *q*-axis inductance, *Ld* and *Lq*.

When a steady state is considered, a vector diagram of the *d*- and *q*-axis is expressed as shown in Figure 4. Here, v_1 and i_1 represent the fundamental wave components of the phase voltage and phase current, while ϑv and ϑi represent the fundamental wave phase angle of the phase voltage and phase current respectively. From here the control parameters equation (1)-(4) can be derived by user defined function (UDF) with a power analyzer as equation (5)-(8).

$v_d = -v_1 \sin\vartheta_v$	(1)	$\mathrm{UDF}_1 = -U_{fnd1} \sin\vartheta_{U1}$	(5)
$v_q = v1 \cos\vartheta_v$	(2)	$\mathrm{UDF}_2 = U_{fnd1} \cos\vartheta_{U1}$	(6)
$i_d = -v1 \sin\vartheta_i$	(3)	$\mathrm{UDF}_3 = -I_{fnd1} \sin\vartheta_{I1}$	(7)
$i_q = v1 \cos\vartheta_i$	(4)	$\mathrm{UDF}_4 = I_{fnd1} \cos\vartheta_{I1}$	(8)

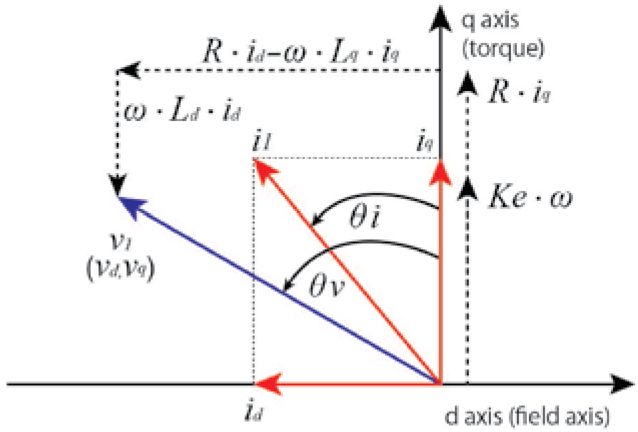

Figure 4: PMSM Vector Diagram

Here, Figure 4 and equations (1)-(8) are expressed based on the following assumptions [2].

- The spatial distribution of magnetic flux in the spaces between the stators and rotors takes the form of a sine wave aligned with the gap.
- The harmonic components of voltage and current can be ignored.
- The core loss can be ignored.

Using equations (1)-(8) and Figure 4, motor parameters *Ld* and *Lq* can be derived and determined by UDF in a power analyzer as follows:

$$Ld : \mathrm{UDF}_7 = \mathrm{UDF}_2/(2\pi f_1 \bullet \mathrm{UDF}_3) - (2\pi Kef_1 + \mathrm{R} \bullet \mathrm{UDF}_4)/(2\pi f_1 \bullet \mathrm{UDF}_3) \quad (9)$$

$$Lq : \mathrm{UDF}_8 = (R \bullet \mathrm{UDF}_3 - \mathrm{UDF}_1)/(2\pi f_1 \bullet \mathrm{UDF}_4) \quad (10)$$

The induced voltage constant *Ke* and the phase armature resistance *R* can be obtained as follows.

For inducing *Ke* ([3], [4]), place the motor terminals of the PMSM being analyzed in the open state ($i_d = i_q = 0$), connect the motor terminals to the “CH 1”, “CH 2”, and “CH 3” voltage inputs on the power analyzer. Then connect the encoder’s A-phase pulse output to “CH B”, the B-phase pulse output to “CH C”, and the Z-phase pulse (origin signal) output to “CH D” (Figure 5).

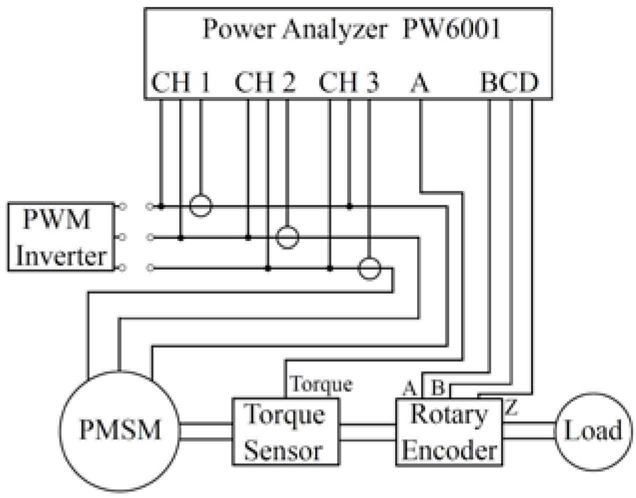

Figure 5: Wiring for phase zero-adjustment and induced voltage constant Ke identification.

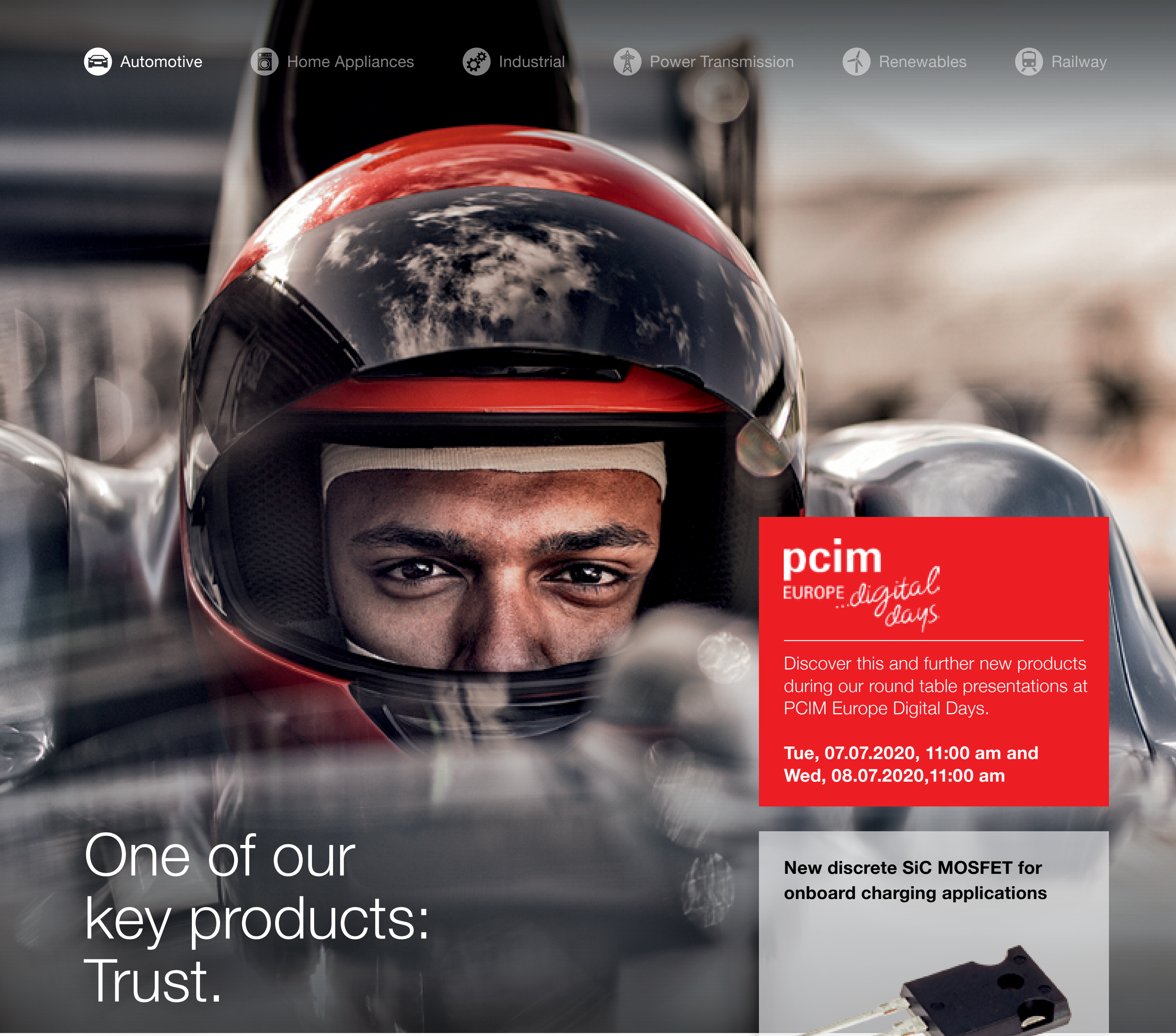
Automotive
Home Appliances
Industrial
Power Transmission
Renewables
Railway

Configure the power analyzer by setting the motor analysis operating mode, the measurement parameter to “Torque, Speed, Direction, and Origin ”, and “CH B” input to “Pulse”. Then set the wiring for “CH 1”, “CH 2”, and “CH 3” to “3P3W3M”, the synchronization source to “Ext1”, and ∆ - Y conversion to “ON”. Setting the synchronization source to “Ext1” allows the voltage and current phase angles to be measured using the inputted encoder pulse as the reference, and setting ∆ - Y conversion to “ON” allows the line voltage to be converted to, and measured as a phase voltage.

Operate the motor from the load side in this state to generate an induced voltage and perform phase zero-adjustment on the power analyzer. This step will ensure that *v* and *i* represent phase angles (I.e. electrical angles) based on the phase of the induced voltage generated along the *q*-axis.

At this time, the induced voltage v_q will equal to v_1 and *Ke* is identified by equation (11).

$Ke = v_1/2\pi f_1$ (11)

The phase armature resistance *R* can be measured by a resistance meter with the 4 terminal method.
The motor torque is calculated by following equation (12).

$T = Pn \{Ke\ iq + (Ld - Lq)\ id\ iq\}$ (12)

Pn is number of motor pole pairs.

The first term on the right side is magnetic torque, and the second term is the reluctance torque. Magnetic torque is generated by attraction and repulsion force between the rotating magnetic field of the stator and the permanent magnet rotor.

Then, drive the motor by invertor under test to measure motor and control parameters. Measured results are displayed as follows:

Figure 6 shows the calculated and measured torque. Calculated torque is derived by equation (12) with use of derived motor parameters (*Ld, Lq*), control parameters (*id, iq*) and *Ke*, and it fits well with the measured torque. This also means that motor torque can be identified without a torque sensor in case it is not possible to adopt a torque sensor into utility drive system.

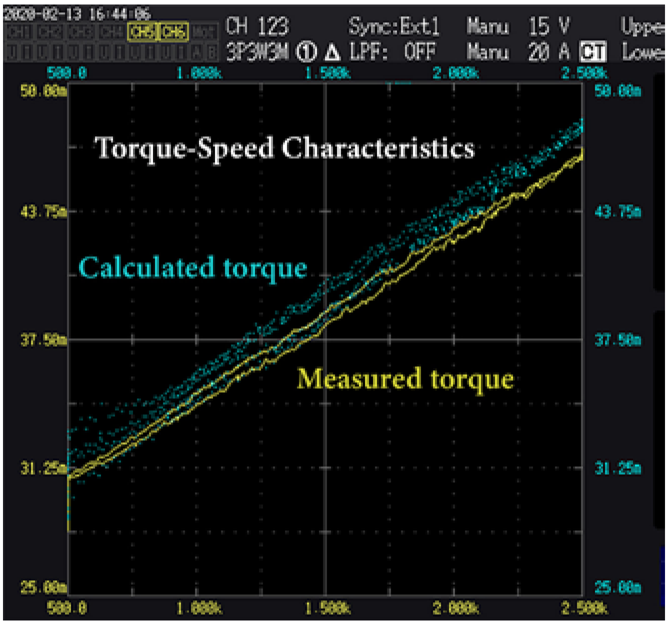

Figure 6: Comparison of measured and calculated torque

Figure 7 illustrates the results of identifying the *Ld* and *Lq* motor parameters while the motor’s rpm varies and the current phase angle is held constant, showing the current dependence of *Ld* and *Lq*. *Ld* remains roughly constant regardless to *id*. By contrast, *Lq* exhibits a high degree of current dependency due to magnetic saturation and varies significantly with *iq*. These characteristics exemplify that it is not possible to use an LCR meter or similar instrument to identify *Ld* with a high degree of precision while the motor is at a standstill. Instead, the value must be identified while the motor is operating.

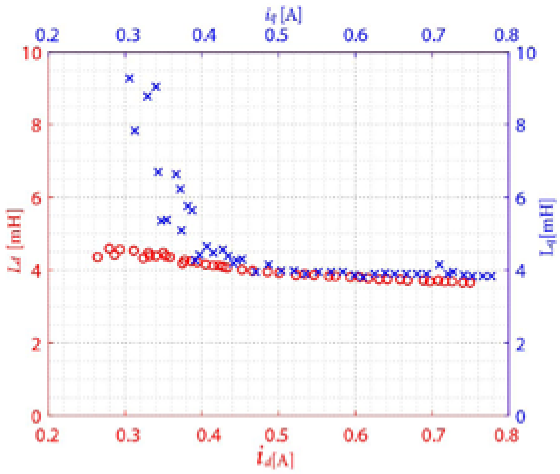

Figure 7: Relationship between the d-q axis current and the identified d-q axis self-inductance

In this article, we introduced a method for identifying PMSM motor parameters with a power analyzer easily yet with a high degree of precision. As an analytical model, we assumed that core loss can be ignored. However, by measuring mechanical loss and identifying the equivalent core loss resistance in advance, it would be possible to develop the described method for identifying motor parameters while taking core loss into account. This would be a next step for us to identify core loss in electric drives.

Conclusion

With a high level of processing power, actual motor parameters can be identified simultaneously with accurate power measurement when executing this method with the HIOKI Power Analyzer PW6001. The power analyzer’s enhanced functions therefore enable effective research on vector control technology of PMSM motors to aim for ever more efficient power conversion, and ultimately contribute to finding solutions how to decrease energy consumption on a larger scale.

References

[1] International Energy Agency: World Energy Outlook 2016, IEA Paris 2016
[2] Shigeo Morimoto, Yoji Takeda, and Takao Hirasa: “Method for Measuring a PM Motor’s dq Equivalent Circuit Constants”, IEEJ Transactions on Industry Applications, Vol.113-D (1993) No.11, pp.1330-1331 (in Japanese)
[3] HIOKI white paper: “Identification of PMSM Parameters with the Power Analyzer PW6001(Theory and setting apparatus)”, 2015 https://www.hioki.com/file/cmw/hdTechnicalDataEn/53/attached_file/
[4] HIOKI white paper: “Identification of PMSM Parameters with the Power Analyzer (Actual measurements)”, 2016

www.hioki.com

SEMIKRON
innovation+service

Power Electronics for Motor Drives

www.semikron.com

Today SEMIKRON offers the complete industrial standard power module portfolio that serves a power range of 0.4kW to several megawatts.

GENERATION IGBT 7

Features

- Rectifier, IGBT and Silicon Carbide power modules
- Latest IGBT technology including Generation 7 IGBTs
- Serving $200V_{AC}$, $400V_{AC}$, $690V_{AC}$ applications
- Plug-and-Play IGBT drivers and stacks for shortest time-to-market
- Covering air- and water-cooled multi-megawatt applications with the SKiiP high power IPM
- Excellent application support

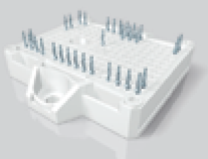

SEMITOP® E1/E2
0.4kW - 30kW

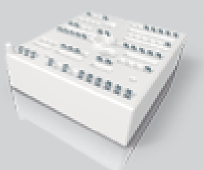

MiniSKiiP®
0.4kW - 110kW

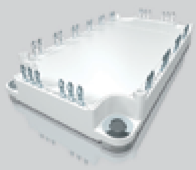

SEMiX® 6 Press-Fit
15kW - 75kW

SEMiX® 3 Press-Fit
55kW - 250kW

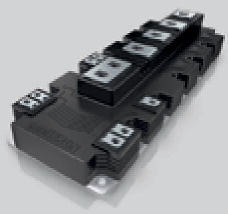

SEMITRANS® 10
300kW - 1MW

IGBT Driver for 2-Level and 3-Level Industrial Applications with Enhanced Isolation Capability for DC Voltages of up to 1500V

SKYPER IGBT drivers isolate and transfer the microprocessor generated control signals from a low voltage side to the high voltage environment of power semiconductors. Besides this essential signal transfer function, this publication will also cover the isolation capability and the robustness of the SKYPER driver alongside dedicated protection strategies for 2-level and 3-level solutions realized through state-of-the-art ASICs.

By Marco Honsberg and Niklas Hofstötter, SEMIKRON INTERNATIONAL

1500VDC –Low Voltage Directive list

With the trend being to utilize power electronics up to the upper limit defined in the Low Voltage Directive, 1500V DC or 1000V AC have become one of the design aims in photovoltaic (PV) and battery storage applications, resulting in more stringent design and materials selection requirements in the development of suitable IGBT driver electronics. Put simply, the required safety isolation capability, a key feature of the SKYPER IGBT driver family, was designed to meet greater clearance and creepage requirements on the printed circuit board (PCB) for applications that exploit the low voltage directive's operation voltage limit of 1500V. A further focus has been on looking into the ways to design converters that operate at a DC-link voltage of up to 1500V. Indeed, a simple 2-level system would require IGBTs with blocking voltages of more than today's industry standard of 1700 Volt to cover transient switching over-voltages and achieve a suitable long-term DC stability (LTDS) performance. The upcoming 2.0…2.3kV IGBT modules facilitate operation at 1500V DC-link voltage in 2-level topology and may be the solution to those semiconductor applications that do not require 3-level topologies known for their lower losses under certain application conditions and lower inductive filter requirements. A typical 3-level configuration is the neutral point clamped (NPC) topology which is also known as "I-type" 3-level configuration. This topology requires a proper shutdown sequence in the event of error detection, avoiding greater potential damage to the power stage resulting from erroneous or simultaneous switching of the NPC power stage. A suitable IGBT driver therefore has to meet the requirements for safe turn-off sequences for 2-level and 3-level topologies.

Outline of the SKYPER 12 PV and the SKYPER 42LJ PV

Figure 1a and figure 1b show the SKYPER 12 PV and the more powerful SKYPER 42 LJ PV driver, respectively, illustrating the compactness of both IGBT drivers despite the enhanced clearance and creepage requirements resulting from the 1500V DC operation. Remarkably, the PCBs shown in figs 2a and 2b combine a creepage distance enlarging pattern milled into the FR4 based substrate with a high quality substrate which boasts a comparative tracking index (CTI) of 400 and 600 in the SKYPER 12 PV and the SKYPER 42 LJ PV, respectively. The milled pattern ensures the realization of the essential creepage distances according to international standards. In both of the SKYPER IGBT drivers shown here, the gold-plated terminals connect to an interfacing PCB through standard 2.54mm double row pin headers. Achieving the same normative compliance for the signal isolation and the isolated power transmission is somewhat more challenging.

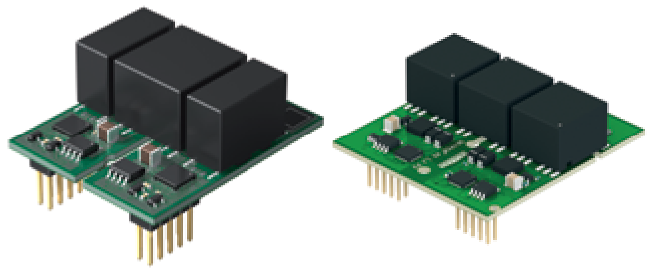

Figure 1: SKYPER 12 PV and the more powerful SKYPER 42 LJ PV driver

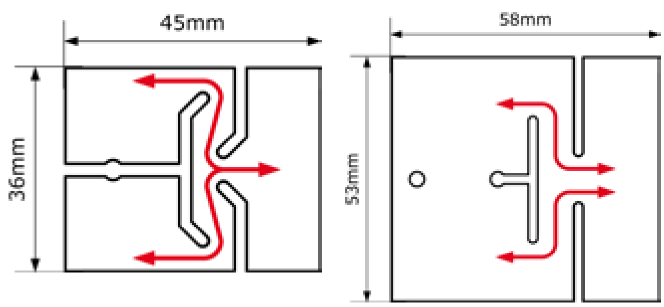

Figure 2: PCBs with creepage distance

Figure 3a and 3b show SEMIKRON's solution, providing additional gaps that incorporate the extra creepage required into the transformers housing without enlarging their dimensions in comparison to transformers used for 1200V IGBT applications. Both design highlights—the milled pattern on the PCB as well as the "gapped" design used for the transformer housing—ensure compliance across the 1500V range of the low-voltage directive.

Introducing a New Generation of AVR® Devices

AVR-DA Flexibility in Design

The Functional Safety Ready AVR-DA family is the new generation of AVR microcontrollers running up to 24 MHz across the full supply voltage range 1.8V to 5.5V featuring intelligent analog and core independent peripherals.

The AVR-DA family uses the latest Core Independent Peripherals and low-power capability to handle real-time control functions in industrial control, home appliance, automotive and Internet of Things (IoT) applications. The Event System and Configurable Custom Logic (CCL) peripherals offer near-zero latency for time-critical functions. Intelligent Analog peripherals like 12-bit differential Analog-to-Digital Converter (ADC), Zero-Cross Detect (ZCD), 10-bit Digital-to-Analog Converter (DAC) and the latest-generation Peripheral Touch Controller (PTC) put the AVR-DA family in the center of sensor interface, system monitoring and human interface applications. 5V operation for increased noise immunity and low-power features ease power supply concerns.

- Product certifications made easier with Functional Safety supporting documentation and development tools.
- Add IoT and connectivity to your application, thanks to the high memory densities and SRAM-to-Flash ratio.
- Design robust and noise-immune applications with built-in safety features and 5V supply.
- Create state-of-the-art capacitive touch interfaces using the latest-generation PTC.

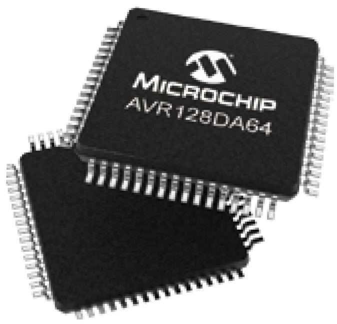

Functional Safety Ready

www.microchip.com/avr-da

MICROCHIP

Looking at the PCB used with the SKYPER IGBT driver, it can be seen that only very few external electronic components are placed on the printed circuit boards around the central ASIC control circuit. Both SKYPER drivers incorporate the latest generation of SEMIKRON's proprietary ASIC circuits that employ power supply management, supervisory control circuits, logic state machines, and signal- and error processing units in addition to the basic IGBT driver output stage. These ASICs substantially reduce the number of external components, in doing so improving the reliability of the entire driver system dramatically to levels of $12x10^6$h for the SKYPER 12 PV and $7.5x10^6$h for the SKYPER 42 LJ PV according to a reliability calculation carried out according to SN29500.

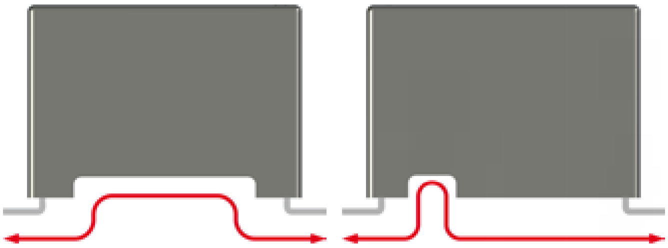

Figure 3: Additional gaps that incorporate the extra creepage

Block diagram and electrical performance of SKYPER 12 PV and SKYPER 42 LJ PV

Figure 4 shows the block diagram of SKYPER driver cores, structured into three major functional blocks. The red-framed functional block on the left depicts the primary side, and the two red-framed blocks on the right comprise the two separate secondary sides of the driver core. The driver's primary side processes the input signals and provides error management functionalities. Here, the signal integrity is largely ensured by dead-time observation and generation as well as short pulse suppression and interlock functions.

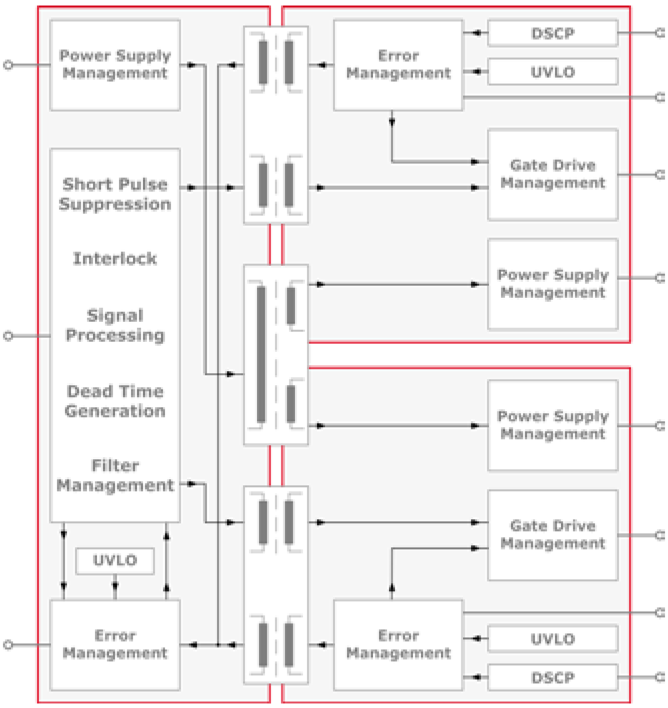

Figure 4: SKYPER driver cores, structured into three major functional blocks

The aforementioned transformers connect the primary side to the two independent secondary sides contained in the two blocks on the right side of the diagram. The secondary sides host the IGBT supervisory control circuits and the power output stage. Both drivers permit a maximum switching frequency operation up to 100kHz and are able to feed an IGBT gate with up to 20µC of charge per pulse. Especially the more powerful SKYPER 42 LJ PV, boasting 35A peak output current and 4.2W output power per channel, meets the challenging requirements of the 7^{th} generation IGBTs manufactured by several companies. This means that PV driver cores from the SKYPER family are suitable for use in inverter designs from a few kW to the lower MW range.

Protection functions included/incorporated:

The SKYPER IGBT driver comprises complete protection functions that ensure proper operation and turn-off of abnormal operating conditions. The under-voltage "UV" protection detects a low supply voltage that would be dangerous for the IGBT and deteriorate the switching speed and conduction losses, leading potentially to thermal "wind-up" failure.

The SKYPER short circuit "SC" protection is based on a dynamic desaturation detection approach. Instead of comparing the saturation voltage of an IGBT with a constant threshold value only during its conductivity, the SKYPER driver cores are able to detect short circuit conditions already during the transient turn-on process of the IGBT. When the blanking time period tbl(VCE) has elapsed, the integrated SC detection circuit in the SKYPER compares the instantaneous voltage across the Collector and Emitter of an IGBT VCE(IN) during the transient event of IGBT turn-on with a down-ramping reference value VCE(ref) that can be tailored for the utilized IGBT. This special feature inside the ASIC turns-off the IGBT only in the event that the desaturation of the IGBT does not happen as defined or expected. Thus, the SKYPER essentially allows for the elimination of the commonly used waiting or blanking time and can monitor the turn-on behaviour of the IGBT on-line even during its transient state.

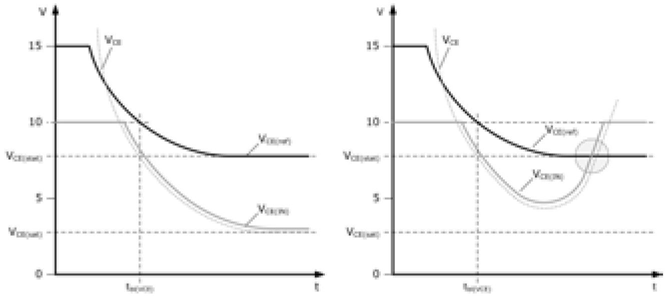

Figure 5: IGBT turn-on behaviour

Figure 5a shows the normal IGBT turn-on behaviour. After initiating the IGBT turn-on process through the driver, both voltages $V_{CE(IN)}$ and $V_{CE(ref)}$ reach their steady state level $V_{CE(sat)}$ and $V_{CE(stat)}$ without crossing each other. The SC detection feature is active from the moment the voltage $V_{CE(ref)}$ falls below the fixed value of 10V set by the ASIC. The detection of an IGBT desaturation event is shown in Figure 5b. The example chosen illustrates a desaturation event that occurs shortly after the IGBT turn-on process starts. When the voltage $V_{CE(IN)}$ exceeds the instantaneous value of the reference voltage $V_{CE(ref)}$, the driver starts its error routine; depending on the user's error mode settings, the driver either turns off the IGBT via the soft-off channel and reports the error condition, or only the error condition is reported and the driver waits for a specific turn-off sequence defined by the controller.

Most of standard IGBT modules employ an NTC on the ceramic substrate to provide the module temperature information. The SKYPER IGBT drivers can use this signal from the NTC to detect an over-temperature situation (OT) if the threshold voltage is chosen correctly.

The SKYPER can turn off the IGBT once the over-temperature level has been detected.
However, although the SKYPER might have detected an error what may not be wanted is for the detected error to automatically result in turn-off of the corresponding IGBT without interception from the microprocessor supervisory circuit. Especially in 3-level neutral point clamped (NPC) configurations, such “automatic” error response behaviour is undesired, since a specific turn-off sequence must be kept to prevent greater damage to the IGBT, the power module and the system. Hence, in a selected 3-level operation mode the SKYPER would only signal the error at the fault output, but not turn off the gate signal. In this case, the turn-off signal will come from the microprocessor supervisory control circuit to ensure a suitable turn-off sequence for all semiconductors to bring the 3-level power stage to a safe state.

SKYPER product range
The table below and figure 6 show a selected range of SKYPER IGBT driver cores. Remarkably, the two proposed types SKYPER 12 PV and the SKYPER 42 LJ PV boast the 1500V ready feature and are suitable for different IGBTs sizes. All other models are suitable for DC-link voltages of up to 1200VDC.

Driver	P_{out}	$I_{out(peak)}$	V_{DCmax}	3-level option
SKYPER 12 R	1.25W	20A	1200V	-
SKYPER 12 PV	1.25W	20A	1500V	yes
SKYPER 32 2nd edition	1.6W	20A	1200V	-
SKYPER 32 PRO R	1.1W	15A	1200V	-
SKYPER 42 R	3.5W	30A	1200V	-
SKYPER 42 LJ R	2.75W	24A	1200V	-
SKYPER 42 LJ PV	4.2W	35A	1500V	yes

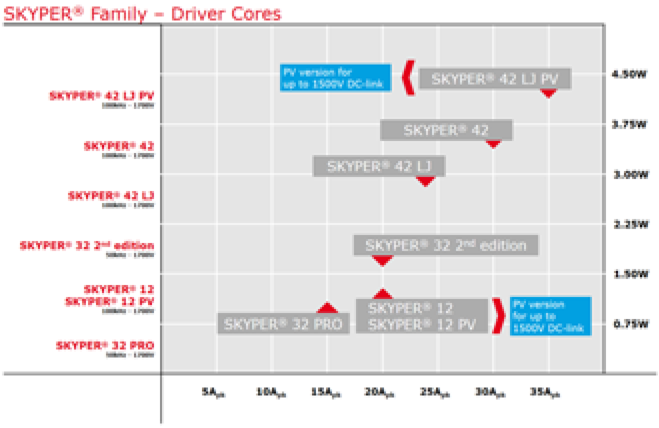

Figure 6: Selected range of SKYPER IGBT driver cores

Accessories
It’s easy to test the SKYPER 12 PV or the SKYPER 42 LJ PV driver core on a standard module if test and evaluation boards are used. For that purpose, SEMIKRON has developed a set of application sample boards for quick, easy and efficient evaluation of the features of the SKYPER driver cores. These evaluation boards, also known as SEMIKRON's "blue PCBs", are available for several 2- and 3-level IGBT modules. Consequently, the boards for the SKYPER PV series allow evaluation operation at voltages of up to 1500V DC according to EN 62109 and EN 61800-5-1 standards. The SKYPER 12 IGBT driver technology is also used in dedicated plug-and-play drivers that can be plugged onto 17mm modules like the SEMiX IGBT and compatible module series. The SKYPER 12 press-fit is suitable for 650V, 1200V and 1700V IGBT modules and is available with 2 different types of connectors.

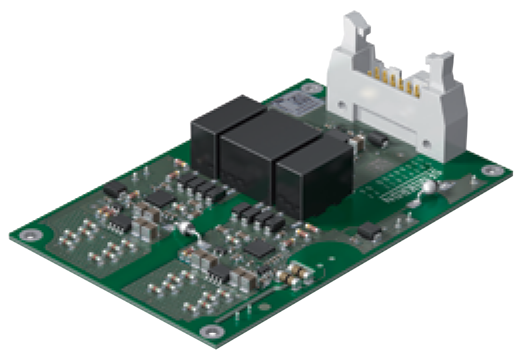

Figure 7: Standard IGBT driver

Customized SEMIKRON plug-and-play drivers
Usually, IGBT gate drivers are adopted for the IGBT in its specific environment and application conditions. For this reason, standard IGBT drivers as shown in figure 7 should be customized, since “standard” drivers can rarely take an application to its maximum performance limit. Custom modifications of SKYPER plug-and-play gate drivers help to get highest performance and robustness out of a given power stage design. Thanks to the proprietary design of SEMIKRON’s ASICs, which boasts a high degree of customization flexibility, changes in the gate resistor value or adjustments to thresholds or timing values are easily feasible in most cases. Do not hesitate to get in touch with us if you need a slightly more customized SKYPER.

www.semikron.com

High-speed Hybrid Modules for Fast Switching Applications

By Ryosuke Usui, Yoshiharu Kato, Seiichi Takahashi, Electronic Devices Business Group, Fuji Electric Co., Ltd. and Lukas Kleingrothe, Power Semiconductor Technical Devision, Fuji Electric Europe GmbH

In recent years, the number of applications that require power conversion systems in the high frequency region in order to reduce size, weight and increase efficiency, has grown significantly. Leading this trend are applications such as Electric Vehicles (EV) and Hybrid Electric Vehicles (HEV), charging systems as well as distributed photovoltaic power generation systems. But also UPS, welding or medical systems are following the idea into fast switching devices. To fulfil the requirement for high-speed and low loss switching, Fuji Electric has developed high-speed hybrid modules which combine silicon insulated gate bipolar transistors (IGBT) with silicon carbide Schottky barrier diodes (SiC-SBD). As a result, power dissipation during high-frequency inverter operation can be reduced by approximately 50% compared to existing products.

Introduction

To reduce the emission of greenhouse gas CO2 in order to suppress global warming, the efficiency of power conversion systems, especially renewable energy generation needs to be increased. Also the switch from combustion vehicles to electric vehicles targets a more sustainable environment. To realize this change, a close-knit network of charging infrastructure is required. These EV charging systems needs higher switching frequencies to achieve a high level of compactness of the overall system and an increased efficiency. Besides the field of EV chargers also UPS systems tend to operate at higher switching frequencies. Figure 1 shows the target applications in relation to the power capacity and the switching frequency. Some of the main applications of high-speed hybrid modules are power conversion equipment, used for renewable energies, automotive applications and uninterruptible power systems (UPS). All these need to convert power at high frequencies.

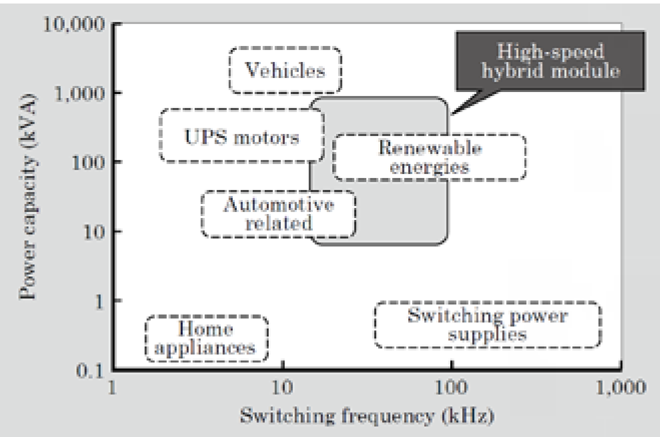

Figure 1: Main applications of high-speed hybrid modules

Features of the high-speed hybrid modules

To achieve a further improvement, switching frequencies of 20kHz or higher are needed for semiconductor devices. Therefore, Fuji Electric developed a high-speed, low loss IGBT which can operate in a switching frequency region beyond 20kHz. These Si-IGBT's are combined with SiC-SBD's to reduce the switching losses and are offered in a half bridge configuration. To maintain the compatibility, the high-speed hybrid modules make use of the same packages like conventional Si-modules, for example the 62mm standard package and the EconoDual™3. The following chapters describe the characteristics of the high-speed IGBT and the SiC-SBD chip.

High-speed IGBT turn-off loss improvement

The IGBT utilizes an optimized chip for high speed switching which is based on the conventional IGBT technology. In order to improve the IGBT for high-speed switching the generated switching loss needs to be reduced. This could be achieved by changing the trade-off between the turn-off loss E_{off} and the collector emitter saturation voltage $V_{ce(sat)}$. Figure 2 shows a comparison of these trade-off characteristics of the actual "X-Series IGBT" (Fuji Electric 7th IGBT Generation) and the high-speed optimized IGBT for a 200A / 1200V module.

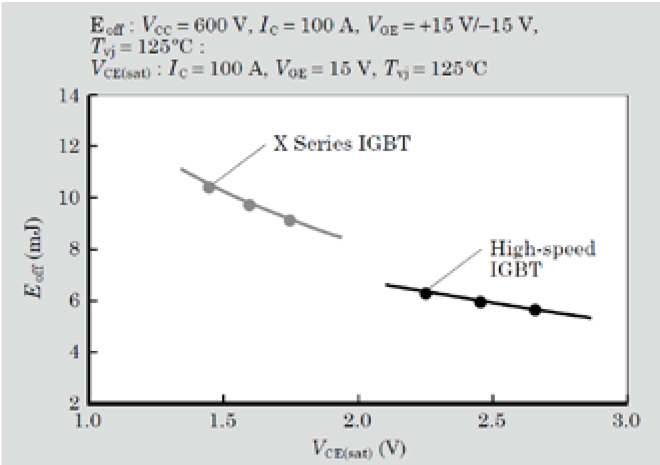

Figure 2: 1200V high-speed IGBT $V_{ce(sat)}$ -E_{off} characteristics

Turn-off losses of the high-speed IGBT are 33% less than conventional IGBT of the 7th generation while the $V_{ce,sat}$ is still suitable for high speed applications[(1)]. This reduction is due to the improved tail current during turn-off. This improvement comes from the drastically reduced parasitic capacitance of the active chip structure as well as on the reduced concentration of impurities in the collector layer which is responsible for suppressing the hole injection[(2)].

SiC-SBD improvement in reverse recovery and turn-on loss

By using a SiC- SBD, the high-speed hybrid module can reduce the reverse recovery peak current by about 60%. The fact that a SiC-SBD is a unipolar device with no minority carrier injection, is the reason for this improvement. The reverse recovery losses ERR are reduced by 92% compared to a Si Free Wheeling Diode of the actual 7th Chip generation.

Besides the improvement during reverse recovery, the enhanced characteristics of a SiC-SBD results in an enhanced behaviour at turn-on of the IGBT in the opposing arm. The reduced current peak during reverse recovery is reflected in the peak of the turn-on current, which is approximately 60% lower. The turn-on loss reduction is therefore about 84% and the overall switching losses of the device are 66% lower[(3)]. Table 1 displays an overview about the explained switching loss benefits of the high-speed hybrid module.

	E_{on} (mJ)	E_{off} (mJ)	E_{rr} (mJ)	Total loss (mJ)
X Series Si module	14.5	19.2	14.4	48.1
High-speed hybrid module	2.3	12.8	1.1	16.2
Reduction rate	84%	33%	92%	66%

Table 1: Switching loss comparison

Contribution for power conversion systems

Figure 3 shows the dependence between the reactor volume and the switching frequency of the power semiconductor device. If the switching frequency of a power conversion system (PCS) is increased from 10kHz to 30kHz the total inductor volume can be decreased by around 50%. By applying high-speed hybrid modules, the size of the entire unit can be decreased and the costs can be significantly reduced because of miniaturizing the passive components, such as capacitors, inductors and transformers which are used for filtering circuits at low frequency operation.

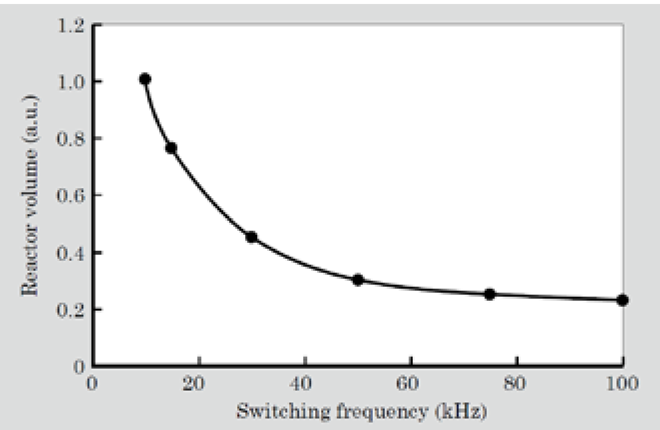

Figure 3: Dependence of reactor volume on switching frequency

To get an impression what the implementation of the high-speed hybrid IGBT module means for an inverter operation, a simulation result is displayed in figure 4. The simulation is done for a 200A / 1200V 62mm standard package in a small capacity PCS.

For a switching frequency of 20kHz an overall loss reduction of about 50% can be achieved. Because of the lower switching losses, these benefit will even increase for higher switching frequencies and will contribute to a high-efficiency operation and miniaturization at the high frequency operation of the inverter system. Even with the slightly increased on-state losses because of the higher $V_{ce,sat}$ the improvement is remarkable.

The chip junction temperature, when mounted to the inverter, is displayed in Fig. 5. Comparing the junction temperature of the chip at a switching frequency of 20kHZ, there is already an advantage of around 18°C for the IGBT and 19°C for the SBD compared to the X-Series Si module. This enables a PCS to further increase the output current during high frequency.

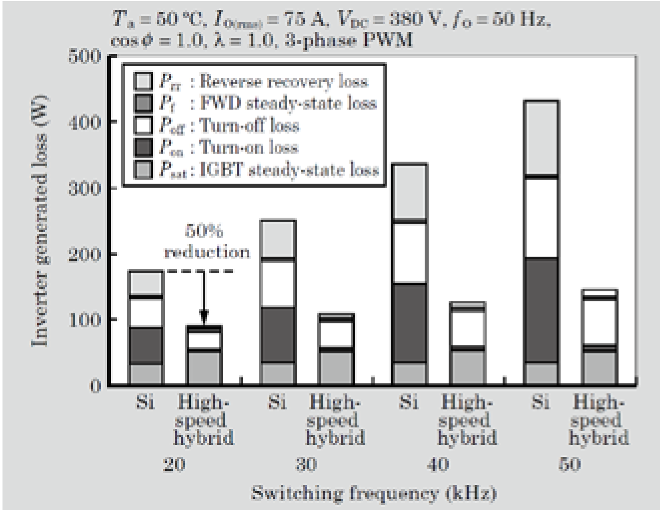

Figure 4: Inverter loss comparison

Postscript

Large volume and mass of filter circuits like capacitors, inductors and transformers can be reduced by higher switching frequency enabled by the use of the high-speed hybrid module. The reduced turn-off losses by the high-speed IGBT and the low losses for turn-on and reverse recovery losses caused by the SiC-SBD allow high switching frequency operation.

These benefits make the high-speed hybrid module to an optimal solution for fast switching applications such as EV quick charger's, PV systems, UPS systems, plasma cutters and welding machines. Fuji Electric will continue pursuing ways to reduce losses to contribute to energy savings and a sustainable society.

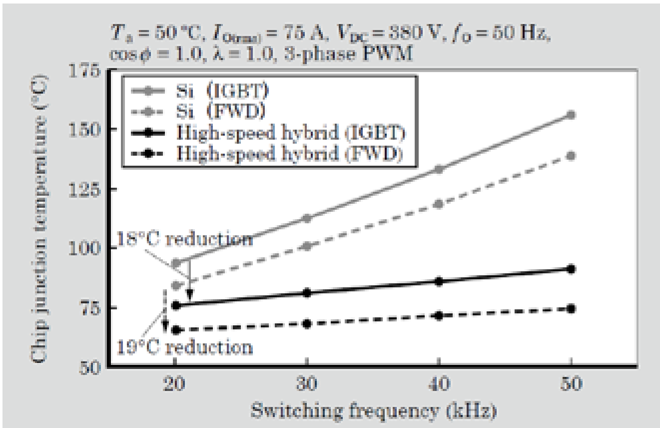

Figure 5: Chip junction temperature when mounted to the inverter

References

(1) Usui, R. et al. High Speed Hybrid Modules Combining High Speed IGBTs with SiC-SBDs. FUJI ELECTRIC REVIEW. 2018, vol.64,no.4, p.176-180.
(2) Hara, Y. et al. High-Speed Discrete IGBT "High-Speed W-Series". FUJI ELECTRIC REVIEW. 2015, vol.61,no.4, p.280-284.
(3) Usui, R. et al. High Speed Hybrid Modules Combining High Speed IGBTs with SiC-SBDs. FUJI ELECTRIC REVIEW. 2018, vol.64,no.4, p.176-180.

Note: EconoDUAL™ 3 is registered trademark of Infineon Technologies AG, Germany

Data-driven Maintenance Planning for Variable Speed Drives

ABB has developed a condition-based maintenance approach for variable speed drives. Operating in the cloud, the data-driven methodology can identify the risk of potential component failures one to two years ahead.

By Stefano Legnani, Global Service Product Manager, ABB

Over a number of years, discussions with users of variable speed drives (VSDs) in critical applications in the oil and gas, metals, water and wastewater, and pulp and paper industries, had revealed that they wanted an approach that went beyond their current time-based, preventive maintenance programs. They knew that some drives in their fleet were probably overloaded and there was a risk of failure before the scheduled replacement date – creating potential issues with unplanned shutdowns and lost production. Equally, some drives, having reached the end of their nominal service life, could still have many years of life left. But without any way of measuring the asset's health they could not take the risk and had to replace the drive components anyway.

To address this challenge, ABB embarked on the development of a data-driven condition-based maintenance approach. The aim was to take the guesswork out of scheduling drive repair and replacement activities by building a clear picture of how drives are actually aging over their time in service.

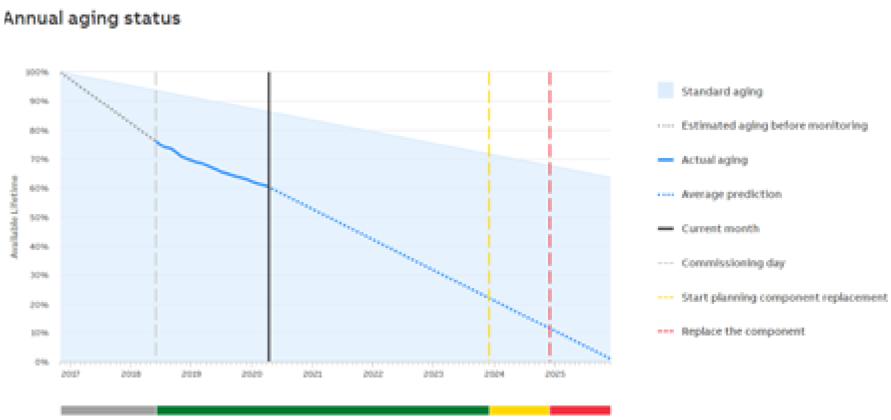

Figure 1: Blue shading indicates the nominal life of a VSD while the blue line shows the predicted life.

Aging of the key drive components

The starting point was to look at the key components in a drive – the fan, the semiconductor converter module and the DC link capacitors – and how they age. The main common aging factor is the temperature at which they operate:

- The lifetime of the main cooling fan is limited by the consistency of the bearing grease. Grease liquification due to high temperature is the prime cause of bearing aging. So, the air inlet temperature of the fan is a key factor in the aging of the fan itself.
- Semiconductor components have a thermo-mechanical aging mechanism related to temperature cycling. In a drive converter module, temperature cycling is induced by the loading of the drive. Variable loading causes thermal cycling which eventually results in component failure.
- The lifetime of the DC link electrolytic capacitor can be limited by the electrolyte. An internal temperature rise in the capacitor accelerates the electrolyte vaporization and diffusion out of the capacitor. This causes an increase in equivalent series resistance (ESR) and a decrease in the capacitance, eventually leading to capacitor failure. The capacitor lifetime depends on the hot-spot temperature of the capacitor and the applied voltage.

Data collection via the cloud

An advantage of modern VSDs is that they already incorporate thermal, voltage and power sensors that collect data on the ambient temperature and load variations of the components, as this is essential for their normal operation. The actual amount of data generated by a drive is huge – with point measurements made at intervals of one second, a single drive might generate 200 gigabytes (GB) a year. Until recently, collecting this level of data and analyzing it would have been impractical. The advent of the cloud computing has proved to be a game-changer in this respect.

Cloud-based algorithms and statistical analysis

Once a method of obtaining the raw data had been established, the next step was to determine how to interpret the information to obtain a life prediction. ABB worked with its component manufacturers to obtain life prediction curves based on L10 probability. In simple terms, the L10 life calculates how long 90 percent of a group of apparently identical components will last when subjected to the same operating conditions. In other words, 10 percent of this sample group of components is expected to fail before they reach their specified L10 life.

The L10 curves were used to develop cloud-based algorithms which process the stress information obtained from the components to estimate their remaining lifetime. The details of the individual components were then used to build an algorithm to predict the life of the VSD. Figure 1 shows how this works in practice on a graph that plots available lifetime against calendar time.

The shaded blue area indicates the nominal life expectancy of the VSD – a gentle slope over 25 years. In contrast, the steeply descending blue line shows the anticipated life under its current stress conditions. Clearly, the drive is predicted to fail when the line crosses the x-axis – some time in mid 2025. Added to the curve are two alarm points – a yellow line that indicates when component replacement should be planned and a red line indicating when the component must be replaced to avoid failure.

This analysis can indicate potential failure up to two years ahead, helping reliability managers to understand why maintenance should be booked for a particular time. The three key drive components covered by the stress analysis are field-replaceable items, and the work could be carried out by a suitably skilled in-house maintenance team.

The data produced by the stress analysis can also be shown in the form of a daily lifetime impact chart, as shown in Figure 2. This helps reliability managers understand if plant setting optimization might be carried out to extend the lifetime of the drive components.

The condition-based maintenance analysis can sometimes bring very good news. Figure 3 shows the actual life curve for a drive with components under lower than usual stress. In this case, the algorithms have estimated how much the maintenance can be delayed

Figure 2: Analysis of the daily lifetime impact of the load on the drive operation.

Figure 3: Condition-based maintenance analysis showing that the drive components are lightly loaded.

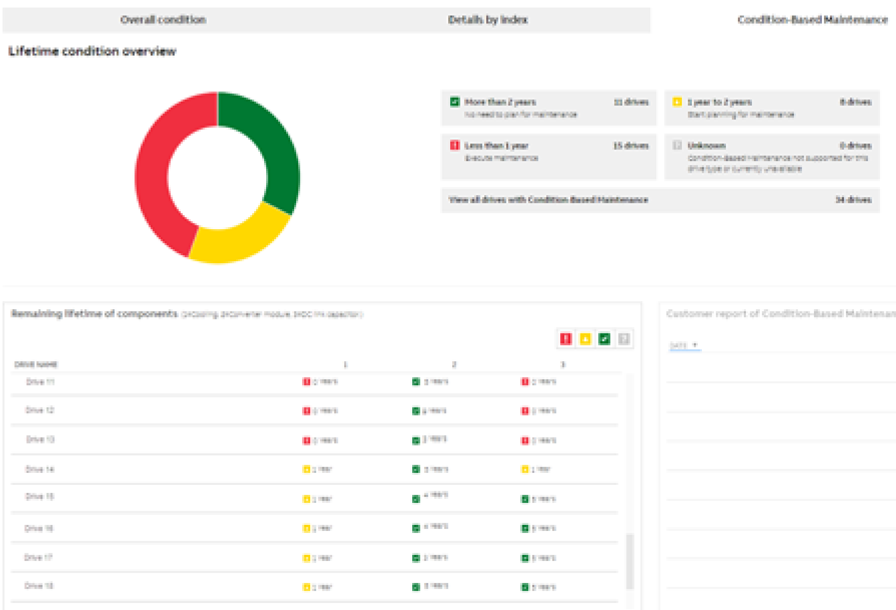

Figure 4: The dashboard provides an immediate overview of the maintenance needs of the complete fleet of drives.

in comparison to the normal preventive maintenance plan (the blue area in the chart). Considering that the aging curve calculation is based on the L10 method, reliability managers can decide to take reasonable data-driven risks and extend their plant production as well as planning their maintenance shutdowns more efficiently to minimize downtime.

Dashboard provides an instant view of maintenance needs
The condition-based maintenance tool provides a dashboard that enables reliability managers to see easily the information needed to plan their next maintenance task. The table of the remaining lifetime of the components clearly shows which drives will need maintenance within one or two years. The pie chart provides a clear view of the maintenance needs for the complete fleet and helps plan maintenance shutdowns. If the pie chart is completely green this means that no maintenance will be needed within the next two years.

If a component is changed, the reliability manager can insert the time of maintenance into the portal. The lifetime plan is then re-calculated accordingly.

Cost optimization for a drive fleet
The condition monitoring service for drives has been designed to be scalable to allow maintenance managers to tailor it to meet their specific needs. For example, critical drives could be protected by condition-based maintenance while less critical drives are given more basic condition monitoring, which are sufficient to follow the equipment's general parameters and stress level.
The service has been developed initially for ACS800 and ACS880 low-voltage air-cooled industrial drives. It enables the failure of a drive component to be predicted one or even two years ahead, optimizing maintenance planning and avoiding costly emergency maintenance in case of failure.

An early success in a practical application
The condition-based maintenance service had an early practical trial with a major customer in the steel processing industry. The converter module in a drive operating the rolling mill was identified as working at a high-stress level. The lifetime estimate showed that the component had reached its remaining useful lifetime. At that point it was not replaced, and four months later it failed. Following its replacement, the condition-based maintenance analysis indicated that the newly installed converter operating in this type of cyclic application requires changing of the power module in seven years to avoid unexpected failure. This was exactly the timescale in which the original converter power module had failed.

Monitoring the world's biggest free-fall simulator
Aero Gravity in Milan, Italy, is the world's biggest free-fall simulator. It enables flyers to experience the thrill of free-fall in a 21-meter high and 5-meter wide transparent tube.
The six 400 kilowatt (kW) fans creating the air updraft are each operated by asynchronous three-phase electric motors and VSDs. With a touch of a joystick, the drives enable the wind tunnel operator to regulate the air flow to meet the needs of the flyers in the chamber – ramping up from 120 km/h to a peak of 370 km/h and back down in a matter of seconds.
To meet the highest safety standards, Aero Gravity uses cloud-based condition monitoring for the drives. The service continuously monitors the status of the drives, collecting data on key parameters such as abnormal temperatures and incorrect operations. The server analyses the data and provides an overview through a dashboard to identify areas that may need extra attention.
The service gathers valuable feedback every day that helps the maintenance team at Aero Gravity to take corrective actions. This reduces thermal stress on the equipment, which will result in longer lifetime and improve its overall efficiency, while helping to maintain comfortable temperatures for the flyers in the chamber.

The next step – neural network computing
Harnessing the combined power of cloud computing, machine learning and deep knowledge of drives has enabled the development of a data-driven condition-based maintenance approach that supports highly targeted maintenance actions for critical drive applications. The next step in this approach will be to use neural network computing to take the data-driven analysis a stage further to develop a greater understanding of patterns and anomalies. This will provide an even earlier warning of potential issues so that appropriate maintenance actions can be scheduled to prevent any risk of unplanned process downtime.

www.abb.com/drives

950 V IGBT and Diode Technology Integrated in a Low Inductive ANPC Topology for 1500 VDC PV String Inverter

In the past two years, with the booming of the global PV market, and the benefits of a lower levelized cost of energy (LCoE), 1500 VDC photovoltaic systems have been established as mainstream. In the meantime, the string inverter solution is also becoming increasingly popular owing to its continuously enhanced power density, flexibility and simplified maintenance.

By Christian R. Müller, Andressa C. Schittler and Sichao Ma, Infineon Technologies

Investigated ANPC topology

To support this market trend, Infineon has developed the new, low-inductive Easy 3B package and a special 950 V IGBT and diode technology. Together with the active neutral-point clamped (ANPC) topology, this combination brings the power density of 1500 VDC PV string inverter to the next level, which leads to a further reduction of LCoE.

Figure 1 shows a typical ANPC topology used in solar inverters. Six subsystems are used and each subsystem consists of an IGBT (T1 to T6) with an antiparallel diode (D1 to D6). VDC is symmetrically applied from DC+ to N and from N to DC-. The investigated ANPC topology uses fast-switching devices in the subsystems 1 to 4, and low-static loss devices in the subsystems 5 and 6. A comprehensive discussion and explanation of ANPC topologies and the relevant commutation paths is provided in Ref. [1, 2].

In active power, e.g., positive output voltage and positive output current, the solid and dotted green lines in figure 1 indicate the typical commutation path. For clarity, T1 commutates with D2, whereas T5 is continuously in an onstate. Consequently, one main commutation path for active-power operation is between DC+ and N and/or N and DC-. Therefore, parasitics should be minimized in these paths by design measures to ensure optimized performance.

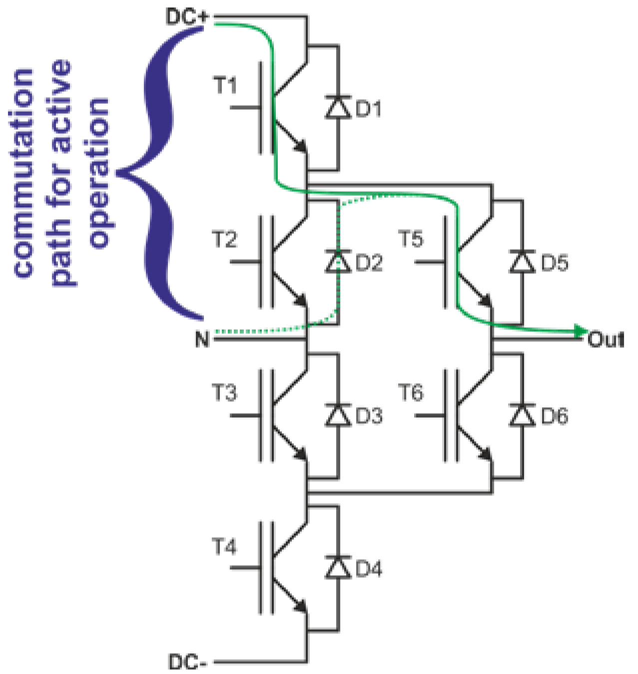

Figure 1: Schematic drawing of an ANPC topology with fast-switching devices and low-static loss devices in the subsystems 1 to 4 and 5 to 6, respectively. The solid and dotted green lines indicate the investigated commutation path

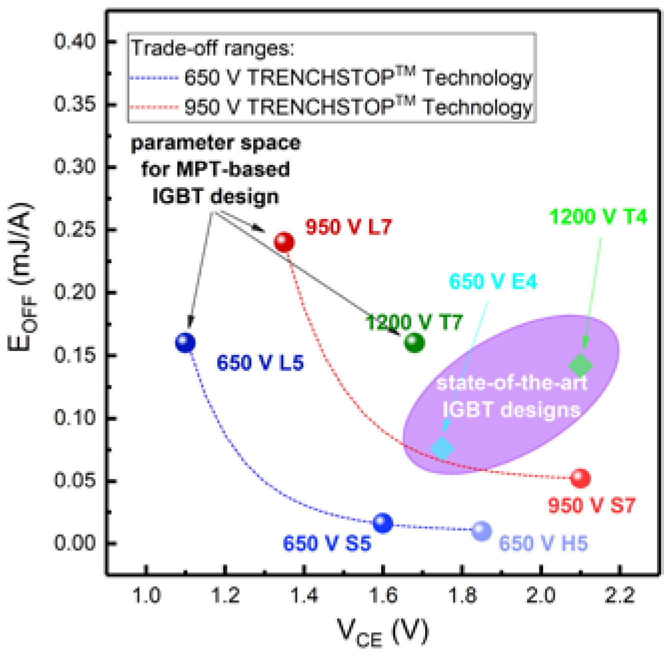

Figure 2: Trade-off diagram of 650 V, 950 V, and 1200 V MPT IGBT technologies. Static and dynamic values are provided at T_J=150°C and with V_{DC}=2/3·V_{CES}. As a reference, 650 V and 1200 V state-of-the-art, 4th generation IGBTs are indicated as well

New 950 V technology for solar applications

The new 950 V IGBT technology is based on a micro-pattern trench (MPT) cell design, which is well known from the 650 V TRENCHSTOP™ 5 and 1200 V TRENCHSTOP™ 7 IGBTs [3, 4, 5]. In order to meet the specific requirement of each subsystem in ANPC topology and to optimize the efficiency of system, two independent device performances were developed: a fastswitching IGBT (S7) with moderate static losses, but significantly reduced dynamic losses, and a low-static loss optimized IGBT (L7). The new 950 V diode is based on the well-known 650 V RAPID technology, and provides adequate softness, cosmic-ray robustness, but also low dynamic losses.

Figure 2 shows the trade-off diagram of 650 V, 950 V, and 1200 V MPT technologies. All values are provided at a junction temperature (T_J) of 150°C, nominal current, and a DC-link voltage (V_{DC}) of 2/3 of the corresponding blocking voltage V_{CES}. As one can see, the 650 V MPT technology offers very fast-switching devices (H5) with higher static losses as well as staticloss optimized devices (L5). The 1200 V MPT technology (T7) combines low static losses with moderate dynamic losses compared to 1200 V T4. At any rate, due to the blocking capability of 1200 V, T7 provides larger (by nearly factor 8) dynamic losses than S5, although both offer comparable collector-emitter voltages (V_{CE}) at nominal current (I_{nom}). Consequently, the 950 V MPT technology closes this performance gap.

L7 provides approximately 50 percent higher dynamic losses than T7 but at significantly lower static losses. S7 shows only a third of T7's dynamic losses at moderate static losses. One should keep in mind that current density decreases with increasing blocking voltage. In the case of L7 and S7, the current density is approximately 50 percent higher compared to T7. Thus, if equal chip areas are used in a power module, the performance benefits of 950 V IGBTs becomes even more pronounced with respect to 1200 V IGBTs. Additionally,

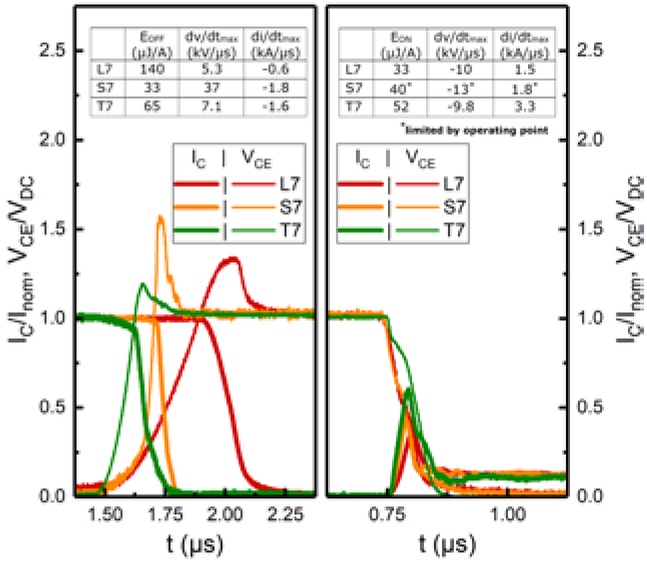

Figure 3: Turn-off waveforms (left-hand side) and turnon waveforms (right-hand side) of L7, S7, and T7 for $I_C = I_{nom}$ and $I_C = 0.1 \cdot I_{nom}$, respectively, with V_{DC}=600 V at T_J=25°C. The tables contain characteristic parameters

comparing L7 and S7 to the state-of-the-art 1200 V T4 and 650 V E4, emphasizes the benefits directly related to the MPT concept and technology used.

In the following, focus is on L7, S7, and T7. Figure 3 displays turn-off and turn-on waveforms of L7, S7, and T7. For turn-off, S7 provides the most aggressive switching behavior, i.e., the highest switching slope (dv/dt) and peak voltage $V_{CE,peak}$. Focusing on S7, $V_{CE,peak}$ are close to its maximum value. L7 and T7 are very soft and do not reach critical values. For turn-on, all devices provide comparable switching performance. S7 might achieve lower switching losses and higher dv/dt values if the gate resistor (R_G) is reduced additionally.

Optimized power module for 1500 V solar applications
As discussed in Ref. [6], an optimized power-module design is mandatory to achieve best performance in the final system. For this purpose, the following steps were taken to develop an optimized power module for 1500 V solar applications:

First, the main commutation paths of the ANPC topology were identified, as depicted in figure 1.

Second, the power terminals were positioned close to each other in a parallel-plate design to minimize stray inductance between DC+ and N and N and DC. The positions of DC+, N, and DC- are indicated in figure 4. The output terminals are situated opposite the input terminals allowing a simplified PCB design.

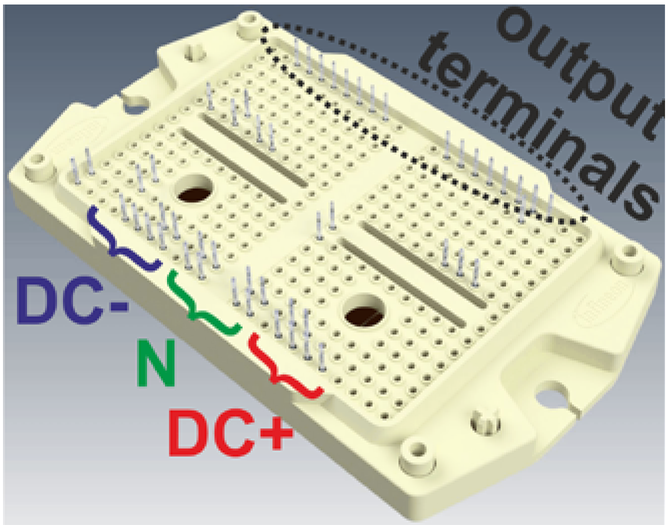

Figure 4: Easy3B package with the corresponding pinout of a 950 V based ANPC topology.

Third, the internal layout was defined in such a way that only very small commutation loops occur on the substrate level for the critical commutation paths. Commutation paths between the module substrates are avoided.

Fourth, a very low inductive and symmetric power module was developed using the novel baseplate-less Easy3B package. Hence, a module-stray inductance of only 15 nH has been achieved on the same footprint as for two conventional Easy2B packages. In addition, the Easy3B package provides a reduced thermal impedance compared to Easy1B and Easy2B.

And finally, the 950 V IGBT and diode technology has been implemented in this power-module design. Thus, an ANPC topology optimized for 1500 V solar inverters with a nominal current of 400 A is fully integrated in a single power module.

The performance of the power module is evaluated using the 1500 V ANPC topology seen in figure 1. S7 and L7 are implemented in the subsystems T1 to T4 and T5 to T6, respectively. Whereas T2 and T3 provide an I_{nom} of 200 A, all other IGBTs have an I_{nom} value of 400 A. With respect to the diode, two main scenarios are analyzed. In the first one, 200 A RAPID diodes are integrated in all subsystems. In the second one, 1200 V SiC Schottky diodes with I_{nom}=60 A replace the RAPID diodes D2 and D3. An ANPC topology with T7 and EC7 is used as reference, and the comparison is performed for the active-power commutation path. In all cases, a maximum increase of the average module temperature of 30 K is presumed, which consequently limits the solution's usability.

Figure 5 shows maximum achieved output current I_{out} versus switching frequency f_{SW} with 1200 V applied between the terminals of DC+ and DC-. The solid lines represent I_{out} of the reference and the two L7/S7-based scenarios mentioned above. All three solutions provide identical nominal currents. At very low f_{SW}, the T7/EC7 solution offers up to 15 percent higher I_{out} than the two L7/S7 variants. At typical f_{SW} above 20 kHz, this benefit is reduced to approximately 7 percent. It is important to mention that only the significantly lower power density of the T7/EC7 solution leads to this imaginary I_{out} benefit. If an equal power density, i.e., identical chip areas of L7, S7, and RAPID diodes, is used, the situation changes. The dashed lines visualize this.

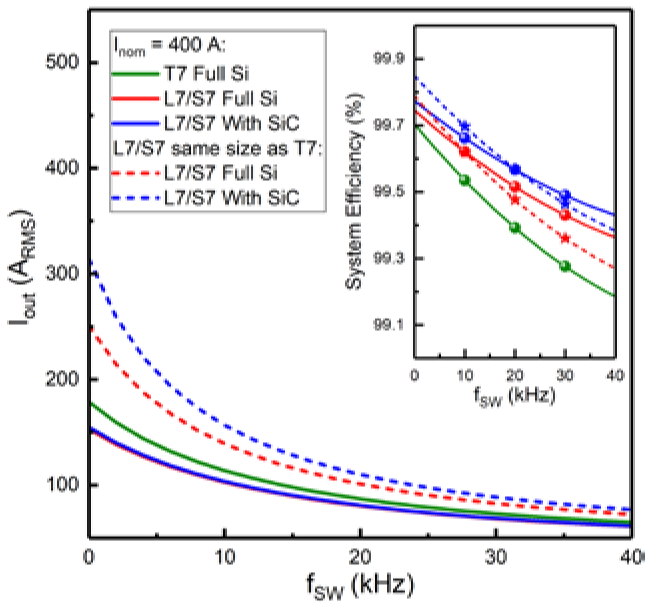

Figure 5: I_{out} versus f_{SW} for different variants and power densities at equal thermal boundary conditions. Inset: System efficiency versus f_{SW} for different variants and power densities at the corresponding I_{out}.

It becomes clear that L7/S7 with RAPID diode and L7/S7 with SiC diode now provide up to 40 percent and 75 percent increased I_{out}, respectively. Even for f_{SW} in the range of 20 to 40 kHz, I_{out} is larger than the T7/EC7 reference by a minimum of 10 percent and maximum of 26 percent. These findings are not surprising, as T7 and EC7 are optimized for general-purpose drives, and thus, lower switching frequencies. Therefore, the benefits of L7 and S7 come to the fore if faster switching is required as in solar applications.

The inset of figure 5 displays system efficiency versus f_{SW} for the corresponding maximum I_{out}. All solutions provide a system efficiency of minimum 99.2 percent. At any rate, L7/S7-based solutions offer a minimum 0.05 percent up to 0.3 percent higher system efficiency than a T7-based one. One should keep in mind that the slightly lower system efficiency for L7/S7 with larger chip sizes (dashed lines) is accompanied by significantly higher I_{out} when compared to the L7/S7-based solution with I_{nom}=400 A (solid lines). Although system efficiency is marginally smaller, I_{out} is 25 percent to 35 percent enhanced at f_{SW}=20 kHz.

Summary

This article presents the new 950 V technology and its inherent design options, and compares them to existing 1200 V technologies. The implemented cell design enabled the development of a static-loss-optimized IGBT (L7) and a fast-switching IGBT (S7). Compared to state-of-the-art 1200 V IGBTs, significantly reduced static losses and/or improved switching performance were achieved, as well as better system performance. With the help of a comprehensive analysis on the interaction of power-module designs and ANPC topology [6], the critical commutation paths and system-limiting factors were identified.

Based on this optimized power-module design, a fully integrated ANPC topology with a nominal current of 400 A for 1500 V solar inverters was presented. The ANPC topology was implemented in the recently introduced Easy3B package, which enables the implementation of a module-stray inductance of only 15 nH. This power-module design together with the presented 950 V technology offers two options in the application. On the one hand, identical output power was achieved at a massively smaller footprint if a given 1200 V technology was replaced. On the other hand, 25 percent up to 75 percent increased output currents were achieved when equal chip areas were utilized.

References

[1] D. Floricau et al., "The efficiency of threelevel active NPC converter for different PWM strategies", Proc. EPE, pp. 1-9, 2009.

[2] C. R. Müller et al., “Using 650-V high speed 3 IGBTs in power modules for solar inverter performance improvement”, Proc. PCIM Europe, pp. 896-903, 2013

[3] T. Kimmer and E. Griebl, “Trenchstop 5: A new application specific IGBT series”, Proc. PCIM Europe, pp. 120-127, 2012.

[4] F. Wolter et al., “Multi-dimensional trade-off considerations of the 750 V micro pattern trench IGBT for electric drive train applications”, Proc. ISPSD, pp. 105-108, 2015.

[5] C. Jaeger et al., “A new sub-micron trench cell concept in ultrathin wafer technology for next generation 1200 V IGBTs”, Proc. ISPSD, pp. 69-72, 2017.

[6] A. C. Schittler, D. Heer and C. R. Müller, "Interaction of power-module design and modulation scheme for active neutral-point-clamped inverters," Proceedings PCIM Europe, pp. 1-7, 2019.

www.infineon.com

High Voltage Thyristors (SCRs) & Applications

WeEn Semiconductors, as an industry leader in thyristors, has successfully introduced high voltage SCRs covering the 1200V - 1600V range. These can be used in industry applications such as Uninterruptible Power Supplies (UPS), Solid State Relays (SSR), Energy storage and Battery chargers where high blocking voltage and high surge current handling capabilities are required.

By Aibin Hu and Brian Xie, WeEn Semiconductors

WeEn's High Voltage SCRs

The SCR, or Silicon Controlled Rectifier, is defined as a switching device having a four-layer p-n-p-n structure, leading to bi-stable behavior which can be switched between a high-impedance, low-current OFF-state and a low-impedance, high-current ON-state. SCR is a power semiconductor device that can block forward and reverse voltage for AC mains and conduct current in the forward direction. It can be considered as a current-controlled power switch. The typical current (I) – voltage (V) characteristic is shown in Figure 1. The reverse behavior is like a diode, which enters the avalanche breakdown region when reverse voltage is higher than the breakdown voltage. With forward bias, the SCR can be turned ON by apply a gate trigger current or a forward voltage larger than the breakover voltage.

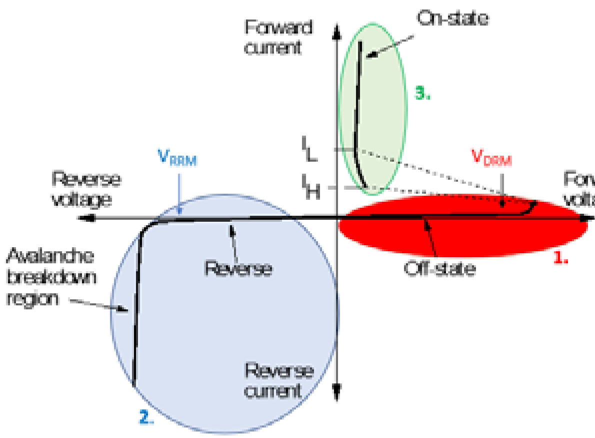

Figure 1: An SCR's typical current – voltage characteristic

I_{TSM}, the maximum surge current – one of the most important parameters in real application – is rated which is 10 times larger than the rated average current $I_{T(AV)}$. This ensures WeEn's SCRs have superior surge current capability for real application circuits. The maximum on-state voltage is lower than 1.5V which yields the benefit of lower conduction loss and lower temperature-rise for the SCR in operation.

High Voltage SCR Application Example

The SCR acts as an AC switch in power converter circuits, which has different function compared with Metal Oxide Semiconductor Field Effect Transistors (MOSFETs). The SCR is a semi-controlled switch in that it can only be triggered ON with a gate current and commutates (self-turns-off when turn-off is not controlled) as the load current reduces lower than the holding current.

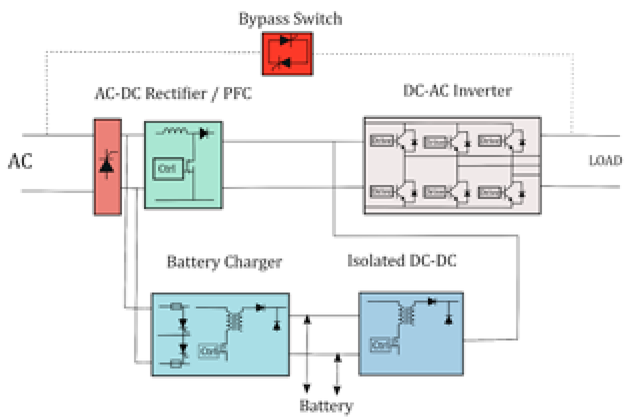

Figure 2: Online UPS topology with high voltage SCRs

Table 1 is an overview of WeEn's 1200V -1600V SCRs. All these SCRs are rated with current from 50A - 80A and packaged in TO247 or TO3P for high current handling capability. Due to the superior planar process passivation manufacturing technology, all WeEn's SCRs are rated with maximum junction temperature of $T_{j(max)}$ at 150 °C for robust and reliable operation.

Part Number	V_{DRM}/V_{RRM} (V)	$I_{T(AV)}$ (A)	I_{TSM} (A) @ t_p=10ms	V_T (V) maximum value	$I_{GT(max)}$ (mA) maximum value	$T_{j(max)}$ (°C)	Package
BT155W-1200T	1200	50	650	1.30V @ 50A	50	150	TO247
BT158W-1200T	1200	80	1100	1.35V @ 80A	70	150	TO247
TYN60K-1400T	1400	60	750	1.35V @ 60A	80	150	TO3P
TYN50W-1600T	1600	50	650	1.3V @ 50A	80	150	TO247
TYN80W-1600T	1600	80	850	1.47V @ 80A	80	150	TO247

Table 1: WeEn Semiconductors High Voltage SCR Overview: 1200V-1600V

Besides UPS, the SCR is widely used in solid state relays (SSR), battery chargers and resistive and inductive load control circuits. In modern online Uninterruptible Power Supplies (UPS), both AC mains and backup DC battery are necessary to make sure the output is continuous at any condition. A typical online UPS topology with high voltage SCRs is shown in Figure 2. The typical SCR waveform is shown in Figure 3.

Figure 3: WeEn SCR: typical waveform used in UPS rectifier circuit (Purple: SCR1 A-K current; Yellow: SCR1 A-K voltage ; Green: AC mains current ; Blue: SCR2 A-K voltage)

In summary, the SCR acts as a power switch in the following functional blocks:

- **AC/DC rectifier circuit**
  There are two types of bridge rectifiers, the diode bridge rectifier and the SCR bridge rectifier. Both have the same function to convert the sinusoidal wave current to rectified sinusoidal wave current. In modern switched mode power supplies, a Power Factor Correlation (PFC) function is necessary to force the current to be in phase with the voltage to reduce the total harmonic distortion of the mains supply. A purified output AC voltage is then generated by the DC-AC inverter. In this UPS topology, a controlled bridge rectifier is necessary and hence the SCR bridge is adopted.

- **Battery charging circuit**
  In the normal AC mains operation, the battery circuit is in the OFF state. In an emergency when mains power is interrupted, the battery circuit needs to be turned ON within 10 milliseconds of the AC mains vanishing. In this circuit, what is needed is a bi-directional blocking switch that can be turned ON with a small control signal. Besides this method of control, good current surge-handling capability and long-term reliability are required. WeEn's 1200V – 1600V SCRs fulfil these requirements in this application.

- **Bypass circuit**
  Static Bypass switches are used to bypass the UPS normal operation in cases of high inrush or fault conditions. Manual bypass switches are an added benefit to allow service and isolation for safety purposes. Due to the phase mismatch between the input AC mains and the output AC sources, large inrush current can flow into the SCR bypass switch. All WeEn's SCRs are rated with an I_{TSM} that is 10 times larger than the rated average current $I_{T(AV)}$, which ensures superior surge current capability for this bypass application.

WeEn Semiconductors High Voltage SCR Process Technology
Figure 4 shows the cross section of a high voltage SCR. The active area is formed with four layers in the silicon. The anode, cathode and gate connection metal are placed on the bottom and top surface

respectively. The SCR functions like a diode after a gate pulse current is applied and current goes from anode to cathode.

In modern power devices it is common to choose the appropriate silicon doping levels and thickness of the silicon N-region in the active area to give the required breakdown voltage. However, the blocking junction must terminate on the surface somewhere, usually the top surface. If the surface depletion reaches the edge of the chip, then there would be a reliability failure. In the case of double-blocking devices such as SCRs, if the surface depletion region reaches the opposite PN junction then there would be a "reach-through" breakdown. In both cases, suitable and adequate passivation of the top termination surface area is necessary.

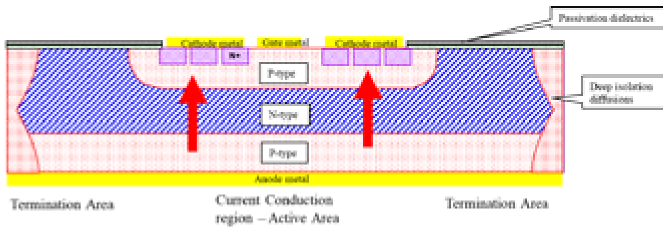

Figure 4: Cross-section of high voltage SCR (both active area and termination areas are shown)

The most commonly used dielectric layer to cover the edge termination region is thermal oxide. This thermal oxide, grown during diffusion, should be very high quality with low surface state density and low oxide charge. An alternative is Semi-Insulating Poly Silicon (SIPOS in short). This is basically a conductor (with very high resistance). Being a conductor, it cannot trap charges, and any charges that are present will simply move along the conductor under bias and out of the device as leakage current. All of WeEn's SCRs have the planar structure and are passivated with SIPOS, which gives better reliability and long-term stability.

This "Planar Process" method of device manufacturing is totally lead (Pb)-free which is another advantage compared with the older but popular "Glass Mesa" termination technology, in which Pb is contained in the glass. Pb-free manufactured SCRs will be an important compliance benefit for users of SCRs as RoHS exemption will expire in July 2021.

Radiation Performance of Enhancement-Mode Gallium Nitride Power Devices

Enhancement-mode gallium nitride (eGaN®) technology enables a new generation of power converters in space operating at higher frequencies, higher efficiencies, and greater power densities than ever achievable before. eGaN devices also exhibit superior radiation tolerance compared with silicon MOSFETs.

By Max Zafrani, CTO, EPC Space
Alex Lidow Ph.D., CEO and Co-founder, Efficient Power Conversion

This article introduces EPC Space's family of eGaN FETs and ICs which have been specifically designed for critical applications in the high reliability or commercial satellite space environments. Some of the failure mechanisms in GaN and how they impact radiation performance are explored. Lastly, the electrical performance of eGaN transistors is compared with the most popular radiation hardened (Rad Hard) MOSFETs in the market.

Radiation in Space

There are three primary types of radiation experienced by semiconductors used in space applications. Regardless whether devices are being employed in satellites orbiting around our earth or incorporated in exploration satellites visiting the most distant parts of our solar system, all experience some form of high-energy radiation bombardment. These types of radiation are gamma radiation, neutron radiation, and heavy ion bombardment. An energetic particle can cause damage to a semiconductor in fundamentally three ways; it can cause traps in non-conducting layers, it can cause physical damage to the crystal, also called displacement damage, or the particle can generate a cloud of electron-hole pairs that will cause the device to momentarily conduct, and possibly burn out in the process.

In eGaN devices, energetic particles cannot generate momentary short-circuit conditions because mobile hole-electron pairs cannot be generated. Thus, this article will focus on the first two failure mechanisms − trapping and physical damage.

Gamma Radiation – Trapping in Silicon MOSFETs

Gamma radiation consists of high energy photons that interact with electrons. Figure 1(a) is a cross section of a typical silicon MOSFET. It is a vertical device with the source and gate on the top surface and the drain on the bottom surface. The gate electrode is separated from the channel region by a thin silicon dioxide layer. In a silicon-based MOSFET, the gamma radiation knocks an electron out of the silicon dioxide layer leaving behind a positively charged 'trap' in the gate oxide. The positive charge reduces the threshold voltage of the device until the transistor goes from normally off – or enhancement mode – to normally on, which is a depletion mode state. At this point the system will need a negative voltage to turn the MOSFET off. Typical ratings for rad-hard devices range from 100 kRads to 300 kRads. In some cases, devices can be made to go up to 1 MRad, but these tend to be very expensive.

Gamma Radiation – eGaN Transistors

eGaN devices are built very differently from silicon MOSFETs. As shown in Figure 1(b), all three terminals; gate, source, and drain, are located on the top surface. As in a silicon MOSFET, conduction between source and drain is modulated by biasing the gate electrode from zero volts to a positive voltage – usually 5 V. Notice that the gate is separated from the underlying channel by an aluminum gallium nitride layer. This layer does not accumulate charge when subjected to gamma radiation.

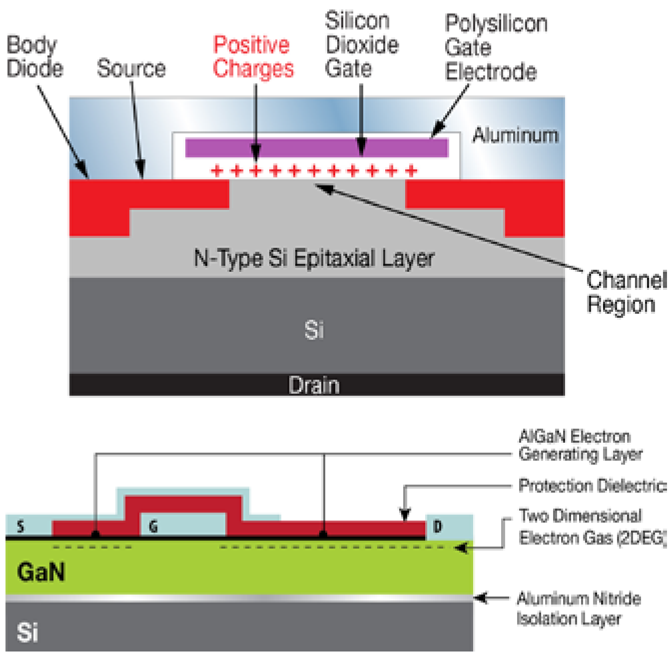

Figure 1: (a) Cross section of a typical silicon MOSFET (b)Cross section of a typical enhancement mode GaN (eGaN®) device

To demonstrate the performance of eGaN devices, EPC Space's 100 V family of eGaN transistors were subjected to 500 kRad of gamma radiation. Throughout the testing, leakage currents from drain to source and gate to source, as well as the threshold voltage and on-resistance of the devices at various checkpoints along the way were measured, confirming that there are no significant changes in device performance. Since the initial testing, eGaN devices have been subjected to 50 MRads, confirming that eGaN devices will not be the first part to fail due to gamma radiation in any space system. Testing results are shown in figure 2.

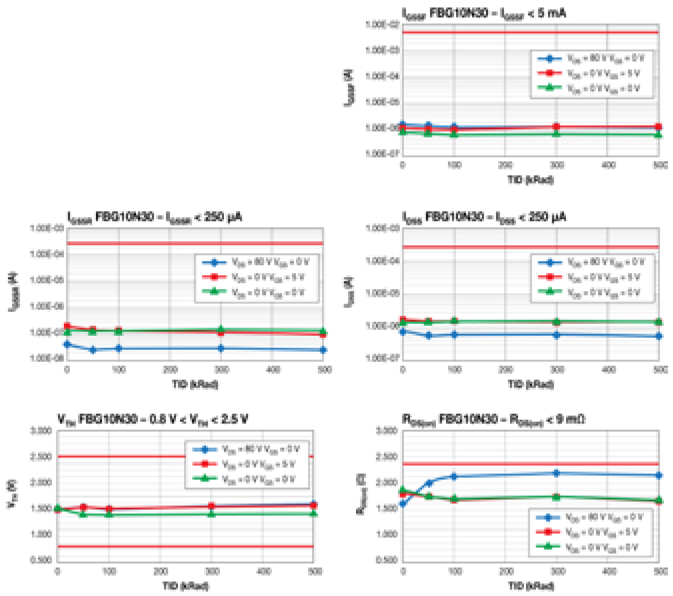

Figure 2: Results of gamma radiation testing of eGaN devices to 500 kRads

Neutron Radiation

The primary failure mechanism for devices under neutron bombardment is displacement damage. High energy neutrons will scatter off atoms in the crystal lattice and leave behind lattice defects. Figure 3 shows the impact of neutron radiation at doses up to 1 x 10^{15} per square cm. As with gamma radiation, the impact of neutrons on the GaN crystal and the entire device structure is minimal.

The reason for GaN's superior performance under neutron radiation is that GaN has a much higher displacement threshold energy compared with silicon.

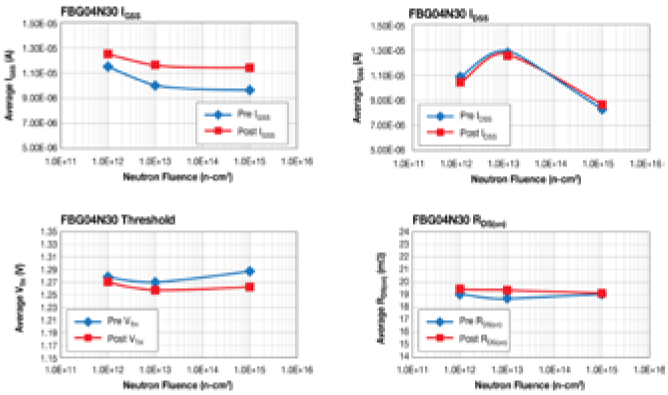

Figure 3: Impact of neutron radiation on eGaN devices at doses up to 1 x 10^{15} per square cm

Single Event Effects (SEE) – Si MOSFETs

SEE are caused by heavy ions generated by the impact of galactic cosmic rays, solar particles or energetic neutrons and protons. This can be simulated terrestrially by using a cyclotron to create beams of different ions. Two of the most common ions used to evaluate radiation tolerance of electronics components are Xenon, with a linear energy transfer (LET) of about 50 MeV·cm^2/mg, and gold, with an LET of about 85 MeV·cm^2/mg.

In a silicon MOSFET there are two primary failure mechanisms caused by these heavy ions, single event gate rupture (SEGR) and single event burnout (SEB). SEGR is caused by the energetic atom causing such a high transient electric field across the gate oxide that the gate oxide ruptures. Whereas, SEB is caused when the energetic particle transverses the drift region of the device where there are relatively high electric fields. The energetic particle loses its energy while generating a large number of hole electron pairs. These hole electron pairs crossing the drift region cause the device to momentarily short circuit between drain and source. This short circuit can either destroy the device, which is a single event burnout, or the device can survive, appearing as a momentary short circuit that can cause damage to other components in the system. This latter case is call single event upset, or SEU.

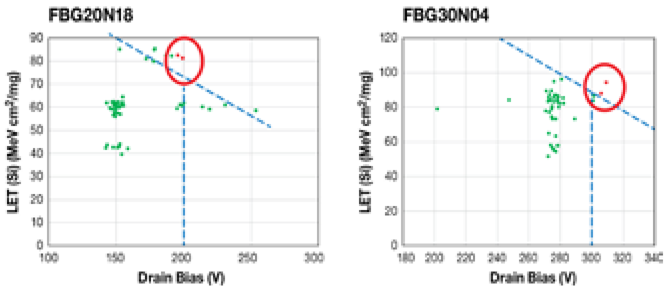

Figure 4: Results from several FBG20N18 200 V products (left) and FBG30N04 300 V products (right)

Single Event – eGaN Devices

Since eGaN devices do not have a gate oxide, they are not prone to single event gate rupture. Also, since eGaN devices do not have the ability to conduct large numbers of holes very efficiently, they are not prone to single event upset. The primary failure mechanism for eGaN devices under heavy ion bombardment is caused by energetic particles crossing the drift region of the device where there are relatively high electric fields. The conditions are about the maximum conditions possible, with an 85 LET beam of gold atoms pummeling the device biased at the maximum data sheet limit. In testing, the gate leakage does not go up during bombardment. The drain-source leakage, however, does start to rise as the displacement damage from the heavy ions increases.

SEE Safe Operating Areas

EPC Space has tested many specially produced EPC eGaN products for SEE under varied conditions. 40 V and 100 V product did not fail under any conditions up to full rated voltage and 87 LET. Figure 4 shows the results from several FBG20N18 200 V products and FBG30N04 300 V products. For the 200 V products, the first failures occurred at 85 LET and 190 V, as shown in the red circle on the left. The FBG30N04 300 V product failed at 85 LET and 310 V as shown in the red circle on the right.

Electrical Performance Comparison

In addition to the superior Rad Hard advantages of gallium nitride over silicon, GaN has superior electrical performance as well. As an example, the electrical performance comparisons of 100 V and 200 V Rad Hard eGaN transistors against Rad Hard power MOSFETs from Infineon are shown in table 1.

The 100 V FBG10N30 packaged part from EPC Space has half the on-resistance compared to the silicon MOSFET, yet is but one-tenth the size and has about one-twentieth the gate and gate-drain charges that determine switching speed. In addition, the radiation resistance is significantly higher.

At 200 V, the difference in electrical performance of the eGaN transistors is even greater. Note that the eGaN device listed on the left side of the 200 V section of table 1 has similar on-resistance to its MOSFET counterpart, yet is one-tenth the size, and has about 30 times better switching performance while demonstrating superior radiation resistance.

eGaN Devices for Space

In summary, GaN power transistors and ICs are the best choice for power conversion applications in spaceborne systems. eGaN devices have proven to be more rugged than Rad Hard MOSFETs, when exposed to various forms of radiation. In addition, the electrical performance of eGaN devices is many times superior to the aging silicon power MOSFET.

100 V

Parameter	FBG10N30	IRHNA67160	Units
I_D	30	35	A
I_{DM}	120	140	A
BV_{DSS}	100	100	V
$R_{DS(on)}$	9	18	mΩ
Q_G	9	160	nC
Q_{GD}	2	65	nC
Q_{RR}	0	1.9	µC
$R_{θJC}$	2.12	0.5	°C/W
Radiation Level	>10 M	300 k	Rad (Si)
SEE @85 LET	100	100	V
Size	23	236	mm²

Parameter	FBG10N05	IRHNJ67130	Units
I_D	5	22	A
I_{DM}	40	88	A
BV_{DSS}	100	100	V
$R_{DS(on)}$	38	42	mΩ
Q_G	2.2	50	nC
Q_{GD}	0.6	20	nC
Q_{RR}	0	3	µC
$R_{θJC}$	3.6	1.67	°C/W
Radiation Level	>10 M	300 k	Rad (Si)
SEE @85 LET	100	100	V
Size	12	78.5	mm²

200 V

Parameter	FBG20N18	IRHNA67260	Units
I_D	18	56	A
I_{DM}	72	224	A
BV_{DSS}	200	200	V
$R_{DS(on)}$	26	28	mΩ
Q_G	6	240	nC
Q_{GD}	1.95	60	nC
Q_{RR}	0	11.7	µC
$R_{θJC}$	2.12	0.5	°C/W
Radiation Level	>10 M	300 k	Rad (Si)
SEE @85 LET	175	170	V
Size	23	236	mm²

Parameter	FBG20N18	IRHNJ67230	Units
I_D	18	16	A
I_{DM}	72	64	A
BV_{DSS}	200	200	V
$R_{DS(on)}$	26	130	mΩ
Q_G	6	50	nC
Q_{GD}	1.95	20	nC
Q_{RR}	0	3.5	µC
$R_{θJC}$	2.12	1.67	°C/W
Radiation Level	>10 M	300 k	Rad (Si)
SEE @85 LET	175	170	V
Size	23	78.5	mm²

Table 1: Electrical performance comparisons Rad Hard eGaN transistors against power MOSFETs from Infineon

www.epc.space

Bodo´s Power Systems®

Special Feature

July 2020

PCIM Europe digital days
7. - 8. July 2020

PCIM 2020 – A leading Event for Innovations in Power Electronics Industry

By Leo Lorenz; ECPE Conference Director PCIM

The first time in the more than 40 years PCIM history we have to re-schedule the event due to the COVID-19 Pandemic. The PCIM today is the leading technology platform for Power Electronics Professionals from Industry, Academia and public Organizations from across the globe engaged in moving power electronics industry ahead in the whole value added chain from new materials to the next generation of power components, advanced packaging technology, full digital controlled power converters up to high level integrated Power Electronic Building Blocks (PEBB). Power Electronic itself is the driving technology for key elements of the global Megatrends e.g. Urbanization, Climate change and Digitalization. Further urbanization depends very strong on Smart home & office (DC-Grid) and full scale integrated transportation systems incl. electric and autonomous driving. To stop the Climate Chance we have to enforce the further development of sustainable Energy Supply by Renewables, to improve the energy efficiency in the whole chain of energy flow incl. the consumer equipment and go for a full Electric Society. The digitalization of our society contributes significantly to self-learning systems in our aging population, factory automation, safe and reliable power supply infrastructure from state grid to smart homes, shopping centers as well as the tremendous increase in data centers and health monitoring in all power electronic systems. To serve all of this fields of applications power electronics has become a very innovative technical discipline and thus very attractive for engineer's and the whole power electronics industry. Initiated and directed by these new fields of applications within the last 2 decades we had a complete renewal of power electronics industry and from 2010 to 2019 nine consecutive years of more than 10% annual growth rate. Last year there was a slow down due to political reasons –like trade negotiations between USA and China, Brexit outcome, etc. - and this year we are suffering from an impact of COVID-19 pandemic.

Today we see the first sign that the economy is picking up again. From the history we know that any economic slowdown is triggering new innovations which will be launched in the market during the next upturn. The power semiconductor market prognosis is always a mirror for the power electronics industry. Nevertheless starting from this year the forecast up to 2030 of all market research Institutions show a very nice development of the power semiconductor market revenue. In the next decade the power semiconductor devices based on Si material is having a growth rate of more than 60 % - from 27 Bill US $ today to up to 38 Bill in 2030. It´s also interesting to see that Si-based devices are still having a nice further development potential and many companies investing in new production facilities such as the 300mm Wafer fabs. Si based devices will remain the driving force for most application in power electronics mass market. Of course – and this is also a mirror of this year's PCIM conference - WBG Devices are on top of the technology development. In the meantime we see many emerging applications for WB Devices with outstanding performance and cost benefits on the system level. According the market forecast within the next decade we will have an increase in the revenue by a factor of 12 from 250 Mill US $ today up to 3 Bill in 2030. 2/3 will be SiC Components and 1/3 GaN Devices.

In addition we have to learn that some segments we are serving with power electronics components and systems are strong governmental regulated e.g. renewable energy generation and E-Mobility. The first push in E-mobility is driven by governmental bonus payments. The free open market will depend very strong on the availability of charging infrastructures, driving range of the car, lifetime of energy storage device and mass production of affordable cars.

For this year PCIM conference again we have seen an increase in the number and quality of papers submitted, and selected the best and most important for inclusion in the program of oral and poster presentations. At this year's event, special focus is paid on technologies for future energy supply systems, E-Mobility including the infrastructure and SMART Battery Management Systems, advanced power converters driven by efficiency and power density. The drivers for these applications include advanced power semiconductor devices based on Si and WBG materials, new materials to improve device and system reliability, and pioneering research on managing parasitic effects in the package and circuit set up. Presentations on intelligent driving of these ultrafast switching devices, digital controlled power converter topologies and control techniques in intelligent motion systems form the backbone of the PCIM Europe Conference. More than 40% of the presentations are covering WBG devices and related emerging application of these. Advanced integrated cooling concepts with new materials on the one side to match the CTE and on the other side with significant elevated operating temperatures. A hot topic this year will be the discussion on ruggedness and reliability of power devices. The first time we implemented a special session on additive manufacturing and 3D printed electronics for ECU´s (electronic control units). A special highlight will be Energy storage systems including Battery Management systems and strategies for Battery Lifetime Maximization.

I am convinced that with its high level technical program and discussion platform this year's PCIM Europe Conference will provide you with an overview of the key technology development trends in power electronics and inspire you to pursue new business opportunities.

I wish you an enjoyable and successful conference packed with new ideas for your future business.

Take care and stay healthy,
Prof. Dr. Lorenz

Detailed Statistics on the PCIM Europe 2019

An increase of visitors and exhibitors as well as high satisfaction rates on all sides confirm that the PCIM Europe, the leading international Exhibition and Conference for Power Electronics and its applications, was a great success.

With 12,182 visitors and 515 exhibitors, this year's PCIM Europe that took place on 7 – 9 May in Nuremberg registered another record result. As far as the Conference is concerned, the numbers were on the same level as the previous year, showing a slight upward trend with 804 international delegates.

More than half of this year's exhibiting companies are based outside of Germany; the number of American enterprises was a remarkable 14%. Furthermore, China, Italy, Great Britain, France and Japan were strongly represented. 76% of the exhibitors rated the PCIM Europe "good" or "very good" and they praised, in particular, the quality of trade visitors at their booths as well as the organization of the event.

The international trade visitors (46%) predominantly came from German-speaking countries, but also from Italy, Great Britain, France and the USA, the large proportion of decision-makers (79%) mirroring the superior quality of the clientele. 93% of the visitors would recommend the PCIM Europe to others and 75% of them intend to attend the exhibition again next year. Information on new products and trends was the most frequently mentioned objective (74%), followed by exchanging knowledge and experiences (62%), gaining an overview of the market (61%) and maintaining existing / establishing new business relations (57% and 55% respectively).

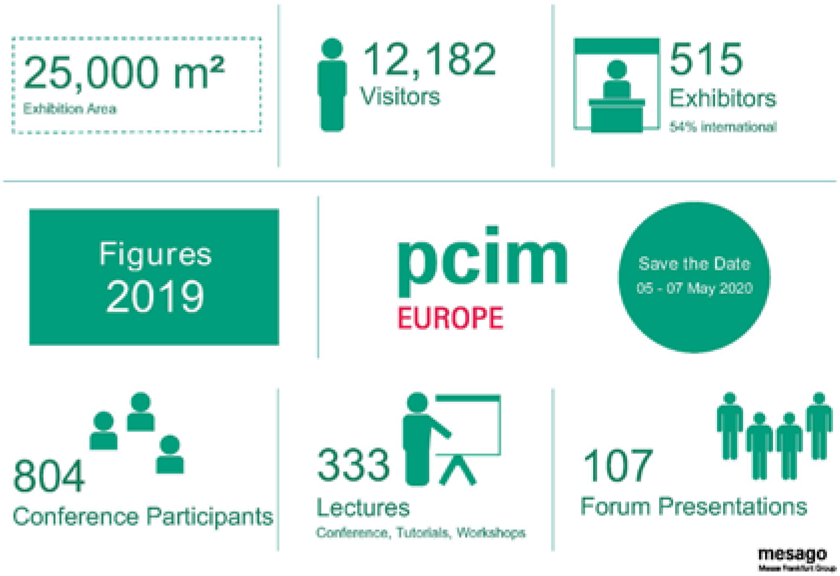

MITSUBISHI ELECTRIC
Changes for the Better

Discover this year's highlights in Si and SiC power modules

CM1200DW-34T

LV100 for industrial and renewable applications, Dual type 7th Generation 1200A/1700V IGBT module with SLC technology

LV100 is the Next Generation Standard Module package for high power. The LV100 package has been optimized for the requirements of industrial and renewable applications. An optimized solution is realized by the utilization of: efficient 7th Gen IGBTs with 1200V and 1700V ratings, thermal cycle failure free SLC (SoLid Cover) package technology, and advanced package layout with the advantages of low stray inductance, easy paralleling and symmetrical current sharing.

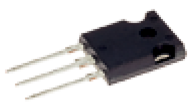

N-series 1200V SiC-MOSFET

New discrete SiC MOSFET in TO-247 package

Mitsubishi Electric added the new N-series SiC MOSFETs to the product portfolio. The line-up is divided into three ratings (RDSon = 22 mΩ, 40 mΩ, 80 mΩ) in the TO-247 package with a blocking voltage of 1200V, which are optionally qualified according to the AEC-Q101 standards. The N-series SiC MOSFETs can be used in applications like solar inverters and on-board chargers for electromobility.

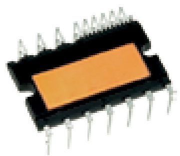

SLIMDIP-W

DIPIPM with RC-IGBT in SLIMDIP package

The high-switching frequency optimized SLIMDIP-W module for home appliances has been released. The integrated drivers and protection functions combined with the RC-IGBT offer a reliable and compact solution for a short time-to-market. The module has a rated 600V blocking voltage and a rated current of 15A.

FMF1200DXZ-24B

2nd generation Dual type 1200A/1200V SiC MOSFET with RTC short- circuit protection

The 2nd gen SiC MOSFET Industrial module for 1200V and 1700V for several applications such as auxiliary supply, elevator, UPS, PV, CT, MRI etc has been released. Mitsubishi Electric's proven 2nd gen planar SiC MOSFET with 2nd gen SiC Schottky barrier diode (SBD) in parallel has been employed to the module. The module is equipped with Real Time Control (RTC) to provide short-circuit protection. The line-up for 1200V has been expanded from 300A up to 1200A widely for several application.

Join our digital round table presentations:

Mitsubishi Electric's highlights of Si and SiC power modules in a wide range of applications for a greener tomorrow.

Tue, 07.07.2020, 11:00 am

- 3.3kV and 6.5kV; high power modules with SiC technology
- 7th gen industrial IGBT modules: delivering excellent performance and high reliability
- SLIMDIP-W, a fully integrated motor driver for high switching frequencies
- SiC technology – when the future becomes a reality

Wed, 08.07.2020, 11:00 am

- Power modules for high power and high voltage applications. Continuously striving for perfection
- Industrial LV100, the next generation standard for high power
- DIPIPM product family; green power devices for white goods
- SiC discrete power devices as a flexible and efficient solution for modern applications technology, overview of portfolio

Mitsubishi Electric Europe B.V. (European Headquarters) – Semiconductor European Business Group
Mitsubishi-Electric-Platz 1 / D-40882 Ratingen / Phone +49(0)2102/4860
Fax +49(0)2102/4864140 / E-Mail semis.info@meg.mee.com / www.mitsubishichips.eu

eco Changes for a greener tomorrow

A Lifetime in Power Electronics

My interest in electronics started with the my brother's electric train set – when I was a five years old! That was in the middle of the last century. After becoming an engineer, I spent a quarter of a century in electronic design and applications. During that time I signed on to serve and support PCIM Europe as an advisory board member. I had a great time, starting in the 80s, working with Gerd and Christine Zieroth, the owners and organizers of the Conference and Show, including the PCIM Europe magazine.

My first contact with PCIM Europe was in the very early days in Munich at the Hilton Hotel. The conference was with simultaneous translation into the local languages of attendees. The exhibitors were on a few dozen table tops in the car park of the hotel. Shortly after that PCIM Europe stopped moving around; Nuremberg became the permanent place for PCIM Europe, and that has continued for more than three decades. Since these early days the conference language has been English. The few table tops have expanded to fill four auditoriums.

Power Electronics has become increasingly important, and an emphasis has emerged on improving efficiency. MOSFETs largely replaced bipolar transistors, and then IGBTs were a key innovation in the early 80s. Module packaging development evolved to better serve system requirements. Great improvements have been realized in system efficiency.

During this time I worked for RCA - that became GE, then Harris Semiconductor. We introduced the IGBT into Europe. RCA had called the new device a COMFET, which was in many ways a very apt name, but a joint Committee (JEDEC) compromised on "IGBT". The first volume design that I assisted in (also a first for the world) was a 10 amp device in a variable speed motor drive for a household kitchen appliance at Braun. That technology was based on silicon and is very much still in use.

Now, wide band gap devices show more potential to reduce losses. We have gallium-nitrate (GaN) covering the voltage range up to about 1000 volts and silicon-carbide covering a range from 1000 volts up to several kilo volts. The emphasis in Power Electronics is moving on from silicon - a sea-change is underway.

But PCIM Europe remains as the place for engineers to come together to discuss these technologies, and the progress in system implementation. PCIM Europe, started by Myron Miller in 1979, gave power electronics an identity. Before PCIM, the main interest of the semiconductor industry was focused on the functionality of IC designs.

We all have to work for a better World for our children. Modern electronics helps pave the way in this. The challenges in life are always unknown. The corona virus has taught the world to minimize physical contact, so large events have been cancelled, including PCIM Europe.

For the first time after many decades we will not meet personally in Nuremberg for the Conference and Show. The plan by the current PCIM Europe organizer is a virtual conference and show in July.

I will have my podium discussion, that was planned for May, now virtually in July. Stay tuned to attend the session about wide-band-gap devices – it will be on

Wednesday, the 8th of July

at 12:00 -12:45 for SiC and
at 12:45 -13:30 for GaN.

I am looking forward to "getting together" with you – yes the format is a new challenge, but technology change is an eternal subject.

Continuing through Corona-times, my magazine will present information, always on time, in print and digitally. Bodo's magazine is delivered by postal service to all places in the world. It is the only magazine that spreads technical information on power electronics globally on a monthly basis. You will find all of our content optimized for mobile devices on www.bodospower.com.

Best regards   Bodo

Cutting-edge solutions for industrial and automotive applications – powered by ROHM Semiconductor

ROHM Semiconductor Europe was looking forward to welcoming you at its booth at PCIM Europe. Even though we won´t be able to meet up personally, we would like to present our cutting-edge solutions for industrial and automotive applications to you.
Our virtual booth provides you with the highlights:

- **Next Generation SiC MOSFETs:** ROHM is shaping the power solutions of the future. Our advanced SiC technology boosts the performance of power systems.
- **GaN HEMT:** GaN devices for the next generation of power devices are in development – extending the offer of high-performance solutions.
- **Gate Drivers for SiC MOSFETs:** The new series of Isolated Gate Driver ICs for power MOSFETs offers new solutions to increase flexibility while improving the design of industrial and automotive power systems.
- **New Super Junction MOSFET Line-up:** ROHM's R6xxxKNx & R6xxxENx series consist of 650V and 600V high-speed switching Super Junction MOSFET products. Both series achieve a higher efficiency via high-speed switching.
- **Automotive IGBT:** ROHM's RGS series consists of an automotive graded switching IGBT with high robustness against short circuit failure.
- **600V IGBT Intelligent Power Module (IPM):** ROHM's BM63xxxS series is an Intelligent Power Module composed of gate drivers, bootstrap diodes, IGBTs, and freewheeling diodes.

Register for our exclusive webinars via our virtual booth:

Tuesday, 7th July, 2pm CEST
ROHM IGBTs – The best fit for HV heaters and e-compressors

Felipe Filsecker, Application Engineer for Power Devices at ROHM Semiconductor Europe, speaks about ROHM's solutions for electric vehicle air-conditioning systems. The webinar targets OEMs that are now thinking of expanding their portfolio to new products, such as high-voltage heaters and e-compressors.

Wednesday, 8th July, 2pm CEST
Gate driving of SIC power devices and ROHM solution

Vikneswaran Thayumanasamy, Application Engineer for Gate Drivers at ROHM Semiconductor Europe, explains SiC power device gate driving challenges and the corresponding solutions ROHM provides.

Start your virtual ROHM tour!

Bodo's Podium

pcim EUROPE ...digital days

12:00 — 12:45
8 July '20

SiC-Devices - The Game Changers

Language: ENG

30 mins. Presentation
+ 15 mins. Live Q&A Session

Efficiency is the most important game changer in systems. Wide Band Gap power semiconductors have paved the way. 16 experts from leading Industry will be part of the presentations and discussions about usage of Wide Band Gap power Semiconductors. 8 experts will present About SiC for the first session and another 8 experts will do the GaN. Efficiency is what counts first in the game.

Invited speakers:

Guy Moxey, Wolfspeed

Anup Bhalla, UnitedSiC

Hugo Guzmán, Littelfuse

Eugen Stumpf, Mitsubishi Electric

Aly Mashaly, ROHM

Andrei Mihaila, ABB

Peter Friedrichs, Infineon

Jan Huijink, WeEn

Subject to changes without notice

12:45 — 13:30
8 July '20

GaN-Devices - The Game Changers

Language: ENG

30 mins. Presentation
+ 15 mins. Live Q&A Session

Efficiency is the most important game changer in systems. Wide Band Gap power semiconductors have paved the way. 16 experts from leading Industry will be part of the presentations and discussions about usage of Wide Band Gap power Semiconductors. 8 experts will present About SiC for the first session and another 8 experts will do the GaN. Efficiency is what counts first in the game.

Invited speakers:

Alex Lidow, EPC

Philip Zuk, Transphorm

Tim McDonald, Infineon

Stephen Oliver, Navitas

Balu Balakrishnan, Power Integrations

Jim Witham, GaN Systems

Eric Moreau, Exagan

Ran Soffer, VisIC

Subject to changes without notice


R6
C18
U2
LFPAK56
LFPAK56
Q2
Q3
Vout

PCIM Asia 2020 Postponed to November

The organisers of PCIM Asia have confirmed that the 2020 edition of the fair will now take place from 16 – 18 November due in part to disruptions to international travel resulting from the COVID-19 outbreak. Scheduled to take place in early July in Shanghai, the exhibition and conference for power electronics, intelligent motion, renewable energy and energy management will now be held four months later, remaining at the Shanghai World Expo Exhibition and Convention Center.

Mr Louis Leung, Deputy General Manager of Guangzhou Guangya Messe Frankfurt Co Ltd commented on the decision: “We have been working tirelessly over the last few months to try to keep the original July date, but after consulting with our stakeholders, we believe it is best to delay the fair until later in the year to minimise the risk, while the autumn timing will help to facilitate the industry’s recovery. Especially given the worldwide profile of the exhibitors and conference speakers, postponing the fair until November gives us more confidence that we can host a well-rounded, international event at this time. These extra few months will ensure that more of our overseas stakeholders can travel to Shanghai at this time. Furthermore, given PCIM Europe 2020 will now take place digitally from 7 – 8 July, we feel it’s important to provide a meeting place this year to further assist with the industry’s recovery.”

PCIM Asia is a specialised event for power electronics, intelligent motion, renewable energy and energy management. In 2019, the fair hosted 81 exhibitors and 6,358 visitors from around the world, while 46 papers were presented to 407 attendees at the concurrent PCIM Asia Conference. Mr Leung continued: “Earlier in the year both the exhibitor and visitor registrations for the fair were tracking around 15-20% ahead of last year, while we also expected the conference participation to increase, however with the COVID-19 outbreak the situation will now be different. We are still confident however that the November date will be a success as the industry will be looking to bounce back as things return to normal later in the year.”

The **higher standard** of DC/DC power supplies.

Low Ripple
High Stability
High Efficiency
Competitive Pricing

Outputs up to 6kV @ 30W
Lead times stock to 3 weeks
Samples are available now

Dean Technology's new UMR Collection of high voltage power supplies is a **form-fit-function replacement** for industry standard modules at a competitive cost. UMR performance meets and often exceeds similar offerings, making them the **best value available**.

The first UMR Collection includes three full product series in two package sizes, as biasing or capacitor charging variations.

Contact DTI today to discuss your high voltage design.

DEAN TECHNOLOGY

+1.972.248.7691 II www.deantechnology.com

Modular Multi-level Converter Technology for Medium-Voltage Applications

Development of MMC sub-modules for medium-voltage applications requires careful consideration and design trade-offs. Amantys shares some details about decisions made in development of a flexible and scalable architecture with some innovative features.

By Mark Snook, Technical Director, Amantys Power Electronics Ltd.

The modular multi-level converter (MMC) is widely studied and a topic of research in many universities and companies around the world at present. High-voltage dc transmission (HVDC) has used MMC technology for many years, and in the last decade voltage-source converter (VSC) HVDC systems based on IGBTs have been a viable alternative to the more mature line-commutated converter (LCC) HDVC system based on thyristor technology [1].

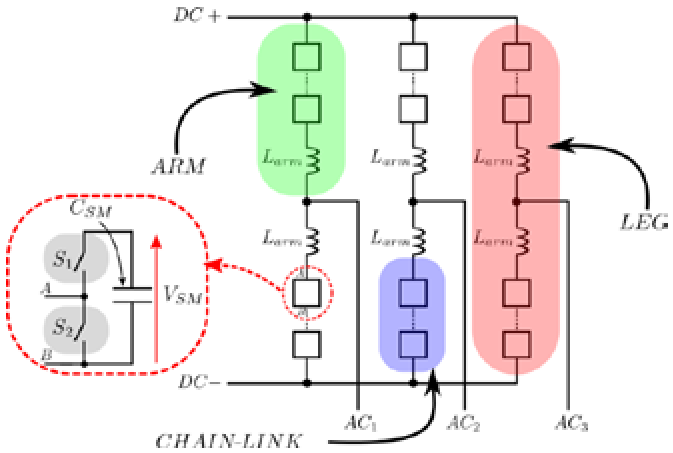

Figure 1: Three phase MMC schematic.

A typical MMC comprises many sub-modules (also known as cells) connected together into chain-links to form, together with arm inductors, the phase arms, see Figure 1. In an HVDC system, there are often many hundreds of sub-modules in a chain-link, which can support hundreds of kilovolts. Each sub-module is usually a half-bridge (as shown in Figure 1) or full-bridge (Figure 4) depending upon the system requirements. The half bridge sub-module is cheaper, containing two switches rather than four, but lacks the ability to block some fault currents. On the other hand, the full bridge sub-module is able to generate negative voltages at the AC terminals (A and B).

Amantys Power Electronics, in conjunction with parent company Maschinenfabrik Reinhausen (MR), has chosen to target MMC converters for medium voltage applications, those in the range of 9-34.5kV, rather than focus on the HVDC market [2]. When the AC voltage is much lower, the number of sub-modules, degree of redundancy, sub-module voltage, bypass strategy, communications infrastructure and modulation scheme need to be carefully assessed.

Amantys chose to use half-bridge IGBTs in the latest module outline, called nHPD2, LinPak, LV100, SEMITRANS 20 or XHP, for the cell switches. This IGBT package, developed primarily for the railway industry, is ideal for modular systems. Devices are available from multiple vendors in voltages from 1.7kV to 6.5kV and are suitable for easy paralleling of multiple modules enabling higher currents. Silicon-carbide MOSFETs are also becoming available in this package, offering higher power density in the future as costs decrease.

MR has developed control strategies for the three-phase wye and delta converter topologies for different applications [3]. The sub-module has been designed with creepage and clearance suitable for up to 4.5kV IGBTs, and initial devices are 3.3kV IGBTs. The sub-module capacitor can be chosen to suit the application with capacitance typically of a few milli-farads. This is crucial as it makes up a significant part of the weight, and cost, of the sub-module. The 3D model of the full bridge sub-module is shown in Figure 2.

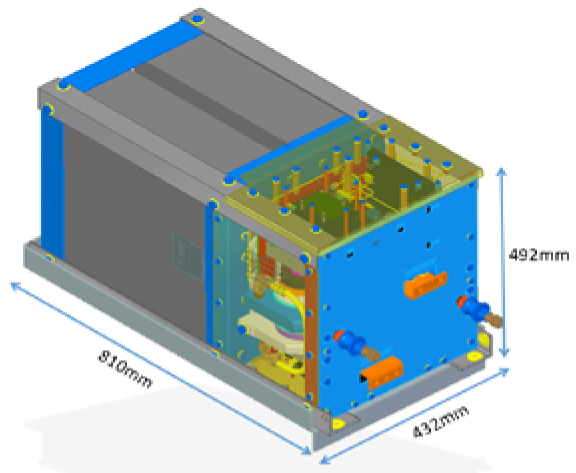

Figure 2: CAD Model of the full bridge sub-module.

Amantys has designed the circuit boards used in the sub-module which are as follows; gate drives, cell power supply, cell controller and bypass controller. The gate drives are standard parts from the Amantys product range. By integrating semiconductor junction-temperature estimation technology [4], converter control based on temperature balancing or condition monitoring can be considered. This technology can also give advanced warning of failure enabling preventative maintenance, a key differentiator for MR.

The cell power supply, Figure 3, is responsible for generating low supply voltages for the gate drives, current sensor and the cell controller. It derives this power from the cell capacitor, starting up at around 250V and delivering full power (20W) when the voltage reaches approximately 400V. The power supply is a critical part for reliability, so the topology is also modular, meaning that there is redundancy in case parts of the circuit fail. There are eight stages (absolute maximum of each stage is 600V) connected in series to achieve the full input voltage which is designed for up to 3kV, but is typically less than 2kV for a cell based on 3.3kV IGBTs. If one stage fails the other stages take up the voltage and it continues to operate normally. If two stages fail, the power supply will continue working, but sends a warning to say there is no further redundancy. Failure of a further stage signals a fault to the chain-link controller, which is continuously monitoring the cell voltage and current and may be able to determine the cause and take appropriate action.

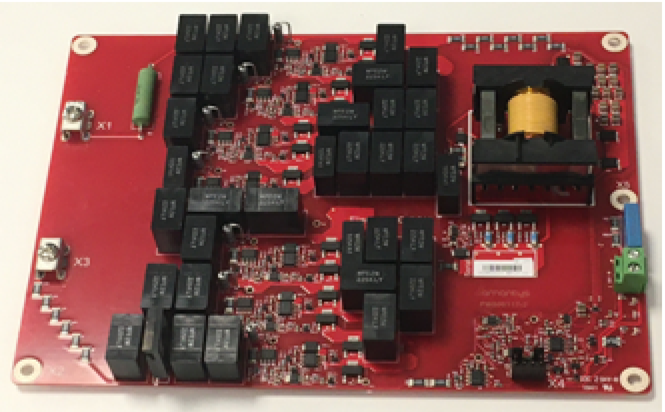

Figure 3: Sub-module Power Supply.

In the event of a sub-module fault, which could be due to the cell power supply, gate drive, IGBT or communications system failure, the cell will need to be bypassed if the converter is to continue operating. A failing or failed cell may be unable to bypass itself, and doing so erroneously in the event of multiple failed communication channels could be catastrophic. In a patent pending alternative method, either of the two nearest neighbours can be sent a message from the chain-link controller to bypass the faulty sub-module. The bypass switch comprises a pair of thyristors connected to allow current flow in either direction as shown in Figure 4. There is no mechanical or pyrotechnic switch, which means the conduction of the bypass can be controlled. This is a useful feature because it means all bypass switches can be tested at start up, and even used as part of the pre-charging circuit. The only requirement is that the state of the bypass switch is maintained even when the switching power from the neighbour is removed. It is also important that during a restart any bypassed cells remain bypassed, unless an engineer has replaced the faulty part and reset the state. The thyristor controller is a unique design that ensures the thyristors are used within their safe operating area, and not exposed to high di/dt which could cause device failure. Bypass controllers for both half-bridge and full-bridge cells have been developed.

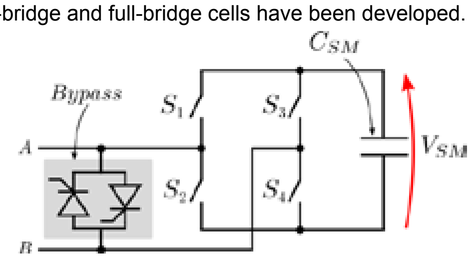

Figure 4: Full-bridge sub-module schematic including the bypass switch.

The cell controller, chain-link controller and valve controllers are all based on commercially available embedded processor modules, which incorporate Xilinx Zynq System-on-Chip (SoC) devices and various communications interfaces, such as USB and Ethernet, which are useful for development. Each SoC has a field programmable gate array (FPGA) and two ARM-based processors. One processor runs embedded Linux and the other a real-time operating system (RTOS). The control and fault handling system is implemented in hardware, being initially developed using MATLAB/Simulink and targeted at the FPGA using a combination of hand written code and automatically generated code using the MATLAB HDL coder. The processors could be used to off-load some lower priority tasks, but they are primarily used for logging, debugging and communication with a converter test bench controller implemented using National Instruments LabView system. Communication between the sub-modules and the chain-link controller is a fibre-optic star arrangement using a custom protocol.

Amantys and MR have dedicated facilities for testing sub-modules in isolation, and as part of a full converter, which clearly contains many more parts than discussed here.

This article introduces some of the technologies Amantys has developed to realise a full-power MMC converter for medium-voltage applications. Whilst the basic structure and building blocks of sub-modules are well known, there are new and interesting challenges in developing reliable electronics for this market. As well as supplying configurable gate drives to the railway traction market, Amantys is now also developing a range of circuits and technologies ready for distribution-grid power electronics. The applications are growing all the time, influenced by the integration of renewable energy generation, battery storage and the fast moving electric-vehicle charging market. If you would like help to develop similar products, we would be happy to discuss them with you.

References

[1] P. L. Francos, S. A. H. Verdugo, S. Guyomarch and J. Loncle, “INELFE — Europe's first integrated onshore HVDC interconnection,” IEEE Power and Energy Society General Meeting, 2012.

[2] A. Bissal, W. Ali and I. Colak, "Effects of phase leg reactor, submodule capacitor, number of submodules and switching frequency on harmonics in modular multilevel converters," in The Journal of Engineering, vol. 2019, no. 17, pp. 4495-4499, 6 2019, doi: 10.1049/joe.2018.8079.

[3] A. Dudin, A. Bissal, I. Colak and W. Ali, "Comparison of Phase Shift and Cell Tolerance Band Nearest Level Modulation for Two Medium Voltage Modular Multilevel Converter Designs," 2018 IEEE Energy Conversion Congress and Exposition (ECCE), Portland, OR, 2018, pp. 3996-4002, doi: 10.1109/ECCE.2018.8557690.

[4] A. Bryant, “Measurement and Datalogging Platform for Junction Temperature Estimation and Converter Diagnostics“, Bodo’s Power Systems, pp. 36-39, May 2019.

Silicon Carbide (SiC) Current Limiting Devices

The Game Changer in Electrical Protection against Energetic and Fast Transients

A known justification for Electrical Protection is to prevent transitory event like lightning, EMI, short-circuit, as well as transitory power-up effects, from disturbing and possibly permanently damage impacted electronic systems.

By Dr Jean-Baptiste Fonder (FAE), Dr Dominique Tournier (CTO), Gonzalo Picun (BDM) and Laurent Martinez (Sales Mgr), CALY Technologies

Most frequent design approach to Electrical Protection is voltage clamping devices (TVS, MOV, GDT) together with current limiting ones (fuses, resistors, polymeric PTC, inductors). Figure 1 shows a typical schematic of fast surge protection for fast surges combining voltage clamping and current limiting devices mentioned above.

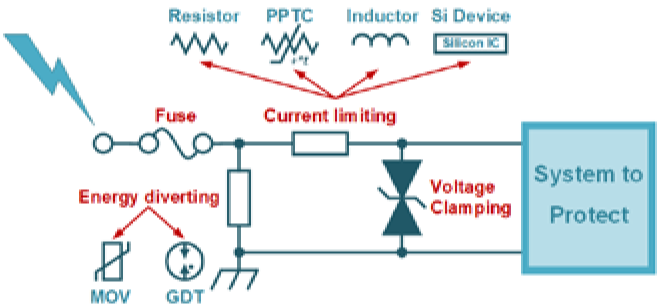

Figure 1: Typical surge protection schematic.

For specific applications, like aircraft lightning protections, tripping speed, reliability and failing mode concerns prevent use of MOV and GDT. This drives aircraft lightning protection designs to use almost exclusively TVS-only structures. To pass Aircraft Lightning Protection Test [1] require sizing up TVS to bulky devices which has cost impact.

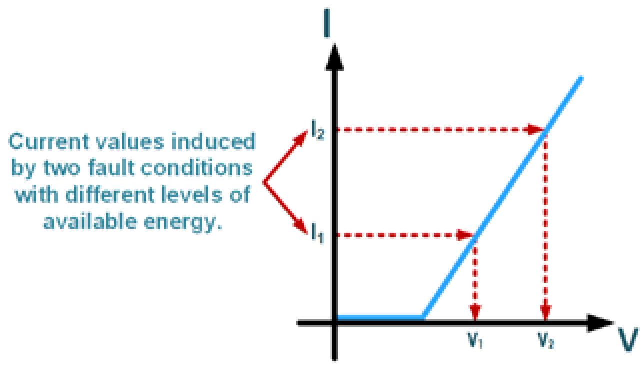

Figure 2: Clamping voltages on a TVS for two current values.

In other cases, standard current limiting devices can be used together with voltage clamping devices.

The following table summarizes drawbacks of standard current limiting devices.

Standard Current Limiting Devices	**Drawbacks**
Resistors	• Same static and dynamic resistance • Bulky • Unsuitable for high ambient temperature • Reduced bandwidth
PPTC	• Long reaction time • Degradation after repeated tripping • Unsuitable for high ambient temperature
Inductors/Chokes	• Behavior dependent on surge rising/falling times • Bulky • Non compatible with high-speed communication
Silicon Devices	• Low voltage capability • High equivalent resistance (high insertion losses) • Only low nominal currents (low power systems) • Disconnection of protected circuit (turn-off)

The next section introduces Silicon Carbide Current Limiting Devices. Such innovative Silicon Carbide Current Limiting Device (SiC CLD) brings advantages summarized in the following table.

Advantages of SiC CLD	**Features**
Fast reaction time	<100nsec
Self-resettable behavior	No external action required
Low nominal resistance	From hundred mΩ
High dynamic resistance	Up to several hundred Ω
No Disconnection	Protected circuit always ON
Small footprint	SMB (DO-214AA)
High transient-voltage capability	Above 1600V
Extreme reliability and robustness	1000's operations without degradation
Wide bandwidth	DC to multi GHz

SiC Current Limiting Device in a Nutshell

A Silicon Carbide Current Limiting component is a two-terminal device. When the CLD voltage drop is greater than its threshold voltage, the device clamps the current going through it to a specific value. This maximum current value is set by its internal topology. As shown on Figure 3, SiC CLDs behave like a current source in DC. When CLD voltage is below saturation voltage V_{Sat}, the CLD behaves like a resistor which value is R_{On}. Above this voltage V_{Sat}, the CLD current saturates at I_{Sat} value. Thus, SiC CLDs can be considered as semiconductor non-linear resistors.

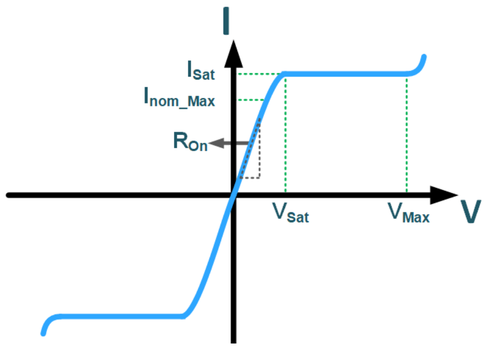

Figure 3: Typical DC behavior of a SiC CLD.

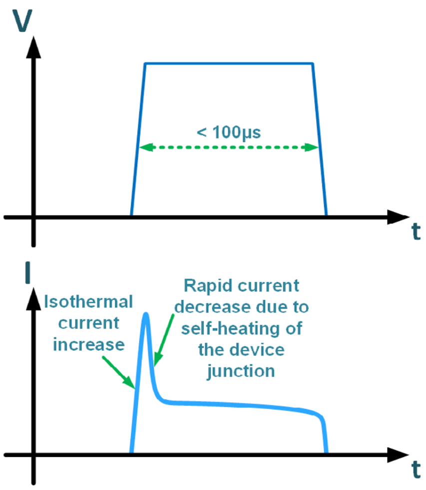

Figure 4: Typical dynamic response of a SiC CLD.

In dynamic behavior, current through CLDs decrease as the junction temperature increases. This is due to self-heating (i.e. junction power dissipation) which increases the equivalent CLD resistance (Figure 4). This resistance increase limits the current inside the device and constrains the self-heating. Therefore, by default the device remains in a safe area of operation. Figure 9 shows the dynamic response of a typical SiC CLD to a short square pulse.

SiC CLDs are described by four principal parameters:

- R_{On}: ON-state resistance
- I_{Sat}: saturation current
- I_{Nom_Max}: Maximum nominal current before saturation
- V_{Max}: maximum use voltage before breakdown.

Parameter	Typical values for available SiC CLDs
R_{On}	from 500mΩ to 10Ω
I_{Sat}	from 1A to 30A
I_{Nom_Max}	From 400mA to 3A
V_{Max}	up to 1.7kV

CLD design took care to comply with 1.2/50µs from IEC 61000-4-2, 40/120µs from DO-160 section 22 making CLD a remarkable fit to it. To ease design with CLD datasheet provides a simple-to-use accurate Safe Operating Area (SOA) graph to assess quick suitability of the CLD device to a specific application. To manage the CLD electrothermal performances a SPICE simulation model is available (Figure 5). More information can be found at application notes of [2].

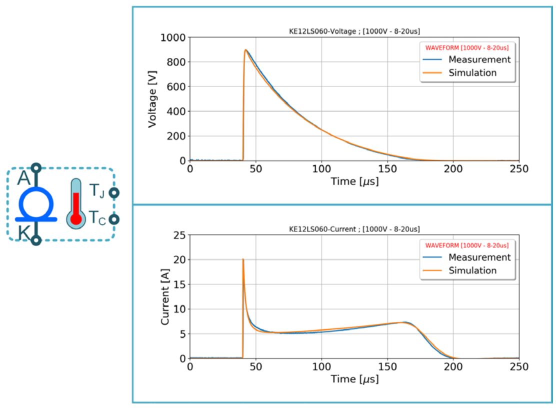

Figure 5: Model of a SiC CLD and measured and simulated dynamic response to a normalized 1000V/1000A, 8-20µs waveform.

Multiple flavors of SiC CLD

SiC CLDs are either unidirectional or bidirectional (see Figure 6). A bidirectional CLD clamps both positive and negative current.

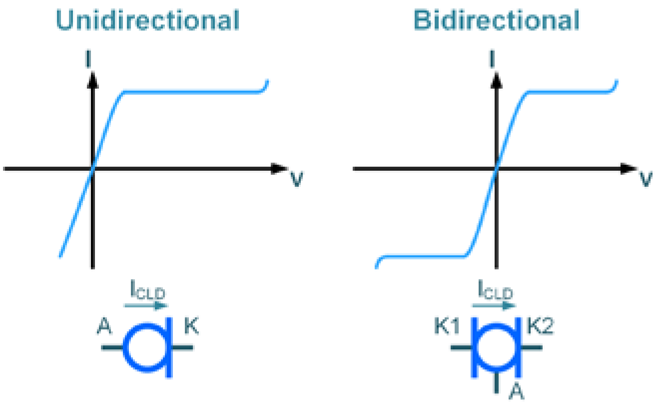

Figure 6: Unidirectional and bidirectional behavior, with corresponding device symbols.

Application benefits of SiC CLDs

SiC CLDs are well suited for many different types of applications such as (Figure 7):

- lightning protection on data or power supply lines,
- reduction of inrush current during start-up of converters,
- protection of sensitive equipment against line transients,
- protection of submarine cable communication repeaters against cable short circuits.

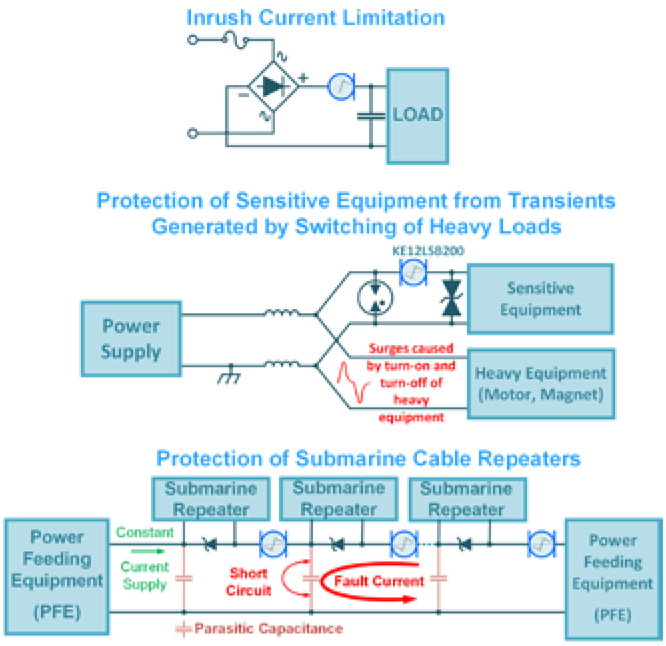

Figure 7: SiC CLD applications in different markets.

SiC CLD is a current-clamping device which is dual to a voltage clamping device such as MOV, TVS or GDT. Combining both in a π (Pi) topology protection circuit ends up with a very compact solution (Figure 8).

In common practice a resistor is implemented in between the GDT and the TVS. Purpose of this resistor is to protect the TVS against current surges. At the same time, this resistor value has to be as low as possible to limit the power dissipation in normal operation. SiC CLDs supplies a new response to deal with this dilemma thanks to its non-linear resistor characteristics. In nominal conditions, SiC CLDs present a low resistance, and this one highly increases when the voltage across the device is high due to a surge condition. This allows using low-power rating TVS, which in turns reduces system footprint and cost. Additionally, for communication lines, SiC CLDs offer lower insertion losses than the needed equivalent resistor, presenting also virtually zero parasitic inductance.

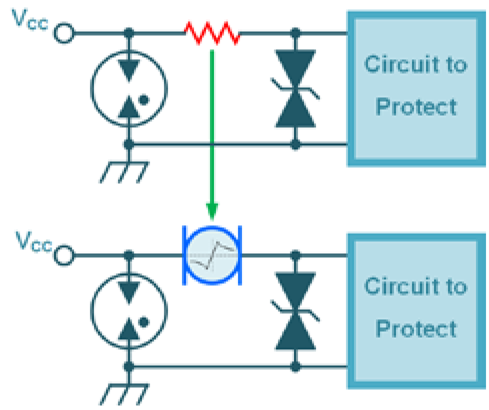

Figure 8: Pi-configuration protection circuit.

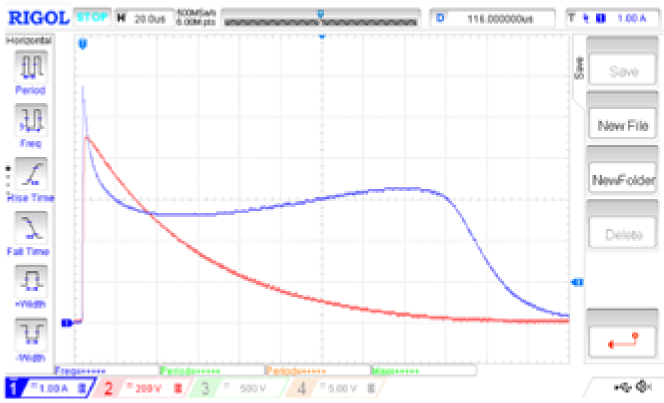

Figure 9: Measured dynamic response (blue) of a SiC CLD (KE12LEB150T20 bidirectional mode) to a normalized 900V/900A, 1.2-50µs waveform (red).

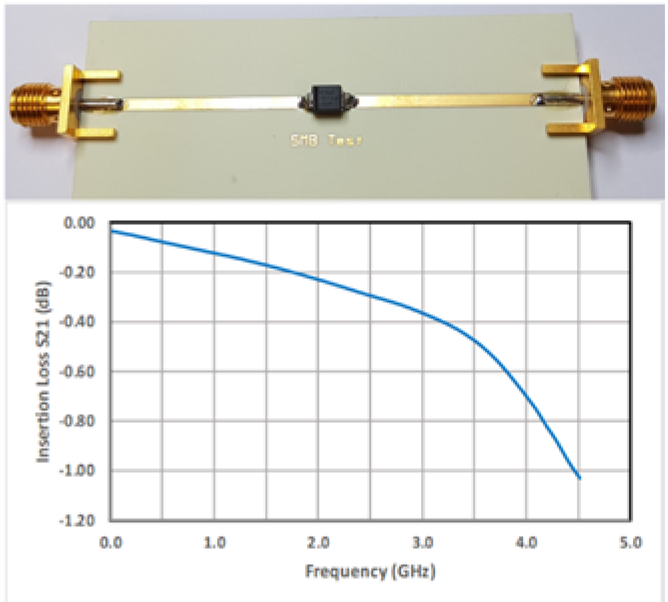

Figure 10: Measured insertion loss S21.

Fast and Safe!

Exhibiting very low parasitic inductance and taking advantage of the SiC material properties, SiC CLD is ideal for ultra-fast current clamping while sustaining high energy. Perfect Fast and safe!

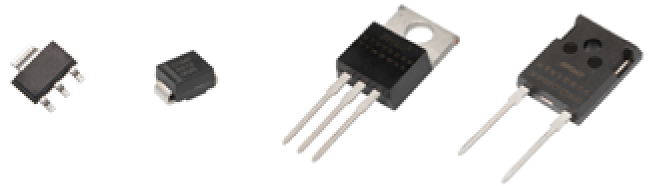

Figure 11: Caly's SiC CLD Packaging options.

Figure 12: Full set of evaluation boards for SiC CLD assessment.

Figure 9 shows Off-The-Shelf SiC CLD (KE12LEB150) real time dynamic response to a normalized 900V/900A 1.2-50µs lightning waveform. At the beginning of the waveform, current through the SiC CLD is clamped almost instantaneously (50-100ns) to I_{Sat} and then it drops quickly per device self-heating.

As mentioned in previous sections, SiC CLD is a perfect fit to high-speed data communication line protection. It brings wide bandwidth performance whilst current clamping is still ensured. Off-The-Shelf SiC CLD insertion losses (S21) up to 4.5GHz is shown on Figure 10.

What does a CLD look like?

Depending upon intended use and targeted market, SiC CLDs are available in diverse forms and packages. Package selection must consider DC power dissipation as much as required AC characteristics. Multiple choices are available to you to fit your need in package size and application requirements.

To facilitate your CLD experimentation various flavors of demo boards are awaiting your call.

References

[1] "Environmental Conditions and Test Procedures for Airborne Equipment", RTCA/DO-160G, RTCA Inc. December 16, 2014

[2] http://www.caly-technologies.com/wp-APPNOTE/AN-00038-17-CLD-Improving Performance of Surge Protection Circuits with Current Limiting Devices.pdf

www.caly-technologies.com

LLC Resonant Converter Topologies for DC-DC Stage of OBC

Selection of dc-dc converter scheme for On-Board Charger (OBC) is based on efficiency, performance and power density targets, for which resonant converters are preferred choice. This article presents popular LLC and LLC derived bidirectional converter topologies described in the literature.

By Milind Dighrasker, V. Thiagarajan, Vishwas Kedlaya, Enstin Labs Pvt Ltd.

Introduction

A typical OBC architecture, as in Figure 1.1, has a bidirectional front-end ac-dc stage followed by an isolated bidirectional dc-dc converter charging the high voltage battery. The designers must meet the performance, efficiency and power density targets for entire range of grid and battery voltages. For the ac-dc stage, Totem-pole PFC is the preferred solution. The charging algorithms are implemented in dc-dc stage. The dc-dc is switched at high frequency and requires a topology with soft switching in both directions, even with use of wide bandgap devices.

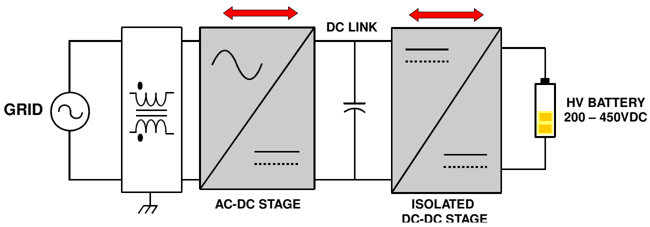

Figure 1.1: Typical OBC power train

The Phase Shifted Full Bridge [1] is a suitable topology but suffers with issues like limited Zero Voltage Switching (ZVS) range, loss of duty to get ZVS, snubbers for secondary devices etc. The Dual Active Bridge also operates with ZVS but has best performance for fixed output. For high power, resonant converters are preferred as they offer soft switching in all devices even at high frequency with low EMI.

Low component count, utilization of transformer leakage inductance for resonance and absence of snubber/clamp circuitries are other added advantages. FETs based rectifier makes converter bidirectional. This article describes LLC and LLC derived topologies for dc-dc and describes OBC design challenges with these converters.

Parameter	Value	Remarks
Battery Charging Mode		
Input voltage	400V	With 40Vpk-pk ripple at double line frequency
Output voltage nominal	330V	
Output voltage range	200V – 450V	
Output power	6.6kW	
Output current max	20A	For 330V and below
Discharging Mode		
Input voltage nominal	330V	
Input voltage range	200V – 450V	
Output voltage	400V	Input to grid tie inverter stage
Output power max	3.3kW	
Common Specifications		
Efficiency target	>98%	For overall efficiency of 96%
Isolation	3 kV	

Table 2.1: Specifications of dc-dc stage of OBC

Resonant DC-DC Converter for Bi-OBC

The specifications for dc-dc stage of a typical 6.6kW OBC is shown in Table 2.1. The design is for the highest power and the current and thermal stress are determined for charging mode. Note that the efficiency requirement is stringent in both modes.

LLC Resonant Converter

An LLC power stage is sown in Figure 2.1. The circuit has two full bridge circuits separated by an isolation transformer. The transformer ratio is set for nominal operating voltage. The resonant tank gain is function of resonant elements (Lm, Lr and Cr), load and switching frequency.

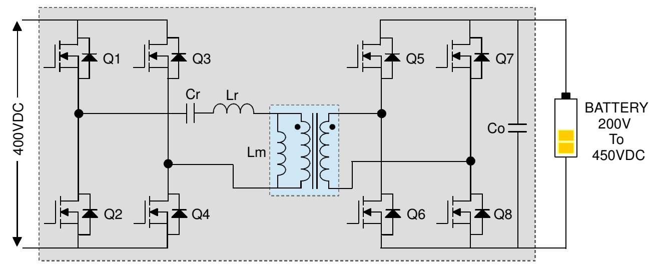

Figure 2.1: LLC converter power stage

LLC converter design procedure is not direct and finalizing the optimum resonant tank component values will need some iterations. The design steps are summarized below

1. Set transformer turns ratio (N) based on nominal operating input and output voltages (400V input and 330V output)
2. Determine the maximum and minimum gain requirements from converter parameters in Table 2.1.
   The maximum gain is evaluated with maximum output voltage and minimum input (which is the minimum voltage considering the line frequency ripple content in PFC output). Similarly, peak of input voltage is to be used for minimum gain calculation
3. Calculate the switching frequency ranges. This will be an iterative process and will need tuning of tank parameters Q (quality factor) and M (ratio of Lm to Lr)
   - Set a resonance frequency value. High frequency is preferred to reduce the size of transformer. Also, output filter capacitance and resonant capacitance value reduce with frequency. However, the transformer and FET turn OFF losses must be monitored while deciding the frequency.
   - Determine the maximum Lm value at resonance which is required to discharge Coss of FETs and aid in ZVS turn ON of primary devices

- Set a value for M to start with. A high value of M indicates high magnetizing inductance and low circulating energy but the gain achievable is limited. For low value of M, high gains can be achieved at narrow frequency ranges. The resultant magnetizing inductance is less and associated circulating current and losses are high. A value between 6 to 10 is good enough to start with [6].
- Select Q based on the maximum gain requirement at full load. If the gain is not enough, then the M value must be reduced. The gain range should be achieved for entire load range or Q range.
- The frequency range for associated gains should be small and the minimum frequency should have low impact on the magnetics size and losses. Reiterate design of Q and M to meet the gain and frequency range criteria

4. With value of M and Q, the values of Lr, Cr and Lm are finalized

The LLC converter has bidirectional power flow capability. But in discharging mode, the magnetizing inductance directly appears across the battery followed by the Lr and Cr which yields an series resonant converter type configuration. The gain curves for a LLC in charging and discharging curve from [4] is shown in Figure 2.2. The discharging curves show no voltage gain from converter and will result in unregulated output. In [2], LLC is switched at resonant frequency in discharging mode and additional boost converter stage after LLC regulates input to PFC stage. The boost stage is bypassed with a relay in battery charging mode. This method however adds to component cost and system size.

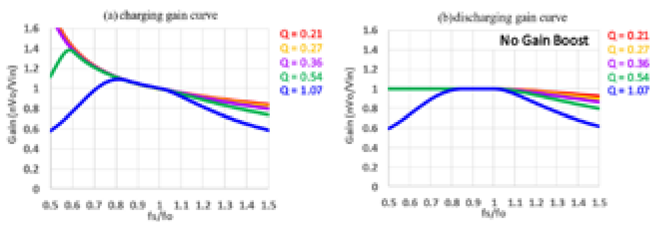

Figure 2.2: LLC charging and discharging mode gain curves

CLLLC Resonant Converter

A bidirectional CLLLC resonant converter with 5 resonant elements is shown in Figure 2.3. The resonant tank is symmetrical, and the converter has approximately similar gain curves for charging and discharging mode.

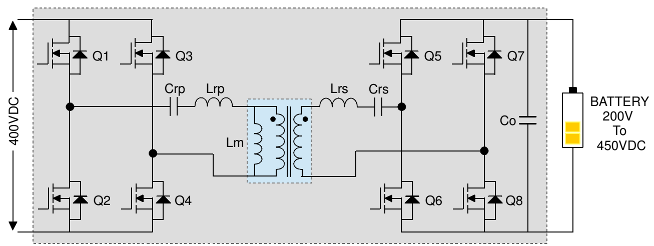

Figure 2.3: CLLLC converter power stage

The design method for CLLLC power stage is similar to the LLC converter. The resonant elements in secondary are all referred to primary and the equivalent circuit yields the transfer function. To simplify design step, reflected Lrs is assumed same as Lrp and a ratio of reflected Crs to Crp is set. The equivalent M and Q values are tuned to meet the gain and frequency range criteria in both modes. When deciding the M value, it is ensured that the gain curves are monotonically decreasing without multiple peaks to enable linear control over the entire operating frequency range.

The CLLC resonant converter is derived from CLLLC wherein the secondary side resonant inductance is eliminated. The Crs is however required to tune the gain curves for discharging mode. If the transformer leakage inductance is also to be made use of, then equivalent configuration becomes CLLLC type. Design example and experimental results with CLLLC for 3.5kW OBC is presented in [3].

CLLLC with Variable DC Link Voltage

The frequency variation for output regulation deviates the converter from resonance, the point for which the converter is optimized. To keep the frequency swing to minimum, the dc bus voltage is varied based on output voltage required. The transformer ratio is adjusted such that at minimum output voltage corresponds to 400V dc bus and then dc link is varied linearly as per set output reference. The design in [4] presents the gain curves as in Figure 2.4 shows significant reduction in frequency range.

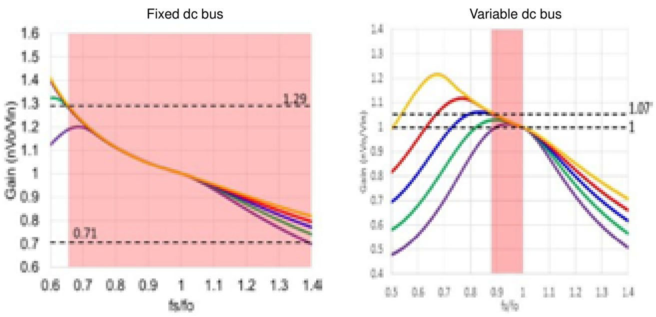

Figure 2.4: Gain curves for fixed dc bus and variable dc bus CLLLC

Conclusion

Resonant converter is undoubtedly the preferred choice for dc-dc conversion for OBC. With modern day wide bandgap devices, designer can easily target the high efficiency at high frequencies. Popular resonant converter configurations based on LLC converter are described in the article. The design methods in literature to suit bidirectional OBC specifications are presented.

Acknowledgement: The authors would like to thank VisIC Technologies, Israel for supporting this work.

References

[1] Y. Kim, C. Oh, W. Sung and B. K. Lee, "Topology and Control Scheme of OBC–LDC Integrated Power Unit for Electric Vehicles," in IEEE Transactions on Power Electronics, vol. 32, no. 3, pp. 1731-1743, March 2017.

[2] H. Li et al., "A 6.6kW SiC bidirectional on-board charger," 2018 IEEE Applied Power Electronics Conference and Exposition (APEC), San Antonio, TX, 2018, pp. 1171-1178.

[3] Z. U. Zahid, Z. M. Dalala, R. Chen, B. Chen and J. Lai, "Design of Bidirectional DC–DC Resonant Converter for Vehicle-to-Grid (V2G) Applications," in IEEE Transactions on Transportation Electrification, vol. 1, no. 3, pp. 232-244, Oct. 2015.

[4] B. Li, F. C. Lee, Q. Li and Z. Liu, "Bi-directional on-board charger architecture and control for achieving ultra-high efficiency with wide battery voltage range," 2017 IEEE Applied Power Electronics Conference and Exposition (APEC), Tampa, FL, 2017, pp. 3688-3694.

[5] Li, Hongbin et al. “A 300-kHz 6.6-kW SiC Bidirectional LLC Onboard Charger.” IEEE Transactions on Industrial Electronics 67 (2020): 1435-1445.

[6] Application note AN2012-09, “Resonant LLC Converter: Operation and Design 250W 33Vin 400Vout Design Example”, Infineon Technologies

Versatile LED Driver Can Be Used with Input Voltages Above or Below the Level of the LED String

The LTM8042 is a μModule® LED driver capable of supporting LEDs with up to 1 A current and a 3000:1 dimming ratio. It operates from input voltages of 3 V to 30 V and a wide frequency range of 250 kHz to 2 MHz, enabling its use in a wide array of applications, such as scanners and automotive and avionic lighting.

By Victor Khasiev, Senior Applications Engineer, Analog Devices

The LTM8042 can be easily configured in three topologies—boost, buck, and buck-boost—to meet a wide variety of specific application requirements. For low input voltages and high string voltages, a boost topology is appropriate, whereas a buck is more suitable for high input voltages and low string voltages. A buck-boost topology is used for a wide range of inputs where voltage can be below or above the LED string. This article covers the process of selecting the suitable topology and its corresponding connections.

Boost LED Driver

The most common topology for an LED driver is a boost application, as might be used for an LED array powered from a 12 V input rail, where $V_{IN} < V_F$. An LTM8042 boost solution is shown in Figure 1 with a block diagram shown in Figure 2. The input voltage is connected to the BSTIN/BKLED– terminal and the LED string cathode is connected to GND. When transistor Q is on, the current builds up in the inductor L. Once Q turns off, the voltage across L changes polarity and the inductor current begins flowing to output filter capacitor C2. LED dimming is implemented in the PWM section, which regulates the duty cycle, and by extension the average LED current (set by resistor RCLR). Capacitor C1 is an input voltage filter.

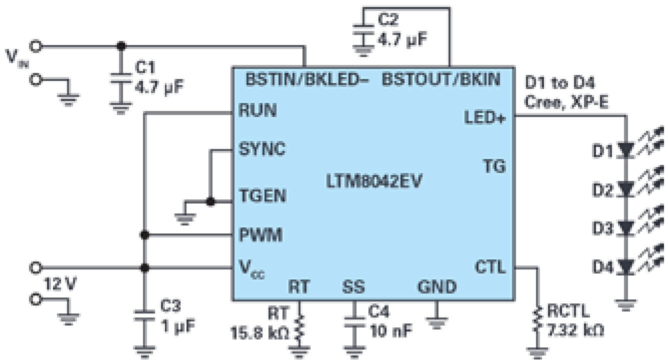

Figure 1: The LTM8042 driving four LEDs where V_{IN} = 5.75 V to 10.25 V and I_{OUT} = 0.5 A.

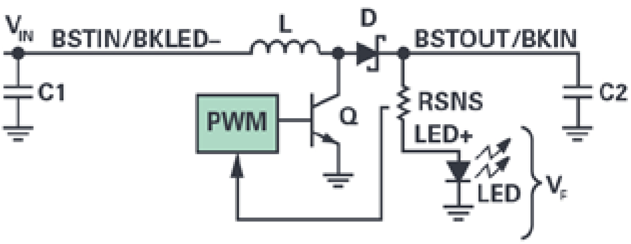

Figure 2: LTM8042 block diagram connections in boost configuration.

Buck LED Driver

A buck topology is used for relatively high input voltages, such as automotive and industrial 24 V rails. Figure 3 shows a block diagram for a configuration for $V_{IN} > V_F$. The input voltage connected to the BSTOUT/BKIN terminal and LED cathode connected to the BSTIN/BKLED– terminal. When transistor Q is on, current flows from the input through the LED string and inductor L to GND. Once Q turns off, the voltage across L changes polarity and diode D becomes forward biased, pulling the LED cathode below the input voltage level, providing the set value of the current in the LED string. C5 creates an output filter for this topology.

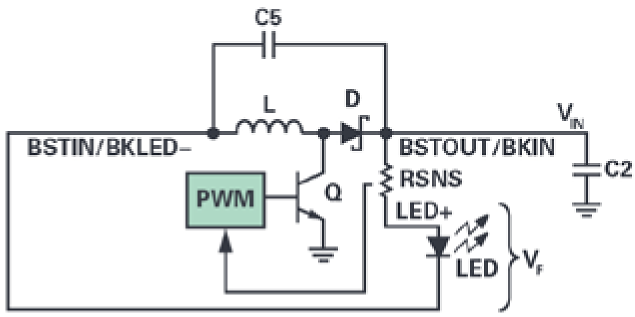

Figure 3: LTM8042 block diagram connections in buck configuration.

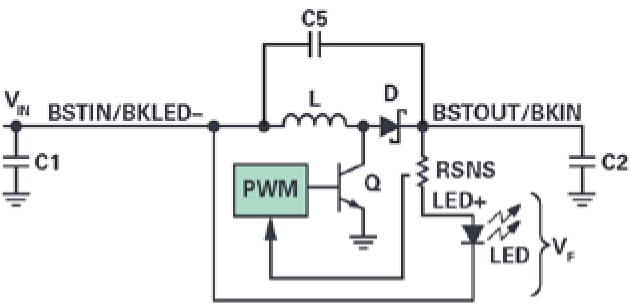

Figure 4: LTM8042 block diagram connections in buck-boost configuration.

Buck-Boost LED Driver

In many commercial, battery, and solar-powered applications, the input voltage varies over a wide range. In these situations, the buck-boost topology shown in Figure 4 is best. The input voltage and LED cathode are connected to the BSTIN/BKLED– terminal. When transistor Q is on, the current builds in inductor L. Once Q turns off, the voltage across L changes polarity, forward biasing diode D while the voltage climbs above the input level. The PWM maintains the set value of current through the LED and C5, and the C2 functions as an output filter. The LED string voltage V_F can be below or above V_{IN}.

Test Results for the Three Topologies

All three topologies were tested using the DC1511 demonstration circuit featuring the LTM8042—using the same LED string, output current, and switching frequency in all cases. To make sure that bias power dissipation is the same for all three settings, the same V_{CC} (shown in Figure 1) was supplied as well. The V_{CC} pin can be tied to V_{IN} in most cases. Figure 5 shows the resulting efficiency curves. All three topologies were also modeled in LTspice® environments and simulation files related to LTM8042 can be found in its data sheet.

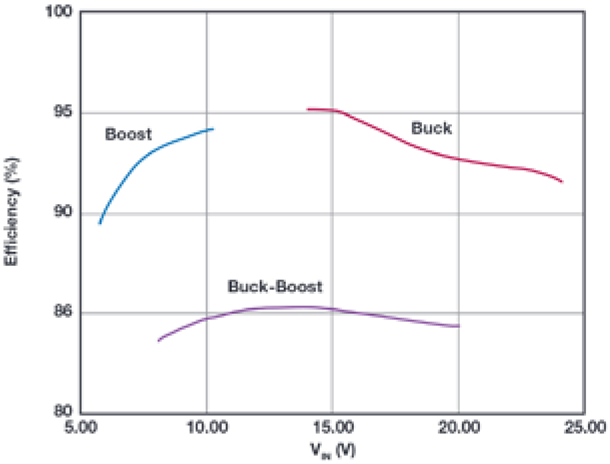

Figure 5: LTM8042 efficiency for boost, buck, and buck-boost configurations.

Conclusion

LTM8042 is a versatile and efficient LED driver capable of operating over a wide input voltage range, while providing up to 1 A LED string current. The LTM8042 is easily applied as a boost, buck, or buck-boost driver to satisfy the needs of a wide variety of applications.

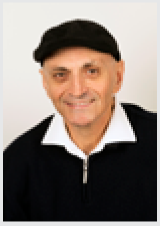

About the Author

Victor Khasiev is a senior applications engineer at Analog Devices with extensive experience in power electronics both in ac-to-dc and dc-to-dc conversion. He holds two patents and has written multiple articles. These articles relate to the use of ADI semiconductors in automotive and industrial applications. They cover step-up, step-down, SEPIC, positive-to-negative, negative-to-negative, flyback, and forward converters, as well as bidirectional backup supplies. His patents concern efficient power factor correction solutions and advanced gate drivers. Victor enjoys supporting ADI customers by answering questions about ADI products, designing and verifying power supply schematics, laying out print circuit boards, troubleshooting, and participating in testing final systems.

www.analog.com

A Guide to the Selection and Proper Operation of Switching Power Transistors – Part 3

With 3 materials and about 8 types of transistors to select from - although not all combinations are available - the choice of the optimum switching transistor is difficult This article is especially also written for the benefit of our young engineers.

By Dr.–Ing. Artur Seibt, Vienna

7. SiC components.

In contrast to GaN SiC is based on > 15 years of practical manufacturing and application experience with diodes and and > 10 years with transistors. SiC jfets and cascodes constitute a solid technology, SiC enhancement mosfets are supported by heavyweights like Infineon, Rohm, Microsemi, to name a few, Also SiC IGBTs and BTs are being developed. SiC easily takes high voltages, even the first ones were specified for 1200 to 1700 V. There is no question that SiC has a very bright future alone in the exponentially growing electric vehicle market where it will replace Si IGBTs in the long run.

7.1 Material properties.

These are the most important advantages over silicon:

1. Wide band gap	3.2 vs. 1.1 eV
2. Far better breakdown field strength	2.4 vs. 0.25 MV/cm
3. Far better thermal conductivity	3.3 ... 4.9 vs. 1.5 W/cmK
4. Far better drift velocity of electrons	1400 vs. 950x10^3 cm^2 /Vs
5. Far higher maximum Tj	250 C

Figure 7.1 visualizes the advantages.

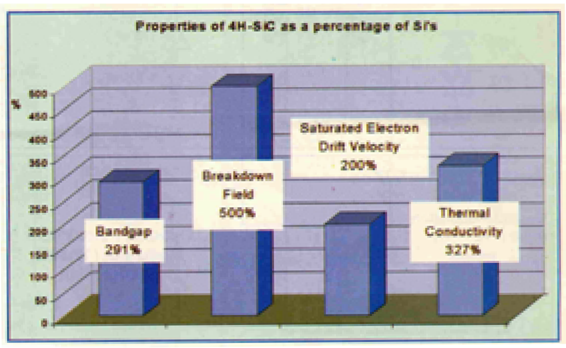

Figure 7.1: Visualizatien of SiC advantages over silicon.

SiC's special properties:

1. High breakdown voltages in the kilovolt range and low leakage currents.
2. Continuous high temperature operation up to appr. 250 C.
3. High switching speed.
4. No increase of losses with temperature.
5. Excellent heat transfer, > 3 times that of silicon.

Serious production problems hampered the introduction of SiC for a long time. Initially, it was only possible to produce small wafers with a high defect rate. The first available SiC products, the diodes, were

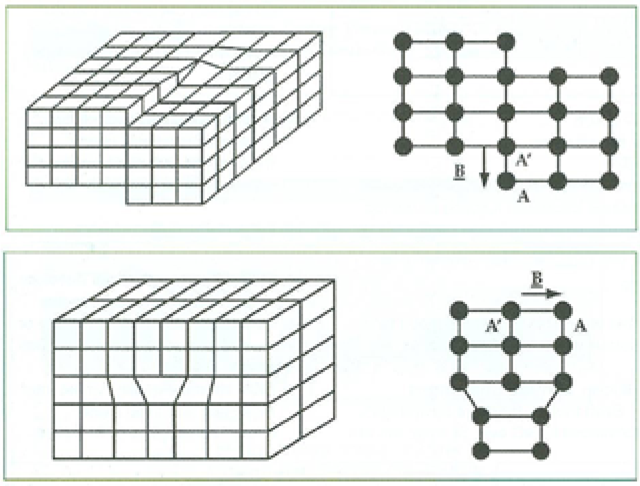

Figure 7.2: Lattice displacements are the cause for the difficulties of producing low-cost SiC semiconductors. A' would be located at A if there were no displacements. There are more lattice defects, all contribute to low yield.

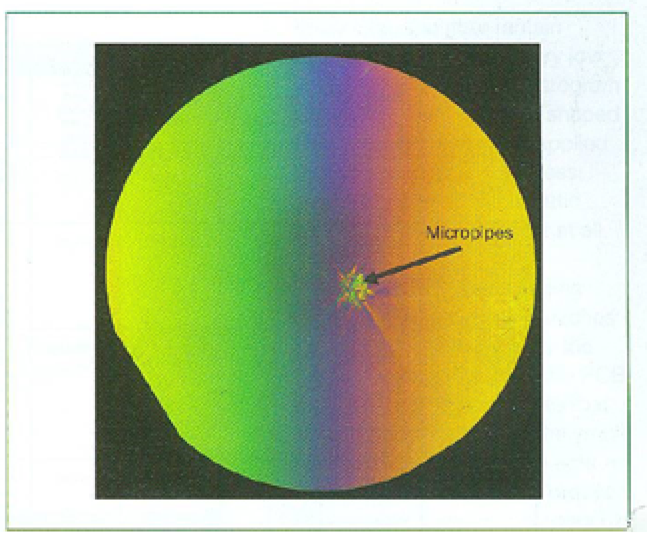

Figure 7.3: The picture shows socalled micropipes which render the material unusable. Those are holes which look like a tornado, they are some micrometers in diameter and go all the way through the whole wafer. For many years they were the main cause of low yield.

very expensive. Still today the wafers are rather small compared to Si wafers, the yield lower, there are only a few wafer manufacturers. A leading firm is Cree where the material is also used for their LEDs.; Cree recently invested heavily expecting big business from the automotive industry, alone from VW, which will certainly materialize. Probably there will be a shortage of SiC within a few years.

Which are the reasons for the limited availability and the high prices? The main reason is the defect rate which caused low yield. Figures 7.2 to 7.5 visualize these problems.

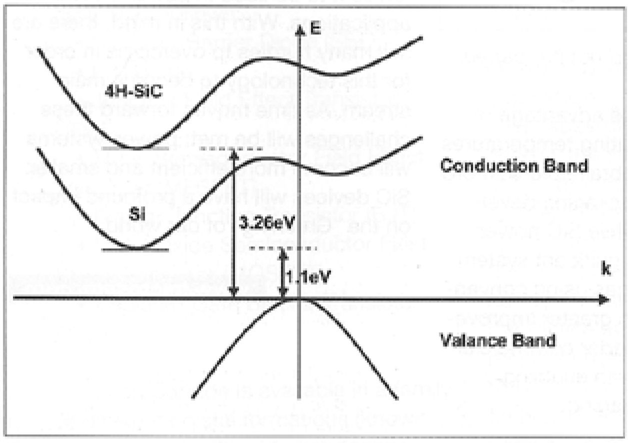

Figure 7.4: The band gaps of Si and SiC. The higher band gap allows high temperature operaton at 250 C and kilovolts. SiC takes 10 times higher fields than Si. Theoretically even operating temperatures of > 500 C were possible.

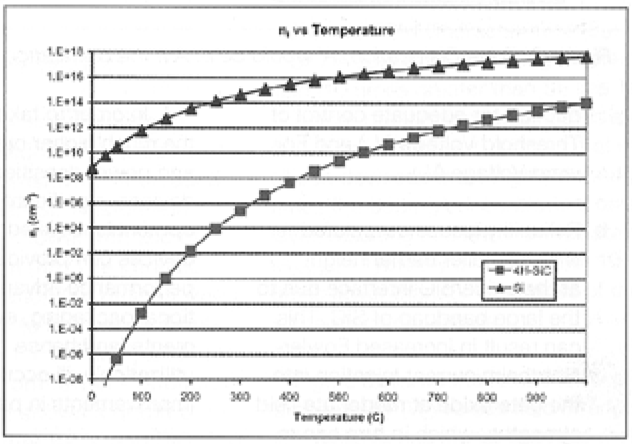

Figure 7.5: Charge carrier concentration of Si and SiC. Apart from the band gap this determines up to which temperatures a semiconductor remains one. This temperature is > 1000 C for SiC. Above the material remains only a resistor.

The higher thermal conductivity means that the thermal resistance between junction and case remains the same although the chips are much smaller. Parts in TO-220 specify 1.5 degrees/W, the same as state-of-the-art Coolmos.

The high permissible field strength allows to reduce the drift zone to 1/10 of Si and to dope it 10 times higher. This reduces Rdson to typically 1/10 of that of Si at the same voltage. Also values of 1/20 to 1/30 are mentioned. Present enhancement mosfets achieve already < 10 mOhms at 1200 V from several firms which is only the beginning. Jfets attain already Rdson's far below 10 mOhms.

The production of SiC parts is more complex, more expensive and requests additional investment, e.g. high temperature chambers, high energy and high temperature (> 500 C) ion implantation equipment. When handling hot ions customary photo masks can not be used because they only take < 200 C¸more durable materials like SiO2 are necessary. It takes more time to manufacture such hard masks. First the material must be deposited, then it has to be defined by photo lithography, then it has to be etched. The next difficulty is the fairly low diffusion coefficient of most atoms into SiC, especially for customary materials like aluminum, phosphorous and nitrogen. Therefore the implantation process has to be repeated several times at different energy levels, up to ten times.

Apart from the high price tag for epitaxial wafers (2 orders of magnitude higher than for Si wafers) the process is complicated and lengthy, and it requires special investments.

- ► All sources unanimously predict that the prices of SiC parts will never reach the prices of Si parts. However, it is wise to be cautious with such comparisons, because SiC chips are much smaller than comparable Si chips.
- ► Comparisons of prices just of parts are misleading. Only complete circuits can be compared. SiC excels in high temperature, high voltage applications and is thus ideal e.g. for the harsh automotive environments. It is clearly superior to GaN.

SiC will replace Si IGBTs because it allows much higher operating frequencies and temperatures as well as savings in inductive and capacitive components. Also it is much more robust than silicon parts, an important argument in automotive applications. Whether the SiC IGBTs being developed make sense when the Rdson's of the jfets and mosfets are so low is questionable. In offline SMPS SiC will probably outperform Si from several hundred watts upwards. GaN is rather a low voltage material, its niche is < 100 V.

With all semiconductors not only the material, but also the crystal structure have great influence on the properties. Of the about 200 various crystal structures those shown in Figure 7.6 only a few are used, for SiC this is 4HC.

Material	Bandgap (E_g) (eV)	Thermal Conductivity (λ) (W/cm°C)	Breakdown Electric Field (E_{br}) (V/cm)	Saturated Electron Drift Velocity (cm/s) (V_{sat})	Additional Information
Silicon (Si)	1.1	1.5	3.1×10^5	1.0×10^7	
Silicon Carbide (3C-SiC)	2.2	3.6	$>1.5 \times 10^6$	2.5×10^7	Superior transport properties, but used less due to smaller bandgap and lack of substrate technology
Silicon Carbide (4H-SiC)	3.26	3.7	3.5×10^6	2.0×10^7	Ideal for power devices. Material well up the learning curve. Can use to develop simple commercial devices. Broad future markets and applications. More isotropic than 6H-SiC
Silicon Carbide (6H-SiC)	3.0	3.7	2.5×10^6	2.0×10^7	The 6H means a hexagonal type lattice with an arrangement of 6 different Si+C layers before the pattern repeats itself. This is the polytype of SiC initially used as substrates for growth of GaN blue LEDs
Gallium Nitride (GaN)	3.2	1.3	3.0×10^6	2.5×10^7	Primarily used in optical devices (blue LEDs); power device type focused on High Electron Mobility Transistors (HEMT). Ideal for RF switching devices (S-Band and up). Cannot be used for IGBTs and MOSFETs. High material cost, high defect density
Diamond	5	20	5×10^6		The perfect power device material. Many decades away from solving basic material problems.

Figure 7.6: Table of the most important substrates for the new materials.

The 7 x higher breakdown field strength recommends SiC also for > 3 KV components in solar and wind generator inverters in addition to electric vehicles, those are the 3 most important growth markets.

7.2 SiC diodes.

Although the yield has been improved SiC wafers are still much smaller than e.g. Si wafers. This is the reason why few chips > 10 A are available. Higher currents are handled by the parallel connection of chips which is possible due to the positive TC.

With Si only socalled "pure" Schottky diodes can only be made up to 100 V. There are 200 V Schottkies the value of which is doubtable. Schottkies also have disadvantages vs. Si Ultrafast diodes, e.g. a markedly higher capacitance and higher leakage currents. The discharge current looks similar to a reverse recovery current. SiC Schottkies have no reverse recovery time, and their losses do not increase with temperature which is perhaps their most important advantage. Their capacitance is 5 x that of GaAs diodes, but the latter never reached their popularity. Due to their positive TC they are sensitive to overloads because the losses rise.

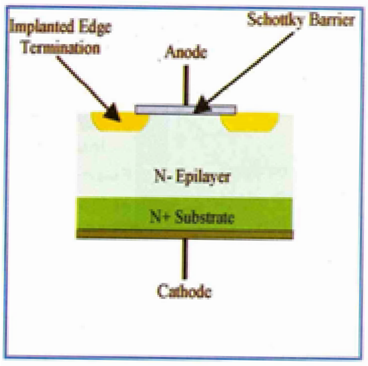

Figure 7.7: Structure of a SiC diode. The diode is constituted by the metal - semiconductor contact, hence it is a Schottky diode with the known advantages. However, the forward voltage is quite high, most diodes are 600 V types with 1.5 V, following the general rule that the forward voltage rises with the blocking voltage.

The main application was sofar in PFC's, manufacturers obviously could not imagine other applications. In fact even the standard 600 V diodes outperform Si ultrafast diodes whereever a transistor switches hard onto a conducting diode, e.g. in the secondaries of flyback converters. (See the article in Bodo's Power Nov. 2009). The 600 V diodes outperform Si ultrafasts even down to output voltages of about 25 V.

Similar to many GaAs diodes a pn diode is integrated in parallel to the SiC diode. The pn diode starts to conduct at high currents resp. a forward voltage of about 4 V and thus protects the "pure" SiC diode.

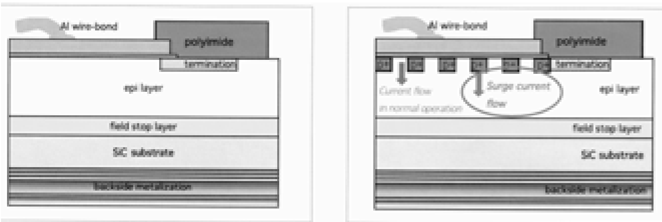

Figure 7.8: "Pure" and 2nd generation SiC diodes with integrated pn diodes.

7.3 SiC power transistors.

Many years of production experience with diodes reduced wafer defects and created a solid base for the introduction of SiC power transistors. The "natural" transistor and first choice is a jfet, firms like Semisouth (defunct)and initially also Infineon and all firms which offer cascodes (e.g. USCI) voted for jfets. Firms like Infineon, Rohm, Microsemi etc. now prefer enhancement mosfets. One company, Transic (Fairchild), made BTs. Also IGBTs are being developed. Designers of power electronics had to become familiar with jfets.The necessity of a negative gate supply which has to be available before turn-on limits the usefulness of jfets to such power supplies which feature an auxiliary supply and to cascodes.

In power applications SiC is in principle superior to GaN, SiC transistors have been on the market for many years. In high voltage applications SiC beats GaN hands down: while even the first SiC transistors, more than 10 years ago, were specified for 1200 to 1700 V GaN has been stuck at 650 V; only recently one firm ventured to specify 1200 V. The problem is that this can not be tested because the tests are destructive. Another advantage of SiC is the vertical structure while most GaN tranaistors are fabricated on Si substrates so they are lateral. While GaN tranistors are destroyed by a single overvoltage pulse, SiC mosfets are expected to achieve an avalanche rating. Jfet cascodes can be made avalanche-proof, see below.

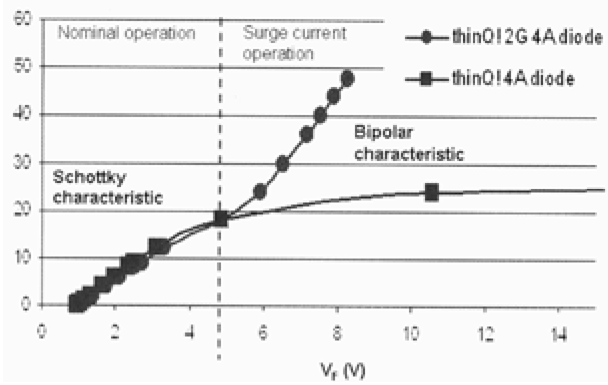

Figure 7.9: The characteristics of "pure" and 2nd generation SiC diodes show the takeover of the current by the parallel pn diode, protecting the former.
Without the protection the SiC diode would be destroyed by excessive power dissipation.

7.3.1 SiC jfets.

Although the natural type of transistor with SiC and GaN is the jfet it is difficult to use in power supplies because jfets are depletion types, i.e. fully on with 0 V of gate voltage. At turn-on of a supply it presents a short circuit, hence it is only usable in a cascode where a standard Si mosfet ensures high impedance at turn-on. Combined with the other advantages of cascodes like very fast switching and low input capacitance, these cascodes as made by USCI are excellent choices. It is hard to understand why major firms insist on mosfets.

Advantages of jfets:

1. Of all transistor types jfets are the easiest to produce.
2. Lower Rdson's than mosfets.
3. Lower switching losses due to lower capacitances. Tests of single jfets, i.e. not cascodes, did not show faster switching than Si Coolmos.
4. Lower losses due to lower Rdson than Si or mosfets.
5. Best suited for high voltages, from 1200 V upward.
6. Continuous operation at 250 C, provided the case can take this temperature.
7. No increase of losses with temperature.
8. Due to the high thermal conductance the thermal resistance remains low inspite of smaller chips.
9. No parasitic elements, no SBD, no dv/dt limits, no antiparallel diode.

Disadvantages:

1. Jfets are by nature depletion type, i.e. with 0 V on the gate they are fully on. In order to turn them off a negative voltage has to be applied to the gate which exceeds the pinch-off voltage. Consequently the gate drive is between 0 V and the pinch-off voltage which does not fit with standard ic's and their positive power supplies.Jfets can not be used as switching transistors in power supplies because that would require a negative supply which is available before turn-on. Hence jfets can only be used in cascodes.
2. No avalanche rating, in cascodes possible, see below.
3. The gate is isolated from the channel by a pn diode. If the gate

voltage exceeds 0.6 V, the diode will conduct so that the gate input becomes low impedance. With mosfets the gate is isolated with glass, SiO2 and high impedance with any positive or negative voltages below the maximum specified voltages.

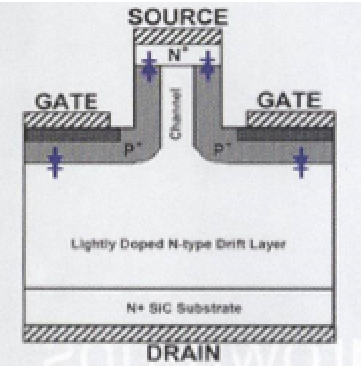

Figure 7.10: Structure of a SiC trench jfet. Like with any jfet there are diodes between gate and channel and drain and channel. At 0 V gate voltage the channel is already fully conducting. If the gate voltage is increased to about 0.6 V, the diode will be on, and the gate input becomes low-impedance. If the drain current is increased the drain potential will rise. If it rises above the threshold voltage, e.g. 6 V, the channel starts to pinch off so that the current can not rise further.

The best switches are the SiC cascodes with jfets which are available from several firms, they are superior to the mosfets supported by major manufacturers and free from their problems. They do not ask for high drive voltages close to the maximum gate voltages nor do they need a negative gate voltage. < 10 mOhms at 1200 V and < 7 mOhms at 650 V are state-of-the-art. As the lower transistor in the cascode is a standard Si mosfet, 12 V drive is sufficient. This Si lv mosfet contributes < 1 mOhm to the total Rdson of the cascode

Regarding the avalanche properties there is a significant difference between SiC and GaN: The manufacturer USCI specifies an avalanche rating for its SiC cascodes. USCI makes use of an old protection circuit known from bipolars e.g. in combustion engine spark generators. If the maximum drain voltage is exceeded a normal - non-destructive - diode breakdown will occur in the jfet. If a sufficiently high resistance is inserted in the gate of the lower mosfet, this leakage current will develop a voltage across the resistance which will eventually turn the cascode on, so it will damp the overload. The drain voltage remains almost constant, see Figure 7.11.

► Obviously this method is not applicble to GaN transistors because they are destroyed in breakdown.

While GaN transistors were limited to 100 to 200 V for a long time, 600 V types came later, 1200 V types were announced for years, but did not come forward. even the first SiC transistors were specified for 1200 to 1700 V. They will replace many Si IGBTs alone because they allow much higher operating frequencies. Higher power cars use already 800 V supplies. The question is rather whether the semiconductor industry will b able to deliver high volumes of SiC. The manufacturers of Si IGBTs came up with the 7th generation. The intrinsic advantage of IGBTs: their saturation voltage rises very little

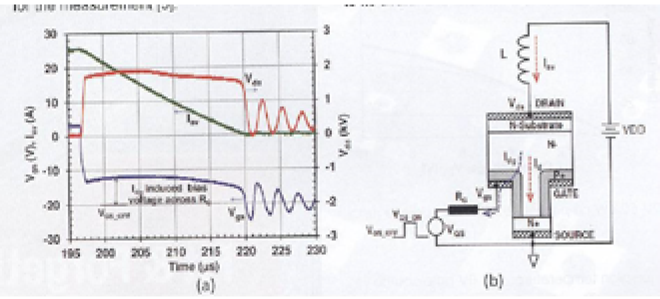

Figure 7.11: Avalanche behaviour of USCI cascodes. The cascode is turned on by the leakage current of the jfet, damping the overload.

with the current. Fets are resistors so the losses rise with the square of the current. SiC transistors can compete due to their extremely low Rdson's even at 1200 V. Si IGBT's profit from the fact that there are no Si wafer supply problems to be expected.

Information relating to the internal structure of their jfets was only available from Semisouth (now defunct) so it is given here as an example.

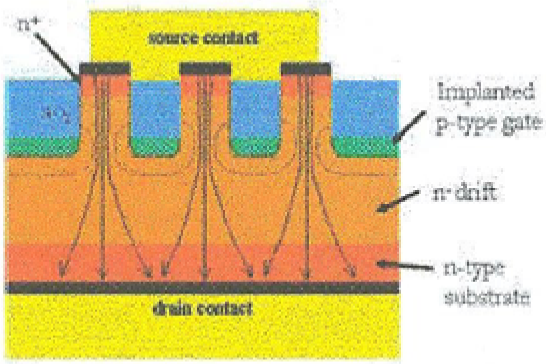

Figure 7.12: Structure of Semisouth jfets. It is purely vertical, the current flows from the bottom contact to the drain and through the drift zone to the source. The gate is covered with SiO2 in the valleys.

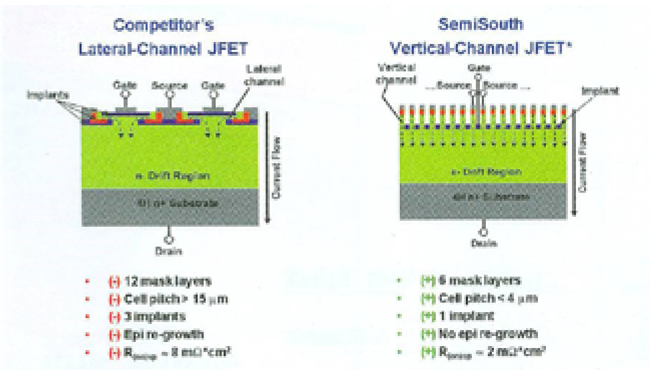

Figure 7.13: Comparison of Semisouth's jfet with that of a competitor.

Other firms showed only samples and some data on exhibitions but neither disclosed more information nor were samples or documentation available. Most firms only offer cascodes, single jfets are presently only available from USCI. The author had an intense correspondence with Semisouth and Cree. Samples in TO-247 were tested in a 200 W offline supply vs. Coolmos. At an operating frequency of 125 KHz only a modest improvement of the efficiency was noted. In cascode the improvement was marked, but as well with the SiC and the Si Coolmos transistors.

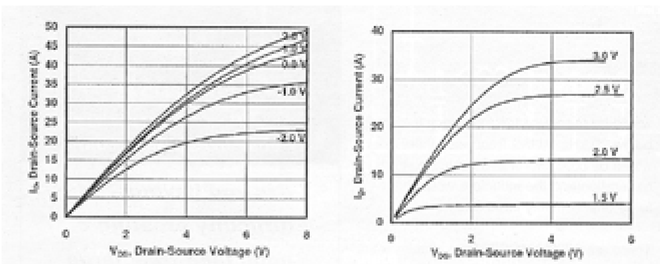

Figure 7.14: Characteristics of Semisouth jfets (left) and their socalled "enhancement" jfet, a great flop and possibly the reason for folding up.

An important application of jfets, either single or in cascodes, is in bridge circuits because they allow current flow in both directions.

In contrast to the use of mosfets there are no parasitic elements involved. The inverse diode of the lower lv Si mosfet is very fast.

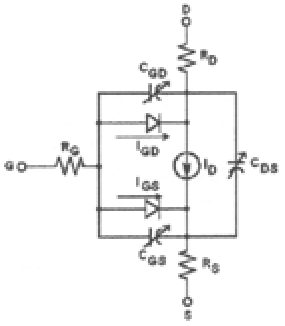

Figure 7.15: Elements of a SiC jfet. The arrows indicate that all capacitances shown are voltage-dependent $V^{-1/2}$. Like all fets these have a TC = 0 point where the increase of the on-resistance with temperature matches the negative gate voltage characteristic of -2.3 mV/degree.

7.3.2 SiC mosfets.

Heavyweights like Infineon, Cree (Wolfspeed), Rohm, Microsemi voted for enhancement mosfets. The reasons are unclear, because the jfet cascodes, as mentioned, are clearly superior in every respect. Patent problems are unlikely, because the cascode is known since about 80 years.

Ideally they should be usable in place of Si mosfets, but this goal was not achieved: the drive levels are - 5 to + 22 V, and these voltages are close to the maximum permissible voltages which are typically - 6 /+ 23 V. It is good engineering practice to stay away from the limits. The supporters of enhancement transistors, in the early days, when asked by the author if their transistors did not also need - 5 V, first denied this, but later had to concede that this was indeed necessary. With standard mosfets and Coolmos 12V is enough and comfortably far below the +- 20 V maxima.

Looking at the specs quite a few peculiarities come up. SiC takes easily Tj >=250 C, but some types are only specified for a maximum Tj = 125 C while all Si transistors in the same case types take 150, some even 175 C. SiC should take >= 250 C continuously.

A maximum gate voltage of +23 ...+ 25 V is specified while a gate drive of 22 V is required. Also - 5 V is required while the maximum is - 6 V. This means that 0 V are obviously not adequate for keeping the parts off. Before turn-on no negative gate supply is available. How critical this is follows from the manufacturer's warning that the gate voltage must not overshoot. This rises another question: why - 6 V/ + 25 V? Allegedly it is the same gate oxide which is used in Si parts. Then why is the maximum voltage here unsymmetrical? This question could not be answered by the firms. That the max. - 6 V are no kidding is proven by tests in cascode: all samples were destroyed. As no standard MOS driver ic can deliver - 5 to + 22 V, one firm specified an expensive single-source driver with 0.6 Ohms and 14 A peak current. Probably these high drive levels are specified in order to squeeze the Rdson as mosfets are inferior to jfets.

With SiC mosfets a leakage current between gate and channel is not possible, hence the protection scheme used with the cascodes is not applicable. Due to the structure similar to Si mosfets probably also a parasitic npn exists with the danger of SBD. The author could not get any information about this. The manufacturers of Si mosfets proclaimed for years that their products were free from SDB until independent experts proved the contrary. One SiC manufacturer gave a "single pulse rating" , two more promised such ratings. However, such a spec is useless in practice, if a part fails it can never be proven that the single pulse rating was exceeded.

So the mosfets do not provide any advantage over the jfet cascodes, and it remains the secret of the firms proclaiming them why. The author does not use them.

7.3.3 SiC BTs.

Transic (Fairchild) announed 2011 a SiC BT. This created some astonishment because BTs are considered obsolete. In fact all major firms discontinued their production. However, this might be a product with some future, because BTs do have some advantages: the small and inexpensive chips, the simple process. This product was similar to the obsolete high voltage Si BTs. In contrast to those this SiC BT has a markedly higher beta. Another BT advantage is the low saturation voltage which increases only moderately with the current and its low TC. 2013 technical data were released, but whether this product came ever on the market is not known.

"Lowest losses on the market, lowest Rdson < 2.2 mOhms x cm^2 at 25 C."

Further specs were: 1200 V, 40 A, Tjmax = 175 C, Vce at 40 A: 1.6 V (vs. 3 V with IGBTs), switching times 20 ns, not dependent on temperature, no "current tail", no SDB, short-circuit proof, low leakage, positive TC, can be connected in parallel, Rsat, 125 C = 40 mOhms.

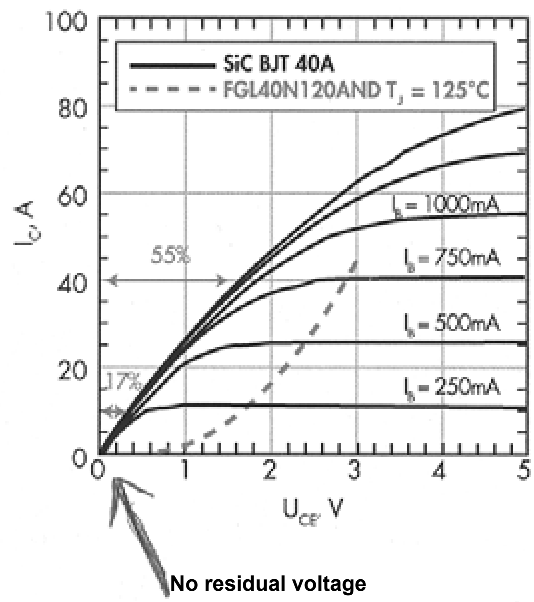

Figure 7.16: Characteristics of the Fairchild SiC BT at 150 C. There is hardly a saturation voltage visible, in contrast to an IGBT. The difference at 40 A is impressive.

7.4 SiC drive circuits.

SiC cascodes use a standard Si mosfet so their drive is identical to any Si mosfet: + 12 V.

Of all power transistors SiC mosfets are the hardest to drive, also their capacitances are quite high and comparable to Si mosfets. The - 5/+ 22 V needed by most are beyond the output levels of standard control/driver chips and their positive supply voltages.

Before turn-on of a power supply no - 5 V is available unless an auxiliary supply is provided. This is already a serious drawback. The + 22 V drive level also requires an uncommon + 22 V supply. But even if this is available, the designer will need one of the rare and expensive, mostly single-source special driver chips for SiC mosfets. Due to the rather high capacitances these chips must deliver high peak currents. Overcurrenr and desaturation control are as a rule provided. External Schottky clamping diodes are necessary from the gate to the minus and plus supplies.

Decoupling should consist of a MLCC of e.g. 0.1 uF directly at the pins in parallel to a 10 uF MLCC. Note that these capacitors must not be used above ½ of their nominal voltage. Or the designer makes his own driver. Here it can be wise to use a transfomer in conjunction with a standard control ic. If the control ic's output can not deliver enough current it may be necessary to add a high current driver.

8. GaN transistors.

8.1 Claims.

For many years manufacturers of GaN transistors touted statements like these:

- "GaN will wipe out silicon within 2 years."
- "usher in a new era in power electronics."
- "the specific on-resistance of GaN is orders of magnitude smaller than that of silicon or SiC."
- "performance now 5 to 10 times better than the best silicon,... GaN will increase that gap to 1,000 times better."
- "GaN will allow switching frequencies > 100 MHz"
- "90 % savings in volume, weight, cost ... 50 % higher efficiency."

None of these claims could be proven. Never a new technology was introduced with such claims. Managers of these start-ups concede that this language is directed towards their investors which expect huge short-term profits, but do not understand the difference between a software start-up which writes a software program and a new hardware technology which requires investments and can only offer long-term profits.

On the other hand articles appeared like: " The question is: Who really needs GaN or SiC power devices?". The authors, market researchers, trying to sell their reports, lacking technical knowhow, tell a lot of nonsense like "GaN will extend the limits of Coolmos", not understanding that one can not compare a 650 V avalanche-rugged Coolmos wth a 650 V GaN which is destroyed by a single overvoltage pulse, being neither faster nor excelling with a lower Rdson and suffering from at least 5 physical problems like dynamic Rdson.

All major semiconductor firms have GaN research programs, a few actually produce components in volume for selected applications. Earlier introductions of new semiconductors came from the established manufacturers, not start-ups. The situation was summed up by a manager of ON (formerly Motorola) at the 2017 PCIM:

"GaN has the opportunity to become mainstream, but it will take up to ten or more years. Regarding applications travel adapters (small chargers for mobile phones etc.) will be a good starting point for GaN, automotive will follow sometimes ... the majority of the market will still use silicon power mosfets, thanks to their proven reliability and good cost performance ratio."

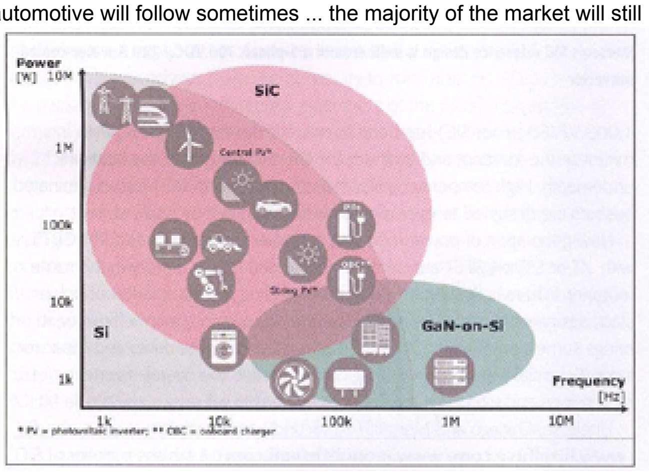

Figure 8.1: Projected application areas for SiC and GaN by Infineon. visualizes that GaN is only applicable to small powers and above 100 KHz. Electric vehicles which requite several ten to hundred KW are out of reach for GaN.

The author goes along with this statement, however, regarding automotive use, SiC will outperform GaN by far. GaN offers lower manufacturing cost, at least for GaN on Si wafers. It may be used in small passenger cars with 400 V systems. The real realm of GaN will be the < 100 V area.

8.2 Strategic considerations.

The introductory claims of GaN start-ups also prove that they lack the knowledge of the end product market. It is not sufficient for a product to be better than another, some basic preconditions must be met before it can be seriously considered by responsible designers: 1. Reliable function. 2. Supply assured for several years with guaranteed quality. Spare parts supply for additional years. 3. At least one second-source of identical quality must exist; its product must be equal in every respect. It is not sufficient if data sheet specs are identical. This is very important because there is no true second source for any of those new transistors. Many start-ups folded up, and their customers had to redesign. The logical consequence of these rules: the products of start-ups are not elegible, one has to wait until major semiconductor firms release products. There is another viewpoint to shun start-up products: their products are continuously being redesigned and change from lot to lot, backward compatibility with formerly delivered samples is insecure. It is possible that a new component is no longer available when the product goes into production.

► A component may have fantastic properties, but if there is no second source it is not eligible.

In a single-source situation. the purchasing department can not negotiate prices but has to succumb to the supplier's price. In times of high demand one can not buy any amount of parts but those are "allottet". The introduction of electric vehecles will most probably cause a shortage of power semiconductors.

If the products of such start-ups are considered seriously quite a few contradictions are evident like: The data sheet says "Operation > 100 MHz" while the evaluation boards operate at 100 KHz, also the sum of rise, fall and delay times amount to 55 ns while the period of 100 MHz is 10 ns. Obviously these start-ups estimate the intelligence level of their prospective customers to be underdeveloped...

It is noteworthy that companies experienced in GaN production for transmitters etc. like Cree or the former RFMD are not engaged in GaN power transistors. Cree only supports SiC and founded Wolfspeed. RFMD offered no GaN but SiC cascodes in 2014, withdrew after the fusion with Triquint. If the future of GaN were that great why did those two firms refrain from entering the GaN power transistor market?

8.3 Structure of GaN transistors.

Most GaN transistors are fabricated on silicon wafers, hence they are lateral. GaN on SiC wafers is better but too expensive. In principle, all transistor types can be manufactured from the new materials. The "natural" transistor is for both the jfet which also has the advantage of bidirectional operation without parasitic elements. Jfets are by nature depletion, hence they can only be used in SMPS in cascodes unless there is an auxiliary supply which delivers a negative voltage before turn-on of the main supply.

Theoretically GaN excels over Si in some respects:

(Similar electron mobility	(> 1250 ... 1600 vs. 1500 cm^2 /Vs))
Higher saturation speed	(> 2.2 ... 2.5 vs 1 x 10t cm/s)
Higher charge carrier density	(1013 cm-2)
Higerh permissible field strength	(> 1 MV/cm vs 0.3)
(Lower heat conduction	(1.3 vs 1.5 W/cmxK))

These properties should theoretically permit power transistors with an Rdson of 1/100 of silicon, lower capacitances should allow shorter switching times and operation to 100 MHz. None of these could be proven sofar. Most GaN start-ups were founded by experts in physics or chemistry who did not know the electronics market. and the requirements on the active devices.

The "natural" type of transistor is the jfet for both GaN and SiC, but for power supplies and similar circuits enhancement types are required. Jfets are manufactured by several companies, but are mostly only available in cascodes The basic structure is shown in Figure 8.2. It is a lateral HEMT (high electron mobility transistor) which is known from other materials. and from GaN hf power transisrors.. Usually GaN is deposited on an appropriate substrate like silicon, simulating a GaN substrate. A "two-dimensional electron gas" is created, although hard to imagine. This conducts current from drain to source if a sufficient gate voltage is applied.

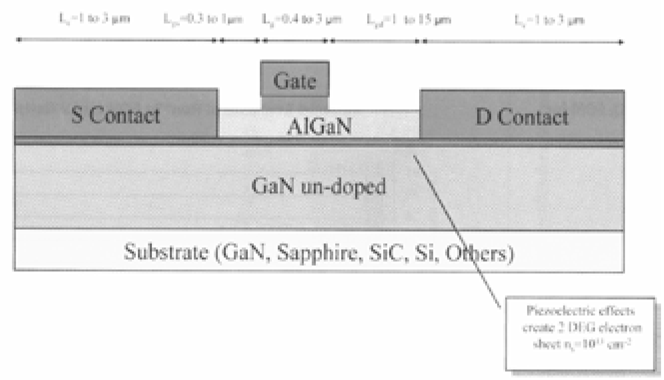

Figure 8.2: Structure of current GaN enhancement transistors.

Figure 8.3: Size comparison of a Si and a GaN transistor of identical Rdson.

However, the area for heat transfer is reduced by the same factor, and the thermal resistance of GaN is higher. Although the operating temperature of GaN is considerably higher than for silicon much less heat can be transferred.

The Si device is shown housed, the GaN device only as a chip. An example of manipulation.

8.4 Advantages of GaN vs. Si.

Claims of GaN manufacturers:

1. Lower Rdson, "orders of magnitude".
2. Lower capacitances, lower gate charges,.
3. Much faster switching.
4. Operating frequencies > 100 MHz.
5. GaN power transistors can be integrated with other circuitry (in contrast to SiC).
6. Takes temperatures up to 300 C. It is unclear what that statement means, because the operating temperatures are the same 150 ... 175 C as those of Si parts.

For years GaN could not even beat the 600 V/19 mOhm Coolmos of Infineon, only lately similarly specified devices were announced. Not to speak of "orders of magnitude lower".

Capacitances are indeed lower, but in practice there are at least 3 devices connected to a node, e.g. in a PFC there are the switching transistor, the diode and the storage choke. Especially the latter has higher capacitances than both transistor and diode. Hence a decrease of the drain capacitance of the transistor has but little effect on the total capacitance.A cascode with a Coolmos has the same switching times as the GaN cascodes on the market, it is much less expensive and features the avalanche robustness of today's Si mos power transistors.

Regarding operating frequencies see the examples in the next paragraph.
Regarding operating temperatures: the product of one firm showed already 4 mA leakage current at 600 V and 150 C which amounts to a 2 W loss.

The GaN cascodes have no advantages vs. SiC cascodes, to the contrary: it is not possible to achieve any avalanche-proofness.

8.5 Disadvantages. Truth and poetry.

► The "higher switching speed" of the GaN and SiC cascodes and the improvement in efficiency compared to a single Coolmos have nothing to do with the new materials but are due to the cascode circuit. It is the lower transistor in a cascode which determines the switching speed, and that is a standard Si mosfet. The upper transistor can be any; if the SiC or GaN is replaced by a Coolmos or even a fast bipolar the same speed will result. See the short description of the cascode in chapter 3.

Suppliers of SiC and GaN cascodes do not mention this. Customers are easily deceived, because these cascodes look like any Si mosfet and can be installed in its place, Suddenly the switching speed is increased, and the efficiency improved. At first sight this seems to be indeed attributed to the SiC or GaN transistor. The cascode has been neglected for decades in SMPS and similar circuits, many designers do not know it. If the customer would just add a small lv Si mosfet to his existing Coolmos he would get the same switching speed and efficiency improvement at much lower cost and retaining the excellent avalanche robustness of Coolmos. If SiC mosfets are used as single switches they are not faster than Si Coolmos. Single GaN 600 V transistors have only lately become available, the author could not test them because of their uncommon packaging, they are not available in standard TO-220's or TO -247's. Manufacturers of GaN cascodes when asked why they did not make enhancement devices answered that they did not believe in their reliability, also investors requested fast profits so they decided to make jfets.

► Also the lower input capacity of the cascodes has nothing to do with the SiC or GaN in the cascodes, but this is one of the intrinsic advantages of cascodes. The lower transistor operates into the source of the upper one, i.e. into 1/S which means a few ohms, virtually an ac short. Hence no ac voltage develops at the drain of the lower transistor, so there is zero Miller capacitance, the input capacitance is reduced to the sum of gate-to-drain plus gate-to. source capacitances. Thus the gate driver can charge the input much faster.

- With the exception of "GaN Systems" all suppliers do not mention that all GaN transistors are destroyed by a single overvoltage pulse, there is no avalanche robustness! Due to the fact that SiC easily attains 1200 resp. kilovolts, this is no problem while GaN sofar is stuck at 650 V, only on firm lately ventured to specify 1200 V. Hence GaN parts can only be used in such circuits where the drain is clamped like in PFC circuits. At lower cost a cascode made of a small Si and a Coolmos has identical performance. GaN parts must not be tested for voltage because such tests are destructive. GaN Systems stated:
"It is necessary for you to recognize that our GaN transistors are similar to ceramic capacitors. That means, at breakdown, they are destroyed." ... "The hard unrecoverable breakdown voltage is about 30 % higher than the rated breakdown voltage, As a general practice the maximum drain voltage must be derated." ... "All GaN HEMTs do not avalanche and thus do not have an avalanche rating." This implies that testing for voltage is prohibited because it is destructive."
- And regarding Rdson which is "orders of magnitude lower"? Infineon has a 600 V/ 19 mOhm transistor since many years. It took until 2018 for a GaN with 600 V/12 mOhm to appear. Also a SiC mosfet with 1200 V/11 mOhms just appeared. SiC jfets < 10 mOhms are available e.g. in USCI cascodes.
- In contrast to SiC GaN suffers from a variety of problems. The worst seems to be the so called "dynamic on-resistance". Similar to the turn-on delay of diodes this effect causes an initial transitory increase in Rdson which decreases the efficiency but can lead to destruction.

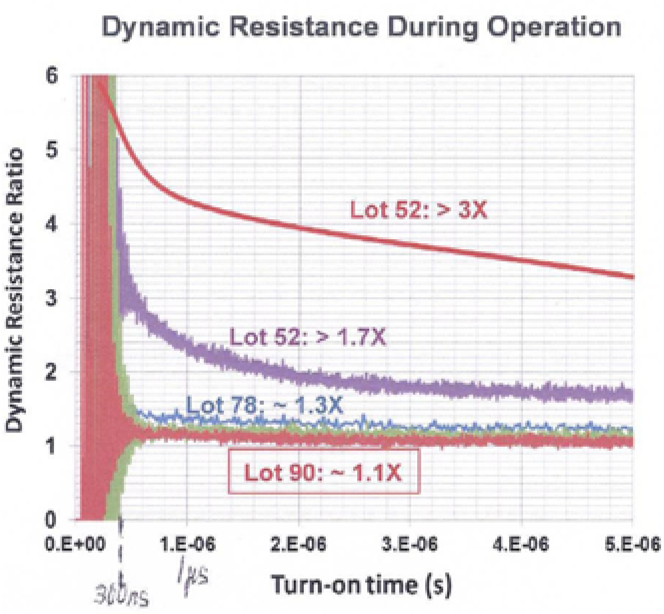

Figure 8.4: Dynamic on-resistance of GaN transistors (RFMD). The picture shows a strong dependence on the lots. The decay to the static value requires microseconds i.e.times far above the switching times. The picture further shows that the increase is far above a 6-fold one where the vertical scale ends.

Some GaN manufacturers claim they had suppressed the dynamic on-resistance, but some warn that it can return with time. Vertical GaN transistors on GaN or SiC substrates are said to be free from this effect. Whether this is true is doubtful regarding the truthfulness of other claims.

- Additional adverse effects with GaN are:
Inverse piezo effect.
Damages by peak electric fields.
Damages by hot electrons.
Electro-chemical oxydation.
- GaN enhancement transistors have a maximum gate voltage of e.g. 6 V, however, a gate voltage of 5 V is required for full enhancement. This the same problem as with SiC enhancement transistors. Good engineering practice requires operation with a substantial reserve to the maximum voltage.
- Last not least: The comparisons with Si circuits are often manipulated. In EVAL circuits unavoidable losses are subtracted, it is a miracle that effciencies do not exceed 100 %. Claims like: "Using GaN transistors will reduce the volume to 1/5, the weight to 1/3" or "90 % savings in volume, weight and cost - an efficiency improvement by 50 %" are absurd. Fotos show Si power supplies which are at least 30 years old and obviously borrowed from a museum.

The credibility of GaN manufacturers' specs is limited. One manufacturer claimed on p. 1 of his data sheet that his device would operate at "> 100 MHz". Some pages further the sum of delay, rise and fall times amounted to 55 ns, the period of 100 MHz is 10 ns. His demo resp, Eval circuits did not operate at 100 MHz, but at 100 KHz. In Sept. 2019 the spec of this transistor, the largest of this firm, was changed:from "> 100 MHz"to: "> 10 MHz"!. A competitor, realizing that for his cascode it is wise not to advertise high operating frequencies, specifies for 10 A and a smaller gate resistor the sum of delay, rise and fall times is given as 32 ns. This is good for operating frequencies < 1 MHz at best, the Eval circuits of that firm run also at 100 KHz to 133 KHz. "> 10 MHz" is false by one order of magnitude. This same firm gives much too high switching times for Coolmos circuits: "200 to 250 ns" is absolutely false and ridiculous by more than an order of magnitude. Also it is false to state that their device had the "same" breakdown voltage as Coolmos: while GaN transistors are destroyed at breakdown all Coolmos will go into nondestructive avalanche operation. Such false specs resp. statements could fill pages.

In the area < 100 V GaN can show better performance than Si.

8.6 Drive circuits.

While the GaN jfets are uncritical and not accessible to the user in cascodes, the enhancement mosfets are critical. The maximum gate voltages are mostly about + 6 V, while drive levels of + 5 are requested. Manufacturers warn that the gate drive signals must not overshoot. Standard SMPS control ic's can not deliver such signals because their minimum supply voltages are higher. External circuitry has to be added like two CMOS inverters with a + 5 V supply.There are special drive ic's on the market, but those are expensive and single-source. GaN on Si allows to integrate the drive circuitry on-chip.

dr.seibt@aon.at

Approaches in the Field of Pressure-Less / Low-Pressure Sintering for Large Surface Areas

In this article we will present the latest results in the area of low pressure/ no pressure silver sintering on using solvent free silver sintering pastes. With these materials sintering with low or no pressure at 250°C results in very dense silver interconnects between electronic components.

By Battist Rábay, Managing Director and Founder of Nano Join, and Michael Doktor, CCO and Founder of Foxy Power

Silver sintering is on the rise. The need of more reliable and better performing interconnects in power- and opto-electronics pushes the limits of the state-of-the-art interconnection materials. Soldering based on tin is becoming the bottle-neck in terms of heat dissipation, electrical resistance, re-melting, and reliability. Furthermore, due to the trend of miniaturization, growing power densities and switching to SiC and GaN challenges tin-based soldering up to its physical restrictions. Silver sintering solves all of the above-mentioned problems with $R_{el.}$ = 1.6 µΩ*cm, $R_{Th.}$ = 459 W/m*K and a melting point of T_{mp} = 961°C the performance of a silver interconnect is superior to the state of the art! Of course, there is a down side. Generating reliable interconnects with a simple process as soldering is, challenges the manufactures of silver pastes. Here, sintering with pressure is an established process, which yields to good interconnects based on silver. But, setting up a pressure of 22 MPa is only applicable for some components and surface areas. In addition, manufacturers tend to avoid the high costs of new production lines which are capable of pressure assisted and wait for solutions which are easy to implement in their already existing infrastructure: pressure-less sintering.

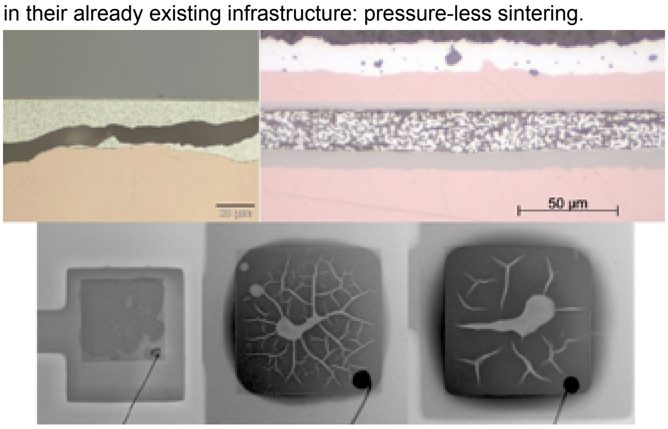

Figure 1: Modes of failure of silver sintered interconnects, via pressure-less sintering. Top left: crack through the layer, with delamination of the substrate.; Top right: High porosity of sintered silver layer.; Bottom: Drying channels, large voids, delamination.

The drawback of current solutions of silver pastes for pressure-less sintering is that they only work reliably for surface areas below 20 mm^2. The modes of failure are common and always can be assigned to the used silver material (Figure 1). All of the modes shown in figure 1 are not favorable for a reliable interconnect and will not outperform tin-based soldering solutions. Two main factors do contribute to such a negative outcome: 1) Wrong sintering process parameters and 2) Poor quality of silver pastes. Finding the right process parameters for several geometries and surface finishes can be really simple, but only if the quality of the chosen silver sinter paste is matched with the scope of the application. Usually, a too high content of organics and the metal particles and additives are not perfectly matched.

Figure 2: Approach of Nano-Join pastes.

The products of Nano-Join distinguish themselves from its competition through a high metal loading (minimum of 92 wt% pure silver) without the addition of any solvents. To make our paste production independent from material suppliers we invented a different approach compared to our competition. We only use two main components for our paste, a highly designed silver salt and our in-house produced silver micron particles, such an innovative process allows us to form a material with an industry standard workability (figure 2). This unique approach leads to a paste-system which is not only capable of sintering surface areas of up to 500 mm^2 in a pressure-less process with very dense silver layers for highest conductivity, but also offers the possibility to sinter surface areas of up to 3000 mm^2 with a pressure of only 5 MPa. In both cases a $R_{Th.}$ = 300 W/m*K and a $R_{el.}$ = 3.0 µΩ*cm are possible, in comparison standard soldering (SAC or Au/Sn) can only offer a maximum $R_{Th.}$ = 100 W/m*K.

Furthermore, there is no limitation in terms of surface finish, silver, gold, copper or even copper alloys can be interconnected. Paired with a long shelf life of at least 6 months at room temperature, the avoidance of silver nano particles in the paste and a large variety of scenarios of applications gives manufactures a powerful tool to improve existing products and processes! Customers, with the desire to switch from soldering to the next generation of interconnection materials in a pressure less process do not have to change the already existing infrastructure. Nano-Join materials can be applied through common techniques: dispensing, pin-transfer, screen or stencil printing. The sintering can be carried out in a standard reflow or convection oven under air or any inert gas. If customers already have a sintering process in line, where pressure is used, switching to our products, will also have a positive effect on the processes. Currently, for the above-mentioned application scenarios we have four products available (figure 2): NJ-One, NJ-Dispense, NJ-Surface and NJ-Force. The latter one for pressure assisted sintering, the other materials for pressure-less processes.

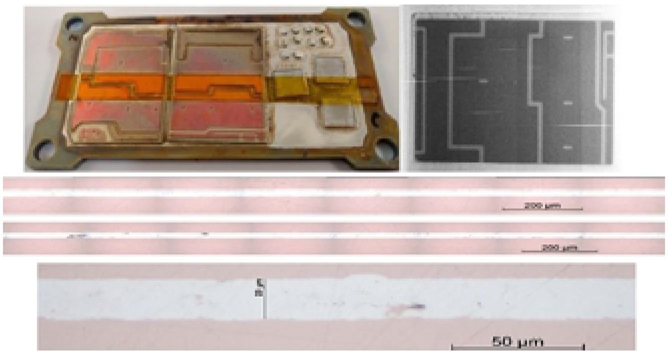

Figure 3: Performance of silver sintered copper-to-copper interconnects. Top left: Demonstrator with a total surface area of 3000 mm^2.; Top right: X-ray scan of one DBC to Cu-plate interconnect.; Bottom: Cross section through two copper plates sintered in a pressure-less process with a surface area of 500 mm^2.

In several projects we have been able to prove the performance of the above-mentioned materials. With industry partners we have been able to demonstrate the capabilities of our silver pastes to interconnect three copper DBCs (surface area above 3000 mm^2) with a copper baseplate (figure 3). Sintering was carried out for 5 min and a pressure of 5 MPa was applied. The resulting C-SAM, X-Ray and Lock-in-Thermography measurements revealed a good interconnection between the substrates, no voids or delamination of the substrates was observed. To evaluate the mechanical performance of the resulting interconnects, small copper shear bodies have been sintered under the same conditions. On average, shear values of 73 MPa have been observed. This approach offers the chance to sinter not only a dye on a DBC and still interconnect the copper ground plate to the DBC via soldering, but also manufacturers can now sinter both interconnects in two or even in one step! The limitations of surface area and pressure are no longer a challenge in the assembly of modern power modules. To stretch the limits of pressure less sintering even further, we have shown in previous results that with our materials the interconnection of surface areas of up to 500 mm^2 is already feasible (figure 3).

The usage of non-toxic and REACH/ ROHS compliant Nano-Join silver pastes offers our customers new possibilities to 1) finally make the switch from soldering to pressure-less sintering without the need of new investments in infrastructure, 2) assemble power modules in a one-step approach by using only low pressure to sinter dyes and DBC together, 3) a superior performance compared to the competition, and 4) the potential for manufacturers to lower the overall system costs.

Please contact sales@nano-join.de for further information.

www.nano-join.de

The Better Design: How IEEE Power Electronics Society is Paving the Way for Power Electronics Design Automation

The megatrends such as climate change, urbanization and digitalization - as well as others - are leading to an ever increasing electrification of everyday life. This development is accompanied by a growing demand for efficient power electronic energy converters.

By Kevin Hermanns (PE-Systems), Professor Miroslav Vasic (Universidad Politécnica de Madrid), Professor Peter Wilson (University of Bath), Professor Alan Mantooth (University of Arkansas)

Introduction

The demands on the systems to be developed are becoming increasingly tougher as we are trying to reconcile antagonistic specifications (miniaturization of power conversion systems and their maximum energy efficiency, for example). In addition to higher targets for energy efficiency, space requirements, weight and reliability, development cycles are also becoming shorter. Together with only a slightly increasing number of available developers, this indicates the stress field to which power electronics is exposed, having to develop more and better systems in less time.

In order to achieve the demanded goals, a considerable productivity boost is needed in development. This cannot be achieved by further developing existing development tools and process steps alone, specialized only for certain parts of the system (magnetics design, layout optimizers or thermal simulators), following the previously established design methodologies. As the system specifications are clearly correlated, we need to set a path towards a holistic approach, that will be the design of a power conversion system as a whole. This rather requires the development and establishment of new design tools and methods for power electronics to address all the specifications, clearly identifying how these specifications are correlated and where are the design limits set by the present technology.

The aim of these new methods and tools must be to reduce the complexity to be mastered by the individual developer to a manageable level, and at the same time, to guarantee the achievement of better technical specifications for the intended application. This trend has already led to the first research projects within the scientific community and the first solutions are pushing onto the market. It is questionable whether these already offer the necessary functional range to master the challenges.

In order to support the modern energy hungry society and push the design envelope, it is required to increase exchange between users, researchers and developers on ideas, their feasibility and implementation. The IEEE Power Electronics Society (PELS) has contributed to this idea by supporting several initiatives that have been launched in recent years in order to master the presented challenges.

The Initiatives

Design Automation for Power Electronics Workshop (DAPE)

The Design Automation for Power Electronics Workshop (DAPE) was the first strategic step in the Power Electronics community to start a discussion about the need for Design Automation tools. The focus of the workshop is to bring together the experts in both Power Electronics and Design Automation and have them presenting their perspectives on the emerging needs. As a result, the workshop helps us to understand the problems of Design Automation in Power Electronics, identify methodologies that have been used so far by academia and industry, identify the tools that have been developed to resolve the issues during design and propose a research roadmap in this area with further steps and actions to be taken.

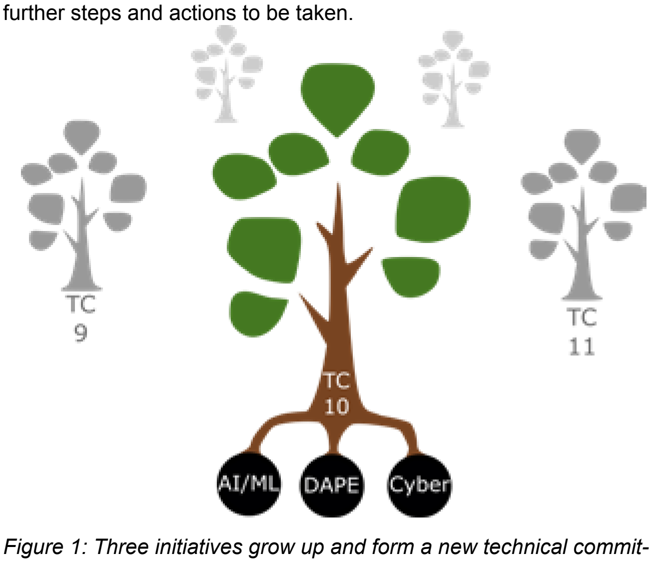

Figure 1: Three initiatives grow up and form a new technical committee on design methodologies

Due to this approach, the DAPE Workshop has become of strategic importance for the Power Electronics Society as modern designs (especially in highly integrated systems) are dealing with multi-disciplinary problems, shorter design time and multivariable optimization to obtain higher efficiencies and more compact designs.

The workshop has been organized twice, so far. The first time it was in September of 2018 in Portland, USA, a day before the IEEE ECCE, and the second time in September of 2019 in Genova, Italy, as a part of the EPE ECCE-Europe post-conference event. On both occasions distinguished academic researchers and key industry players joined to present their vision of the Design Automation and to participate in the interactive discussions with the audience.

This first step has helped us to identify the synergy between Power Electronics and Design Automation and to set the future goals towards which we must aim as a scientific society.

Artificial Intelligence and Machine Learning for Power Electronics
Design Automation for power electronics has used a variety of computational intelligence techniques for optimization and design exploration including evolutionary algorithms, particle swarm optimization, and artificial neural networks; the increased complexity of both the design space and model details required across multiple domains (including electrical, thermal, magnetic, and mechanical) means that expanding the range of computational intelligence techniques are essential for the next generation of new power electronics designs.

As a discipline, power electronics has adopted advanced design automation techniques to achieve more efficient and higher performance designs, and the next frontier is the application of computational intelligence techniques such as Artificial Intelligence (AI) and Machine Learning (ML). Key aspects of any computational intelligence technique are accountability, responsibility, and transparency. Ensuring that design decisions can be justified, trusted and quantified is essential for their effective use. Understanding how AI and ML can be used effectively in power electronics requires fundamental research both into the techniques themselves and how they can be applied in the power electronics context.

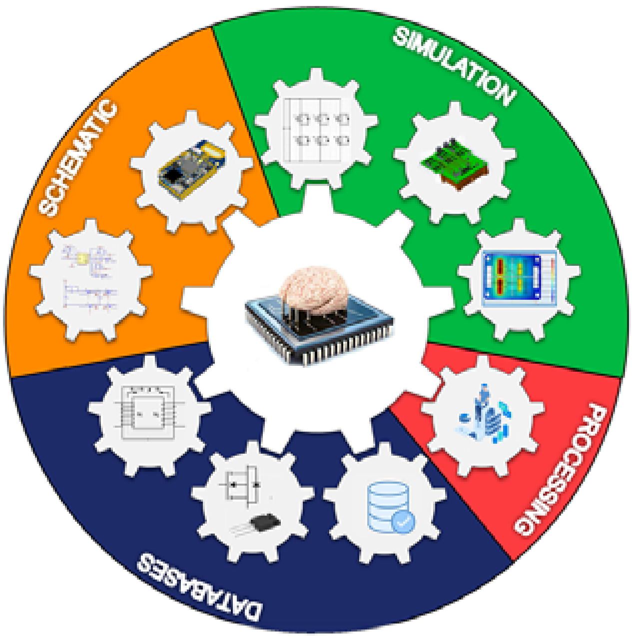

Figure 2: Holistic design approach in modern power electronics using design automation tool

Major questions remained to be explored including how to apply AI for classification and ML for deeper understanding of power electronic design behavior, using ML to explore new design methodologies, architectural design, and evaluation using Artificial Neural Networks, optimization techniques and parameter identification, investigation of multiple domains and their impact on design decisions and trade-offs, understanding the impact of design decisions made using AI/ML techniques, repeatability of outcomes, reliability and robustness of designs obtained using AI/ML and the understanding of risk in the power electronic designs created.

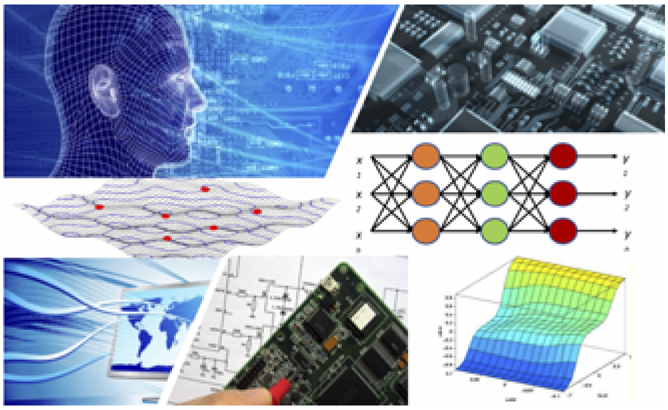

Figure 3: AI and ML techniques are being deployed in many areas for the design and optimization of power electronics

Cyber Physical Security (CyPhy)

The Cyber-Physical Security initiative of PELS began in 2016 with a special session at ECCE on Cybersecurity for Power Electronics. An initial workshop was held in April 2019 in Knoxville, TN, USA with a follow-on scheduled in Miami, FL, USA this past April. The latter of which was postponed and has been re-organized into a single-day workshop on the Saturday before ECCE North America in October.

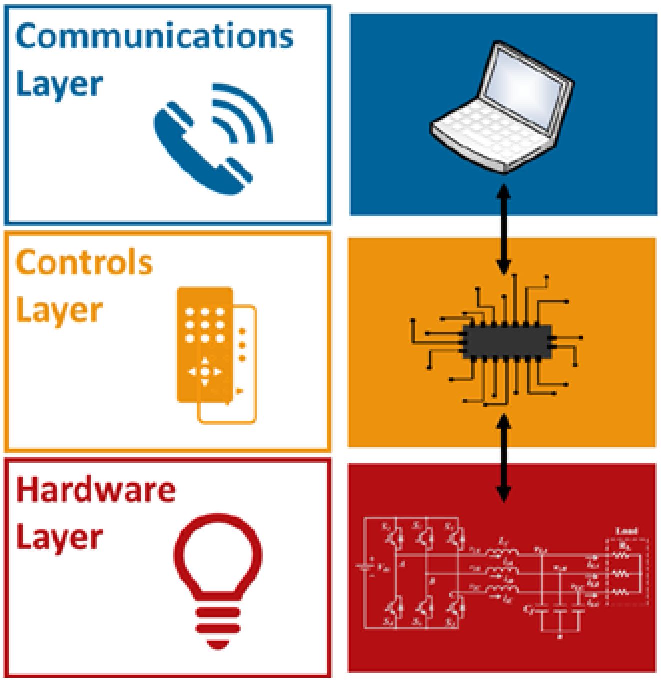

Figure 4: General diagram indicating the defense-in-depth approach to securing power electronic devices

As power electronics become increasingly connected in the IoT era they become more vulnerable to attack. Several events have demonstrated that it is quite possible to penetrate down into the firmware of devices and industrial controls. As power electronics continue to modernize systems such as the electric power grid, transportation platforms of all types, and industrial processes, the future power electronics engineer needs to have a knowledge of best practices, typical vulnerabilities, and design methods that can harden their systems and make them more resilient to attack or to fail safely.

The US Department of Energy has taken this issue to heart by offering millions of dollars in research funding to address these challenges in such systems. PELS feels it is appropriate to ensure that these techniques are disseminated within the power electronics community so that awareness of the issues and solutions are raised and engineers are educated.

Conclusion and Outlook

The activities of all these initiatives over the past few years are increasingly attracting interest from industry and academia. This is reflected both in the rising number of participants in events organized by the initiatives and in new research projects and products in this area. In order to strengthen this trend, it is necessary to give more weight to the topic of design methodologies and to provide further visibility. To this end, the initiatives must become an integral part of PELS. The currently planned reorganization of the Technical Committees (TC) within PELS provides the necessary space for this. Against this background, the activities of the three initiatives will be bundled within the newly planned TC 10 on "Design Methodologies".

The result of this step is a first joint conference on "Design Methodologies" in 2021 in Bath, UK. This conference will bring together the DAPE efforts alongside the artificial intelligence, machine learning and cyber-physical security efforts. The newly established national Institute for Advance Automotive Propulsion Systems (IAAPS) and Centres for Doctoral Research in Advanced Automotive Propulsion Systems (AAPS-CDT) and for Artificial Intelligence: Accountable, Responsible and Transparent (AI-ART) at the University of Bath will provide the appropriate framework. Further activities will be:

- Webinars on selected topics
- Professional exchange with other TCs
- Collection of material and ideas in the field of methodologies
- Specific workshops on selected topics of AI/ML/Cyber
- Support for education in new design methods
- Special sessions in conferences
- Special issues in transactions

A possible mission statement summarizing the activities of the TC Design Methodologies could therefore be the following:

Creates the conditions for the valuable resource of the PE designer to be used where human creativity is needed to create new and better development methods! The repetitive tasks should be done by machines that can do a better job here.

www.pe-systems.de

Teardown of a Variable Frequency Drives Inverter

This teardown looks at the inner workings of the Hitachi SJ P1 Variable Frequency Drive, an inverter for industrial applications and part of a line of industrial inverters. The SJ-P1 inverter achieves high torque at low speeds for heavy loads, making it a suitable option for a wide variety of applications.

By Nilo Mitra, Broadcom

The SJ-P1 inverter can be used to drive both induction motors and permanent magnet motors. While induction motors are more commonly found in motor-driven systems, they are often larger in size and less efficient than permanent magnet motor solutions. While permanent magnet motor solutions tend to have a higher initial cost, they may offer a smaller size for more compact mechanical packages and higher efficiency. Although the permanent magnet motor offers many benefits, there is a problem of permanent magnet demagnetization when the inverter is overloaded over time. The SJ-P1's over-current trip feature uses many isolated current detection and protection components to prevent the inverter from overloading and suppresses the demagnetization of permanent magnet motors.

Figure 1: The Hitachi SJ Series P1 variable frequency drive.

The SJ-P1 Series is designed for easy integration with various networks using optional Fieldbus modules like RS485-Modbus (built-in), RS422 port (built-in), Ethernet, EtherCAT, ProfiNET and Profibus-DP. The SJ-P1 inverter is used in a wide variety of applications including industrial fans, hydraulic pumps, cranes and lifts used in warehouse automation and injection molding machines. Now, let's take a look at the inner workings of this piece of equipment.

General Specifications

- Model and Ratings: SJ-P1, 15kW, 35A, 3-phase 400V class
- Sine-wave PWM system
- 0.00 to 590.00 Hz output frequency range
- Protection functions: Overcurrent error, overload error, brake resistor overload, overvoltage error, memory error, undervoltage error, current detector, etc.

External and Enclosure

- Dimensions: 390mm x 245mm x 190mm
- Weight: 16kg
- Operating ambient temperature: -10° to 40°C
- Installation class: A maximum altitude of 1000m, without gases or dust

Figure 2: The Hitachi SJ Series P1 enclosure.

DC Bus Capacitor

- DC Bus Bulk Capacitor: Nippon Chemi-con (2pcs) 400V/4400µF electrolytic capacitors.

Figure 3: The DC bus capacitor.

Main Controller Board

- PWM MCU: Renesas R5F571MFCDFC industrial equipment-specific real-time engine. A 32-bit microcontroller capable of operation up to 240 MHz.
- Programmable Logic Device: Altera EPM240T100I5N. The MAX® II family of instant-on, non-volatile CPLDs with densities from 240 to 2,210 logic elements (LEs) and non-volatile storage of 8Kbits.
- Isolation: Toshiba
    - TLP2362 (4pcs) 10Mbd high-speed photocoupler.

- TLP2301 (4pcs) 20 kbps photo-transistor with high-speed detector.
- TLP291 photo-transistor.
- TLP290 (4Pcs) photo-transistor with AC inputs.
- Relay: Panasonic JQ1-5V-F general purpose relays 5A, 5VDC, 400mW SPDT (1 Form C).
- Relay: Fujitsu FTR-F3AA012E general purpose relays, 12VDC, 200mW SPST (1 Form A).
- Line input and three-phase output contactor board.
- Current transducer: LEM HLSR 62-P (2pcs) open-loop 62A current transducer with galvanic separation.
- Capacitor: Okaya LE 105 310V 1μF film capacitor.
- Resistor: Iwaki 3.3/6.6ΩJ (8pcs) resistor.

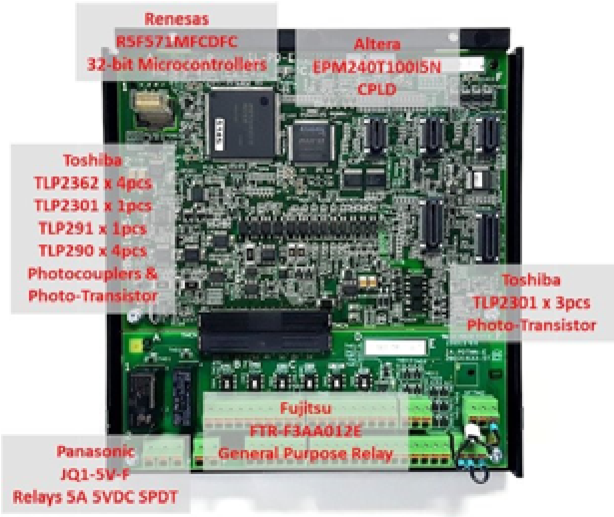

Figure 4: The main controller board.

Line Input and 3-Phase Output Contactor Board

- Current Transducer: LEM HLSR 62-P (2pcs) open-loop 62A current transducer with galvanic separation.
- Capacitor: Okaya LE 105 310V 1μF film capacitor.
- Resistor: Iwaki 3.3/6.6ΩJ (8pcs) resistor.

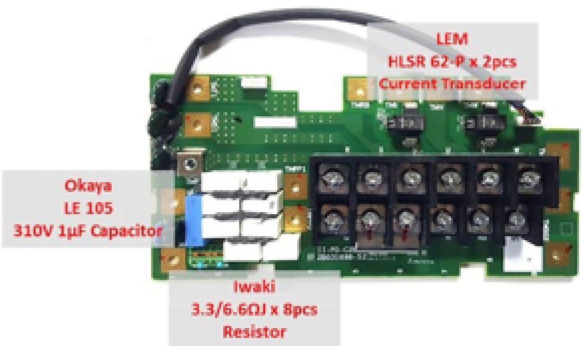

Figure 5: Line input and three-phase output contactor board.

Power Electronics Board

- IGBT: Fuji Electric 7MBR100VR120-50 1200V 100A IGBT module with rectifier, brake, inverter and thermistor stage.
- Isolation: Broadcom (Avago Technologies)
  - ACPL-W61L (3pcs) ultra-low-power 10MBd digital CMOS optocoupler.
  - ACPL-C87A precision optically isolated voltage sensor with 0.5% high gain accuracy.
  - ACPL-C79A precision miniature isolation amplifier with 0.5% high gain accuracy.

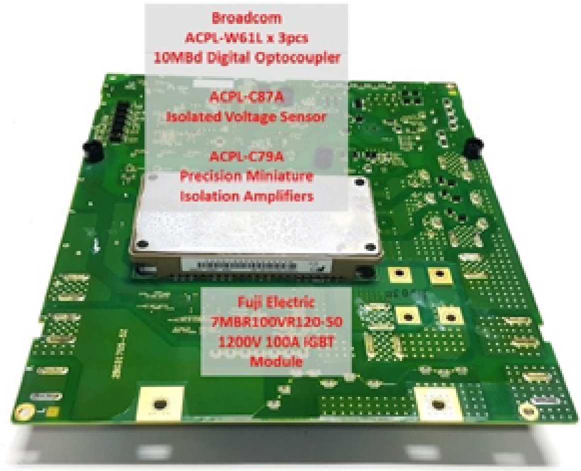

Figure 6: The power electronics board.

- Isolation: Broadcom (Avago Technologies)
  - ACPL-336J (6pcs) 2.5A IGBT gate drive optocoupler with integrated (VCE) desaturation detection, active Miller clamping, fault, and UVLO status feedback.
  - ACPL-W341 3A output current IGBT gate drive optocoupler with rail-to-rail output voltage.
  - ACPL-W61L (4pcs) ultra-low-power 10MBd digital CMOS optocoupler.
  - ACPL-C87A (2pcs) precision optically isolated voltage sensor with 0.5% high gain accuracy.

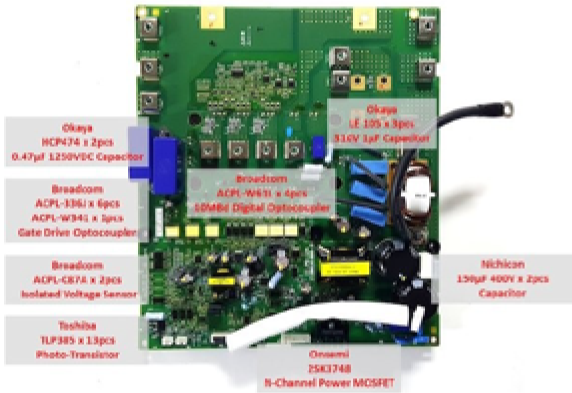

Figure 7: Another view of the power electronics board.

- Isolation: Toshiba TLP385 (13pcs) photo-transistor with 5000Vrms in a 4-pin SO6L package.
- Switching Power Supply: ON Semiconductor 2SK3748 N-channel 1500V 4A power MOSFET.
- Capacitor: Nichicon (2pcs) 400V/150μF electrolytic capacitor.
- Capacitor: Okaya
- LE 105 (3pcs) 310V 1μF film capacitor.
  - HCP474 (2pcs) 0.47μF 1250VDC capacitor.

Modular EMI Filter Selection for AC-DC Converters

Modular AC line filters are often seen in end-equipment, either chassis-mounted or integral to a connector, particularly in environments such as ITE, healthcare and industrial electronics. The purpose of the filter is to attenuate emissions which originate from the equipment from a combination of power supplies, internal electronics, high-speed data lines, etc.

By Gary Bocock, Technical Director, XP Power

Modular AC line filters are often seen in end-equipment, either chassis-mounted or integral to a connector, particularly in environments such as ITE, healthcare and industrial electronics. The purpose of the filter is to attenuate emissions which originate from the equipment from a combination of power supplies, internal electronics, high-speed data lines, etc.

Internal power supplies normally meet statutory emissions standards on their own, typically EN 55011/EN 55032, so why is an additional filter necessary? Compliant components do not necessarily guarantee a compliant system. If there are multiple AC-DC converters, their emissions could add. Also, an AC-DC will have been tested under particular specified conditions of AC line impedance, loading, orientation and positioning of the part with respect to a ground plane, with set lengths and routing of cables and a passive load. Installed in equipment, the converter will not see these same conditions and emissions could be higher. Connections to the end-equipment power inlet could also pick up radiated emissions from other system components adding to conducted interference.

EMI compliance may require additional filters

A typical solution is a modular filter fitted in, or close to the equipment power inlet connector. The selection of the filter from the many available is not trivial though for optimum performance and cost, so to help, let's consider a typical filter arrangement and look at the function of each component. (Figure 1).

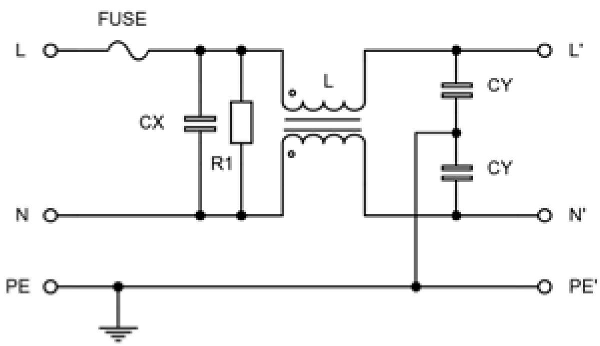

Figure 1: Typical modular EMI filter circuit

CX attenuates differential mode noise, that is, noise from line to neutral. It is an 'X' rated capacitor which can withstand specified AC line transients depending on the 'over-voltage' class of the environment. It is available as X1, X2, or X3 types with peak service voltage ratings of 4kV, 2.5kV and 1.2kV respectively, according to EN 60384-14. If the capacitor shorts due to stress, there is a risk of fire, so the component must be safety agency certified. The capacitance value of CX can be high, limited only by practical considerations: it must discharge within a prescribed time when the AC line is disconnected, either by the downstream circuit or R1 to avoid a potentially dangerous voltage remaining on the connector pins. According to ITE and media safety standard EN 62368-1, the limit is less than 60V after two seconds if CX is greater than 300nF, with a higher voltage allowed for values less than 300nF or in environments only accessible to trained personnel. In medical installations, the limit is 60V within one second according to EN 60601-1 but with no requirement if CX is less than 300nF.

R1 must be rated for the highest continuous line AC voltage and according to EN 62368-1, if fitted before a fuse it must also withstand transient voltages with no more than 10% resistance value deviation. For large values of CX, R1 must be relatively low resistance to achieve the discharge time specifications, with consequent significant continuous power dissipation. This can be problematic when trying to meet limits of no-load or standby losses defined by the US DoE and European ErP directive.

L is a 'current-compensated' two-winding inductor which attenuates common mode noise generated typically by high switching frequency voltages driving noise currents to ground through internal power supply capacitances, returning through line and neutral. Phased as shown, the magnetic field from normal running current cancels and 'common mode' current on both line and neutral together 'sees' a high impedance. The two capacitors CY divert the current so it circulates locally rather than through the AC source. L1 can be a high value as the running current field cancels and prevents core saturation, but sometimes winding coupling is deliberately reduced to allow some leakage inductance, which helps with differential mode attenuation, perhaps reducing the value of CX.

The two capacitors CY also must be safety agency certified because if one fails short and the equipment ground is disconnected, the equipment enclosure can become live. Even without capacitor failure, if the ground connection is inadvertently disconnected, there can be sufficient 'leakage current' to the enclosure to give a shock, so the capacitance values are limited to give a maximum 'touch' and 'enclosure' leakage current according to the applicable standard. Limits could be milliamps in some industrial areas with hard-wired grounds, to less than 10µA in 'cardiac floating' medical environments. Capacitors are also specified according to the AC source class; Y1, Y2, Y3 and Y4, for peak test voltages of up to 8kV.

The fuse in Figure 1 is often included in panel-mounted modular filters such as the popular IEC320-C14 type (Figure 2). Some standards require that only the line connection is fused, others in medical and IT require that both line and neutral are fused. With single fusing, if the input is accidentally reversed, the fuse is then in neutral and is bypassed when neutral and ground are common, leaving protection reliant on upstream fuses or breakers which might be common to other equipment and consequently with a high current trip rating. This current into the filtered equipment could represent a fire hazard. With line and neutral fused, a reversed supply is now covered. However, if the fuse in the neutral connection opens through a fault such as a line to neutral overcurrent, the equipment is apparently 'dead' but has live connections inside. To counter this, the neutral fuse value can be made one step higher than the line so that the line fuse would normally open first.

Figure 2: Typical fused panel-mount EMI filter

Modular filter selection

Various mechanical formats are available for modular filters; chassis-mount types, often with six-sided shielding with direct fixing to a grounded chassis, are very effective with short wiring to a fuse and inlet connector. IEC inlet connectors with a built-in filter are a popular choice with screw or snap-in mounting, with one or two fuses according to the application environment. C14 types are rated to 10A and C20 types available to 20A and higher.

Versions of each type are available without 'Y' capacitors for medical applications with a maximum leakage current of typically 5μA. This reduces common mode noise attenuation which may need to be allowed for with cascaded filters, for example.

The load power sets the current rating of the filter allowing for the lowest input voltage and load power factor. For example, for a load of 300W with a power factor of 0.8 at a minimum of 90VAC, the current draw is 300/ (0.8 x 90VAC) = 4.16A suggesting a 5A rated filter.

Modular filters have published graphs of attenuation with frequency and a type can be initially chosen by measuring performance without the filter then subtracting this from the target to give desired filter attenuation. Performance data for filters is under particular test conditions, typically with 50-ohm source and load impedance, so attenuation in practice depends on the end circuit. AC source impedance can be standardised using a Line Impedance Stabilisation Network (LISN) but the load could be very different to 50 ohms, varying with frequency and even showing negative incremental impedance. There is also the danger of resonances with other series filters causing unexpected results, even amplifying rather than attenuating EMI at particular frequencies.

As an experiment, the EMI performance of an AC-DC converter from XP Power, type PBR500PS12B, was plotted at 230VAC and 180-watt load with results shown in Figure 3. The converter showed compliance with EN55032 curve B emissions limits with a good margin, for quasi peak detection, as the standard requires. An extra filter was added, type XP Power FCSS06SFR, with the attenuation characteristics of Figure 4. The solid line is a common mode and dotted line differential mode attenuation.

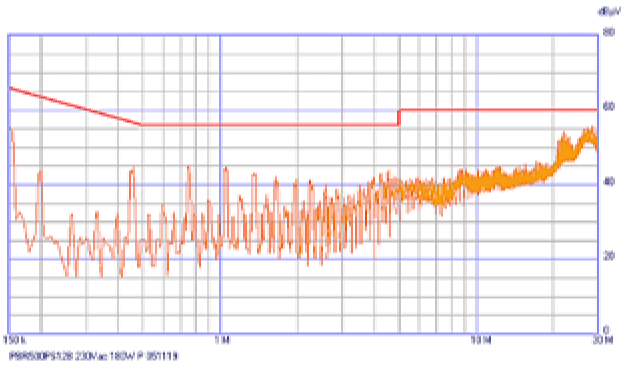

Figure 3: AC-DC power supply, internal filter only

A plot of the combined effect on emissions is given in Figure 5, showing that up to about 1MHz, the overall attenuation in dB is the original plus filter value. Above a few

MHz though, the attenuation is less than expected. This is due to the filter not 'seeing' 50 ohms termination at high frequencies, reducing its attenuation effect and confirming the necessity of practical measurements to confirm compliance with emission limits.

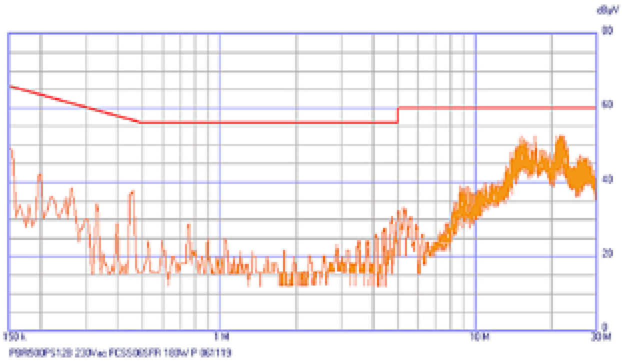

Figure 5: AC-DC power supply with an external filter added

Help is at hand

The type and performance of modular EMI filters is a complex choice and vital to get right to avoid the costs of potential re-design at EMC testing, when product release should be close. Over-kill with a large filter is costly and can even be counterproductive with unexpected results. Manufacturer XP Power is here to help, with a wide range of filters to complement their AC-DC converter products, with a choice of current ratings and attenuation characteristics in IEC and chassis mount formats. Versions are available for all applications including low-leakage types for medical with yet more planned for high current and three phase applications. Multi-stage filters are also available for increased attenuation as well as custom versions as required.

XP Power offers comprehensive application support for their products and can assist in pre-compliance testing of customer products with free use of in-house EMC test facilities in company locations worldwide.

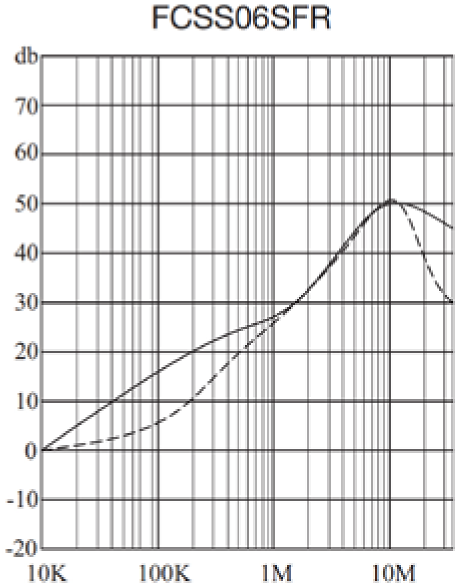

Figure 4: Modular filter type XP FCSS06SFR

www.xppower.com

ClearPower Modules Tackle Designers' Toughest Challenges

There are fundamental truths that every system designer must face when it comes to power electronics. First, most projects will need multiple rounds of design, simulation, and trial to pass strict limits on EMI (electromagnetic interference). Second, there is the issue that introducing EMI components will reduce system efficiency and add to cost and solution size. This latter point is particularly pertinent as there is often very little board space reserved for the power solution, so the option of using large, proven solutions is no longer valid. Finally, the thermal environment will generally be worse than anticipated.

By John Bazinet, Director of Engineering,
Regulator and Lighting Products, Allegro MicroSystems
and Ben West, Applications Engineering Section Lead,
Regulator and Lighting Products, Allegro MicroSystems

Fortunately, where this situation was once little short of dire, recent developments in integrated circuit design, system integration and packaging are serving to lighten the power designer's load. In fact, it is now possible to consistently deliver high-quality designs that pass the strict limits of CISPR 25 Class 5 or EN 55025, while simultaneously reducing overall solution size and managing thermal dissipation.

Allegro MicroSystems' ClearPower module family of products, which adopt a 'system in a package' approach, provide the answer that designers have been seeking for some time. ClearPower modules house all the principal elements of a high-performance switching power supply or LED driver within a compact package, significantly easing the task of designing complete power solutions.

An example of a recently developed ClearPower module is Allegro's APM80900 (Figure 1), which is intended for LED lighting applications. A power inductor, critical bypass capacitors and an advanced switching regulator IC are co-packaged within an envelope that measures just 4 × 6 × 2 mm, while routable substrate technology is employed to connect the various sub-components together, and to the outside world.

By co-locating these critical power stage components within close confines, the high current switching paths that promote EMI are reduced by a factor of 10. Additionally, through direct integration and innovative IC design, overall size can be up to 70% less compared with conventional solutions.

Allegro MicroSystems' ClearPower modules feature an MIS (molded interconnect substrate) routable lead-frame package with the look and feel of a conventional QFN solution. Combining this technology in an industry-standard QFN footprint with wettable flanks ensures reliable operation at the harshest of automotive operating temperatures.

While the task of developing a viable power solution that will pass EMI limits has become far easier with power modules, achieving high performance demands a holistic approach to the design of the module itself. This undertaking involves combining IC design, packaging technology and passive component integration to achieve the desired EMI, thermal performance and size.

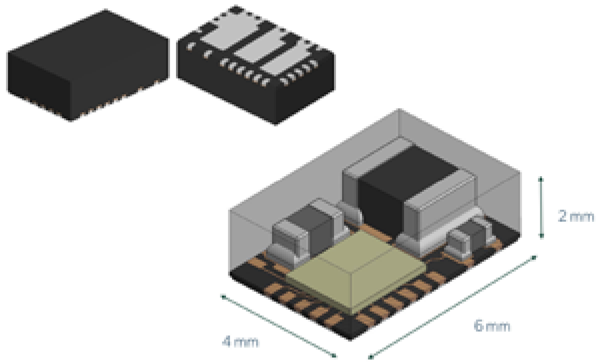

Figure 1: The APM80900 is a 40 V, 1.5 A synchronous buck LED driver ClearPower module by Allegro MicroSystems

Specialised packaging and chip design techniques allow ClearPower modules to achieve excellent thermal dissipation characteristics. This factor is critical as both the IC and inductor are heat sources, and are encased within the same compact package. Notably, deploying multilayer routable packaging technology within the ClearPower module, which is not possible with conventional single-layer leadframes, permits the creation of connections and component spacing that maximises thermal dissipation. The routable inner layer(s) of the module package is used to make contact with the IC and passive components, while the module's heat-generating areas (power switches and inductor) are connected through vias, providing an efficient way to channel heat from the package interior to its large, exposed power pads.

Flip-chip IC technology is often used to lower the resistance and inductance associated with bond wires. Just one flip-chip connection (referred to as a bump) has an inductance around 20 times less than a conventional bond wire. As a result, multiple bumps can be used to connect to each high-power node, producing a total inductance that is immeasurably small. Flip-chip bumps also lower any high-frequency ringing that leads to EMI and, in comparison with conventionally bonded products, serve to decrease power dissipation.

In addition to these advanced packaging techniques, ClearPower module-based regulators (including the AMP80900) use many of the same techniques as conventional switching regulators to further reduce EMI. One method is spread spectrum modulation, which slightly modulates the converter's switching frequency. Here, energy is spread out over a broader frequency span to reduce noise energy peaks. Another effective method of reducing EMI is by reducing switch turn-on losses. ClearPower modules are uniquely designed and configured to minimise such losses.

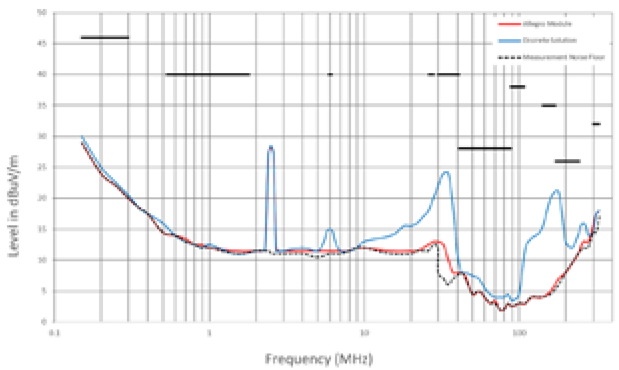

Figure 2: Comparing the radiated EMI of Allegro MicroSystems' ClearPower APM80900 module with a conventional solution

Once a power supply design has gone through its initial stages, EMI is evaluated in a special testing laboratory, often leading to late nights, stressed engineering managers and inconvenient late-stage design modifications. As EMI laboratory time is typically charged by the hour, it is incumbent upon the design team to reach a viable EMI solution quickly. This demand leads to any number of non-ideal solutions being employed to quell EMI, including metal shields, passive snubbers and common mode input chokes. These additional passives add cost, increase overall size and reduce system efficiency, leading to higher heat dissipation.

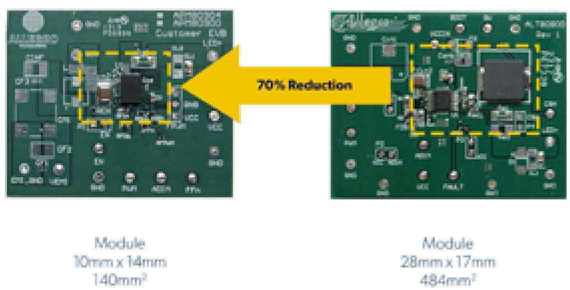

Figure 3: Board space comparison between Allegro MicroSystems' ClearPower APM80900 module and a conventional solution

The promise of ClearPower modules is that there is no longer any need for these somewhat desperate measures. Today, a CISPR 25 Class 5 compliant solution can be delivered with far less effort. To prove this point, a like-for-like comparison between a module solution and conventional counterpart is shown in Figure 2. Both designs employ identical input filters and switch at 2.5 MHz. Note that the module design is typically very close to the noise floor of the measurement system and exhibits considerably less noise than the conventional design.

Alongside EMI concerns, reducing the power solution envelope and profile on the board is an ongoing challenge. While every type of electronic component requires a power supply to perform its function, this notion often occurs late in the process and receives little attention. Treating the power supply as an afterthought means an optimum design will not be achieved, promoting many system problems. Allegro's ClearPower modules are viable solutions that improve performance and simplify design. Moreover, by reducing external components, integrating magnetics and using bespoke power packaging designed to withstand the harshest automotive operating temperature range, ClearPower modules can reduce overall solution size by up to 70%, as outlined in Figure 3.

Ultimately, EMI mitigation is an increasing challenge as more systems become connected wirelessly or are integrated into smaller spaces where there is a higher potential to interfere with other devices. ClearPower modules from Allegro MicroSystems offer a fast, effective and reliable solution for solving these difficult EMI challenges. In addition, ClearPower modules reduce R&D time and cost, and simplify the bill of materials, while the PCB area required for the power solution is significantly reduced, leaving space for more value-added functions. In short, power modules are becoming increasingly mainstream and compare favorably in the overall cost-benefit calculations of system developers.

www.allegromicro.com

Hanna Curve Reloaded

Inductance is the most fundamental parameter to define an inductive component. In a practical application, the inductance normally performs with non-linear features thus three terms: amplitude inductance, differential inductance and energetic equivalent inductance are defined to describe the components during the magnetizing and de-magnetizing process, as shown in Figure1 [1].

By JC Sun, Bs&T Frankfurt am Main GmbH and Yi Dou, DTU Kopenhagen

Among these three definitions, the energetic equivalent inductance is of great significance for energy conversion applications because it matches well with the basic energy charged and discharged operation in the converters, such as DC choppers in buck converters and coupling inductors in Flyback converters [2].

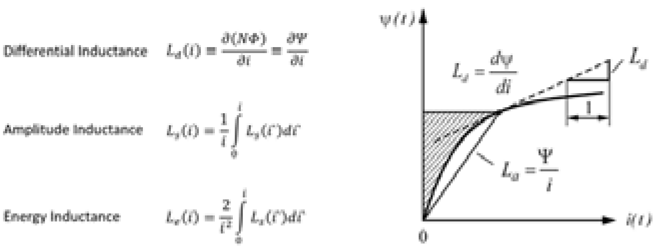

Figure 1: Definition of amplitude inductance, differential inductance and energetic equivalent inductance.

Conventionally, the non-linearity performance of the components is derived from the non-linearity of magnetic materials, where the amplitude permeability, incremental permeability and initial permeability etc. are defined initially [4]. However, the description from materials lacks an important aspect-power loss, for a specific inductive component. Besides, the measurement of the material to distinguish the incremental and reversible permeability is normally insufficient for an inductive component, especially under DC-bias condition and the near-saturation condition.

In order to synthesize the design of an inductor, the Hanna Curve was proposed to connect its energy storage capability to its physical geometry, which has been applied for silicon steel at early 20th century i [3]. In fact, the Hanna Curve is a powerful tool for gapped magnetic components design based on materials study. It was taken over as well for design with gapped ferrite core with consideration of thermal resistance for standardized shaped cores [1].

In this article, the basic concept of Hanna Curve is discussed in the first place and the measurement of the inductance definition and Hanna curve is demonstrated by Bs&T-pulse technology. Two case studies are also presented to discuss the design guidelines from the practical measurement results, to validate the utility of the Hanna Curve as well as the damped oscillation method around the first current peak of voltage-current decay.

Demand of high current power choke design

Currently, higher power density and higher power delivery are the essential expectations for power converters. The recent rapid development of power semiconductors with wide-gap-band materials (GaN and SiC) permits the converters working under higher temperature environment. Correspondingly, the magnetic components are also expected working on different conditions from the prior-art. The current standard IEC62024 edition 2, whose target is to characterize an inductive component, while only specifies the performance up to 22 A. Obviously, it cannot satisfy the requirement for modern inductive components operating under higher current excitation and an extended temperature range. Moreover, the uncertainty caused by higher delivered power (i.e. de-rating), higher current and drastic change of the temperature, may affect the systems` reliability.

An example of the emerging requirement for material evaluation is the cross field inductive heating, as illustrated in Fig. 2 [5]. In this typical application, coils will generate a very strong AC magnetic field and the magnetic materials are in charge of regulating the fields, thus the entire system benefits from a high efficiency and practically no EMC issues during the operation. Nevertheless, the operation condition for the materials is on a harsh one with a large flux bias and a high operation temperature, where the performance evaluation for the materials faces critical challenges. Similarly, the difficulty of the materials evaluation also comes up for high-power filter reactors for DC-link converters and electric traction applications etc. [6] [7].

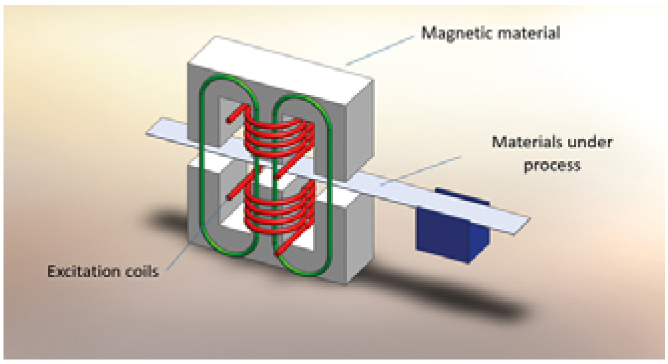

Figure 2: Principle of cross field heating – an application of inductive components working with high temperature and high excitation current.

With the emerging requirement of accurate magnetic measurement, the Bs&T pulse technology offers a unique solution to fulfill the requirement for next-generation magnetic component evaluation. In Bs&T bipolar impulse measurement, the damped oscillation method, which has been described in standard IEEE 389, is adopted and it is able not only to provide the performance evaluation under hundreds even thousands of ampere current excitation, but also to minimize the performance shift from temperature rise during the measurement.

The basic concept for damped oscillation method in *BsT- pulse* micro is illustrated in Figure3. In the first place, the energy for damped oscillation will be charged in the capacitor C, where the voltage can be controlled from 100 V to as high as 1000V to provide enough energy for the oscillation. Once the capacitor being charged, a damped oscillation will be conducted on the D.U.T., during which the voltage and the current of the D.U.T. will be sampled and processed to achieve the performance evaluation, and will complete inductance analysis for magnetization and demagnetization path. The full reversal current enables the loss quantification. Compared with the conventional magnetic measurement with a continuous sinusoidal excitation, this method is particular optimized for high-current application because the total measurement process only persists from tens of nano-second to microsecond. Thus, the measurement temperature of the D.U.T. can be assumed as constant during the measurement. In contrast, the conventional method will suffer the uncertainty from the temperature shift during the entire measurement process, while the systematic error for the total measurement set-up becomes unpredictable either.

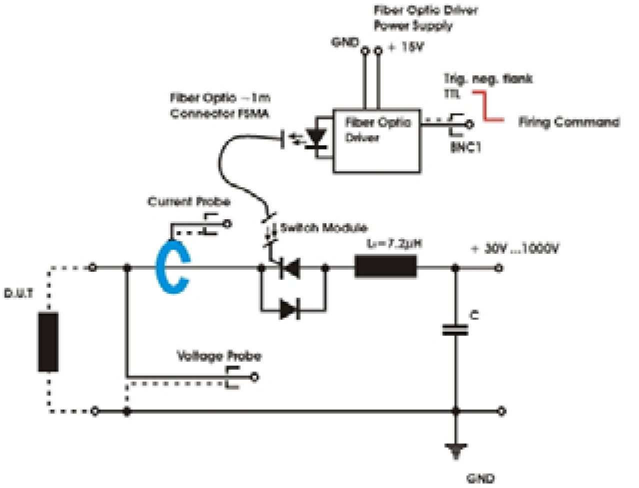

Figure 3: Bs&T measurement system with damped oscillation method.

Hanna Curve validation for Inductors

It is well known that two concerns, which are from windings and from core shape and materials, are main aspects for an optimized inductor design with lower volume and lower temperature rise. Nevertheless, it is not necessary to depict the detailed winding configuration due to the energy storage and delivery of the inductor normalized typically. Correspondingly, the non-linearity from the core materials must be taken seriously, especially for inductors with significant DC bias.

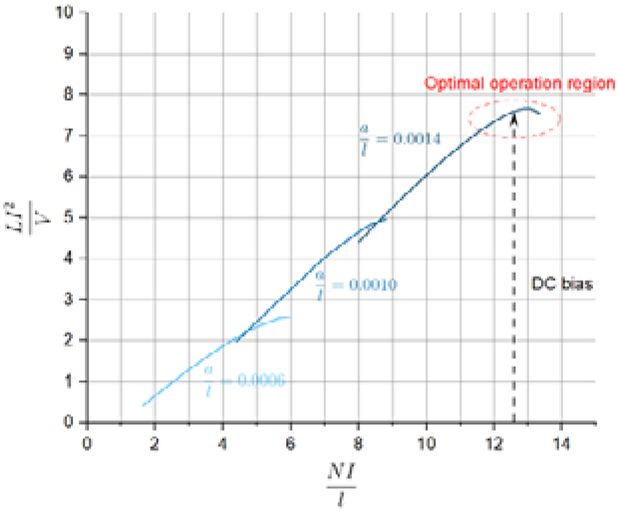

Figure 4: Typical Hanna Curve of a gapped core.

The previous evaluation of the inductor is originally derived from the performance of magnetic materials, which can be qualified by BsT-Pro measurement. Nevertheless, the non-linearity of the inductive components cannot be directly reflected from the features of the materials. The shape of the magnetic core, the winding configuration and especially from the air-gap of the core (distributed or discrete) because they rearrange the distribution of the magnetic flux in the magnetic cores, compared with the components with a closed flux loop, such as toroid cores or typical transformers, due to demagnetization factor. Under these circumstances, the measurement directly for a gapped core should be made before component design, especially with higher current and high temperature applications. In the magnetic materials` measurement, the detailed performance can be describe by “permeabilities”, such as initial permeability and incremental permeability [4], which have been specified by magnetizing condition and measurement configurations. However, the corresponding definition for inductive components has not been established, thus measurement became the only way to specify the components.

A proper description to specify the DC chokes can be Hanna Curve, which was initially proposed by C. R. Hanna in 1927. In the initial curve description, a curve of LI^2/V against NI/l for a specified a/l of a magnetic core is plotted to illustrated the energy-store capability of a magnetic core, as shown in Figure 4, where L is the differential inductance, corresponding to incremental permeability μΔ or the reversible inductance μ_{rev} ,depending on the excitation of the alternating signal; I is the direct current; V is the volume of the core; N is the number of turns; a is the length of the air gap and l is the effective length of the magnetic flux. The Hanna Curve can also be plotted by pre-magnetization LI^2 vs B [8]. Meanwhile, the flux ripple can also be reflected in the Hanna Curve by define as $\Delta I/I_o$, or delta $\Delta B/B_o$ no matter if the magnetic core operates in the linear area.

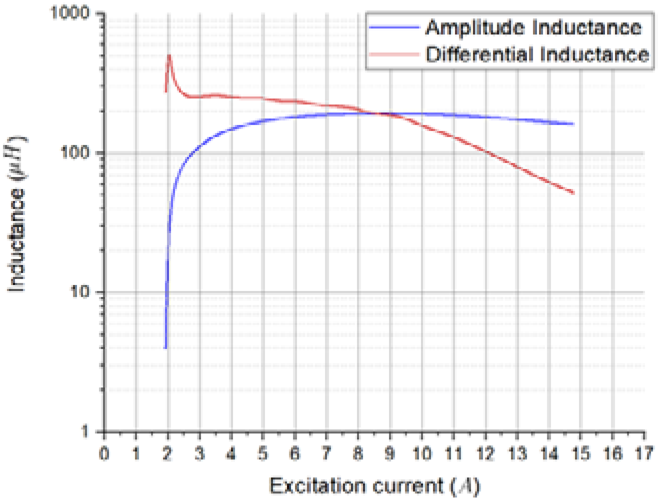

Figure 5: Measurement results for UI 93 ferrite core with Bs&T pulse.

It has been recognized that with the increase of the ratio between the air-gap length to the total effective magnetic length, the energy storage capability will be enhanced in a specific core, which is also described in the Hanna Curve. In the Figure 4, it is noticed that linear accessible flux-linkage extends with the increase of the a/l, which validates the enhancement of the energy storage capability. Moreover, the Hanna Curve for a specific gapped core, which indicates a unimodal function, need to be highlighted because the peak value of LI^2/V indicates a unique optimum point for the energy storage capability can be identified for a specific core, which is an essential design guideline for the inductors. Compared with deriving the optimum operation point from the magnetic materials` features and the winding configuration, the Hanna Curve can directly provide a design

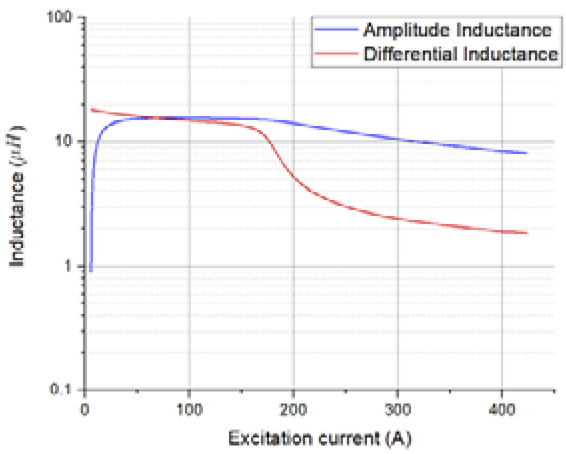

Figure 6: Measurement results for UI 93 ferrite core for leakage inductance with Bs&T pulse.

guide both for optimum H-bias and optimum AC current loop while the optimum current density range can be obtained from the x-axis (NI/l) in the Hanna Curve, which can be provided by the Bs&T pulse measurement.

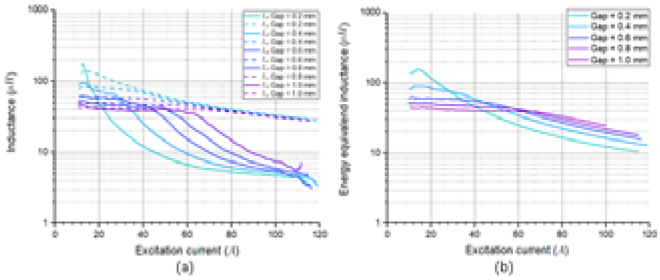

Figure 7: Measurement results for EE65/ D9B material ferrite with Bs&T pulse (a) Differential and amplitude inductance (b) energy equivalent inductance

In particular, the Bs&T micro pulse is able to rapidly provided Hanna Curve for cores of both standard core shapes and customized core, especially under specified operation temperatures. Once the measurement of cores` Hanna Curves are released, the optimum core shape selection can be achieved by reading the Hanna Curve, as well as integrating the evaluation of thermal resistivity, especially for standard Ferrite cores, with proven thermal resistance to limit the uncertainty because of thermal dissipation during the operation.

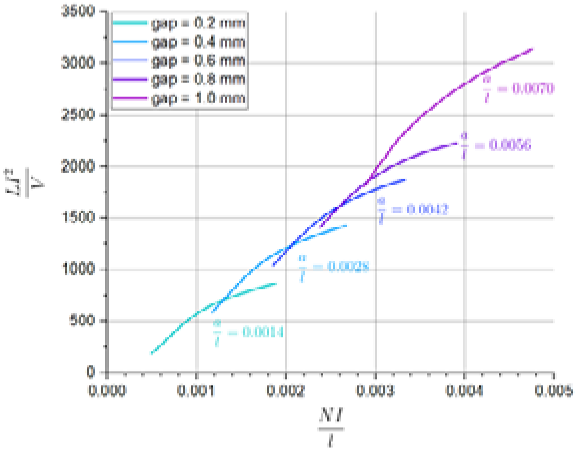

Figure 8: Hanna Curve of D9B in EE65 core with different gap length (in SI).

Case study

In this section, two case studies for the measurement with Bs&T pulse for gapped inductor are presented, where the non-linearity of the components are highlighted with different inductance definition and excitation current.

Case study I

In the first case study, a ferrite core in shape UI 93 and winding with 7 turns are tested by Bs&T pulse measurement for the amplitude inductance and differential inductance, as shown in Figure 5. It can be found that both the amplitude inductance and the differential inductance show a nonlinearity with the different excitation current, which not only come from the original feature of the ferrite materials, but also from the shift from core shape, air gap length and also magnetizing/ de-magnetizing process.

In Figure 6, a secondary winding, which also consists of 7 turns, was added on the same tested core to simulate the core working as a transformer and the secondary winding is short when measured to depict the performance of the leakage inductance, by definition. In this case, the excitation current was pushed to higher than 400 A and due to the flux in air dominates the operation, the linear range of the leakage inductance is found from 50 A to 200 A and then with higher excitation current, the inductance start to show nonlinearity, which should be considered in the component design.

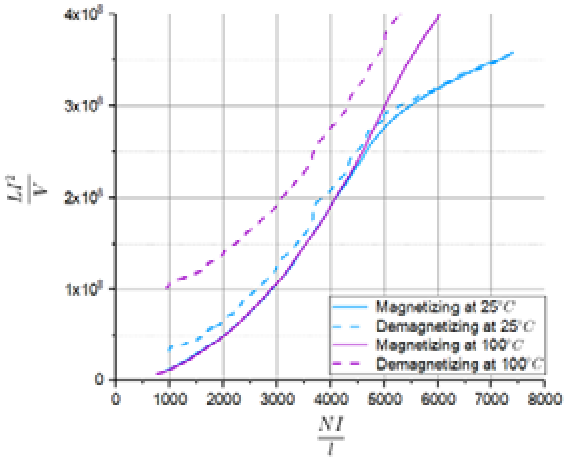

Figure 9: Hanna Curve of D9B in EE65 core with different temperature and magnetizing/demagnetizing process (in SI).

Case study II

In this case study, the measurement was conducted on D9B ferrite material in EE 65 core shape. Firstly, the differential inductance, amplitude inductance and energy equivalent inductance are depicted in Figure 7 with different excitation current.

From the energy equivalent inductance measurement, the Hanna Curve of the specified core can be derived as in Figure 8, from which the energy storage capability can be observed directly. In Figure 8, the original form proposed by C.R. Hannah is adopted, where the y-axis represents the energy density stored in the structure while the x-axis represents the flux linkage in the flux path. It is natural that with the increase of the air gap length, the energy will be enhanced correspondingly. From the Hanna Curve, the designer is able to define the energy charging and dis-charging range for the component and also the voltage-second operation range can be defined.

It is well acknowledged that the temperature has significant influence for the inductors with ferrite core due to lower Curie temperature compared to metal alloyed design and the non-linearity of the components also shifts between the magnetizing and demagnetizing process, because energy loss is generated during each half cycle. In Figure 9, the Hanna Curve is depicted with different testing temperature and magnetizing/ demagnetizing process. With the damped oscillation method with Bs&T measurement system, the performance shift can be clear observed: under the room temperature, the magnetizing and demagnetizing process own similar energy storage capability; while at higher operational temperature, the two curve shows separate trend but generally the energy density will be higher compared with that with room temperature, which indicates an potential optimal operation point for this magnetic core.

Conclusion

With the emerging requirement for high performance magnetic components with higher current and higher temperature working condition, the damped oscillation method enables proper validation for the magnetic cores, especially for DC chokes application. The Hanna Curve is one of the choice for estimating the performance for a gapped core as well as optimizing the design even without specifying the winding configurations. With the two case studies, the complete inductance analysis, as well as Hanna Curve are depicted based on the measurement data by Bs&T pulse. The measurement validates its energy storage capability not only for evaluating the performance of the components, but also for optimizing the operation point for inductive components, which work as an essential reference for component, converter and system designers. Hanna curve can then be reloaded with BsT-pulse for each magnetic component designer, completely, correctly and easily. It provides the designers and users of magnetic components with limited values for specification.

References

[1] Snelling, Eric Charles. "Soft ferrites" Edition 2 (1988).
[2] Valchev, Vencislav Cekov, and Alex Van den Bossche. Inductors and transformers for power electronics. CRC press, 2018.
[3] Hanna, C. R. "Design of reactances and transformers: Which carry direct current." Journal of the AIEE 46.2 (1927): 128-131.
[4] JC Sun, K Seitenbecher Proper specification of magnetic components BodoPower December edition 2019.
[5] private communication with Dr. Rainer Menge
[6] J. Wang, "Challenges Facing Emerging Megawatt Applications: New Technology and Solutions Needed for High-Power Applications," in IEEE Power Electronics Magazine, vol. 6, no. 4, pp. 38-40, Dec. 2019.
[7] Johann W. Kolar, Jonas E. Huber, "Fundamentals and Application-Oriented Evaluation of Solid-State Transformer Concepts".
[8] Hilzinger, R., & Rodewald, W. (2013). Magnetic materials: fundamentals, products, properties, applications. Vacuumschmelze.

IGBT Simulation Software

One of the main tasks of the newly released program is to streamline design of converters based on IGBT modules manufactured by Proton-Electrotex JSC. This tool allows to calculate heat losses in the specified operating modes. The program allows to simulate the entire circuit, determine currents and voltages on all elements, use real models of components, carry out spectral decomposition, determine the power factor and harmonic distortion coefficient.

The program includes 4 main modules:

- Authorization module: signup, login and password recovery;
- Calculation module: calculation of currents and voltages; calculation of losses and temperatures;
- Graphics module: plotting for both HTML and PDF;
- Report module: generating and emailing a PDF report.

This tool allows the user select any of IGBT modules produced by Proton-Electrotex; specify the circuit and its input data – DC bus voltage, output frequency, phase load; set up PWM and choose between calculation for chip or base temperature. Currently calculations can be made for the following circuits:

DC/DC Boost
DC/DC Buck
DC/DC SR-Motor
DC/AC 2L VSC
DC/AC 3L-NPC VSC

Electrical and thermal calculations can be carried out separately or sequentially. Semiconductor elements in the electrical task are assumed to be ideal switches. Energy losses occur instantly when a semiconductor device transitions from one state to another.

www.proton-electrotex.com

750W Regulated 48V-to-12V Converter

The Vicor DCM3717 enables customers in data center, automotive and industrial markets to quickly deploy high-performance 48V power delivery for legacy 12V loads while achieving significant power-system size, weight and efficiency benefits. The DCM3717 operates from a 40 – 60V SELV input, is non-isolated and provides a regulated output with a range of 10.0 – 13.5V, a continuous power rating of 750W and a peak efficiency of 97% in a 37 x 17 x 7.4mm Surface-Mount Converter housed in Package (SM-ChiP). The DCM3717 supports the

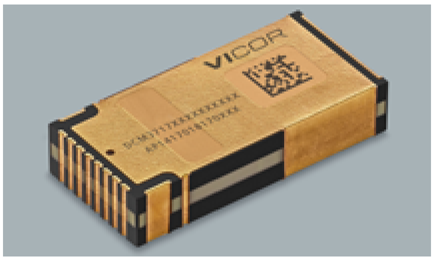

LV148 specification (48V automotive standard) for pure electric and hybrid vehicles and the recent Open Compute Project (OCP) Open Rack Standard V2.2 for distributed 48V server backplane architectures, providing a regulated 48V-to-12V option for downstream legacy 12V multiphase point-of-load converters. Applications not requiring regulation of the 12V supply can take advantage of the Vicor NBM2317, a 800W, 48V-to-12V fixed ratio converter which is available in a smaller 23 x 17 x 7.4mm SM-ChiP with 69% higher power density and higher efficiency at 97.9%.

www.vicorpower.com

JPC Series with AOCT for High Power 3-phase Inverter

The JPC series with an innovative AOCT, Advanced Offset Cancelling Technology, is designed with lightweight and high precision to be suitable for compact high efficiency inverter design. The JPC series which provides a high bandwidth of up to 200kHz, matching increased

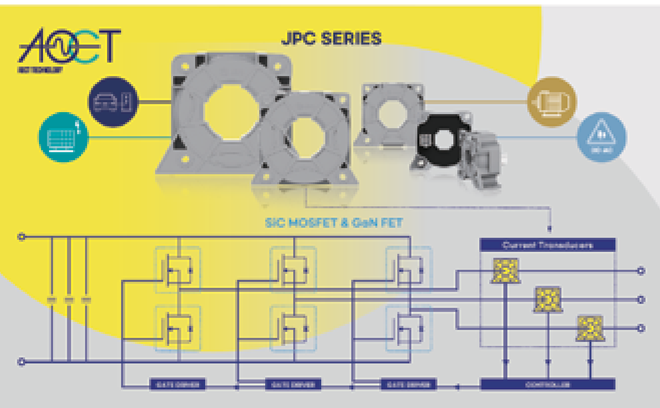

switching speeds especially of SiC and GaN devices, is the most optimized current sensor for High power 3-phase inverter which consists of GaN FET or SiC MOSFET. The JPC Series' superior technical property over the existing current sensors is the AOCT, the J&D's brand-new hybrid technology of zero-drift operational amplifier IC and high permeability permalloy core. This innovative hybrid technology is implemented to high-precision measurement with much lighter and compact size due to its specialized elimination of DC offset. As a result, this impresses with about 30% lighter weight than existing products and an improved precision requirement for the current output signal. The JPC series offers five models in the range of AC or DC rated current 100A – 2000A and supports industries requiring high precision such as train/traction, building automation, power supply and welding for the future of the energy industry. Specifically, it is suitable for DC microgrid applications such as EV charging stations, photovoltaic systems, UPS and ESS.

www.hqsensing.com

1200V αSiC MOSFETs for High-efficiency Applications

Alpha and Omega Semiconductor announced the release of the 1200V silicon carbide (SiC) αSiC MOSFET technology platform. Specifically targeting the industrial and automotive market, this next-generation technology will enable customers to achieve higher levels of efficiency and power density compared to existing silicon solutions. Optimized for minimizing both AC and DC power losses through a low gate resistance (RG) design combined with the low increase in on-resistance (RDS,ON) over temperature, the αSiC technology can achieve the highest efficiencies across a wide range of application switching frequencies and temperatures. This higher efficiency can result in significantly reduced system costs and total bill-of-materials for the many industrial uses, including solar inverters, UPS systems, and EV inverter and charging systems. The first product release for this new platform is the AOK065V120X2, a 1200V 65mΩ SiC MOSFET available in a TO-247- 3L package. For ease of use, the AOK065V120X2 is designed to be driven with a -5V/+15V gate drive, allowing the broadest compatibility with existing high voltage IGBT and SiC gate drivers. Operation with a unipolar drive is also possible with optimized system design. Additional benefits of the αSiC platform is a robust UIS capability, enhanced short circuit performance, and a high maximum operating temperature of 175° C.

www.aosmd.com

LED Driver for Automotive LED lamps

ROHM announces the development of its ultra-compact linear LED Driver suitable for automotive socket type LED lamp applications such as rear lamps, turn, fog and position lamps or DRLs (Daylight Running Lamps). In response to the growing demand for higher levels of reliability, safety, and increased flexibility for the LED's thermal management in combination with an ultra-compact design, ROHM developed the industry-leading Automotive LED Driver BD18336NUF-M. "ROHM is embracing the market trend towards miniaturization with its newest LED Driver without compromising in safety features and performance," says Stefan Drouzas, Senior Marketing Manager Automotive, ROHM Semiconductor GmbH. Its monolithic design ensures stable lighting during battery voltage drops down to 9V. The configurable current bypass function prevents LEDs to turn OFF and keeps a minimum brightness at all times contributing to higher driving safety. An ultra-compact 3.0mm² package reduces the mounting area by 30 % compared to conventional solutions using external circuitry, while providing a high current output of 600mA. Heat generated by the LEDs is suppressed by an integrated current derating function. The thermal adjustable output current limits the heat generated by the LEDs, increasing their lifetime, which makes the LED Driver ideal for white as well as for red and yellow LEDs.

www.rohm.com

DC / DC Power Supplies Collection

Dean Technology announced the introduction of its collection of standard DC / DC high voltage power supply modules. The UMR collection consists of three full series that are form-fit-function replacements for industry standard solutions covering two package sizes, biasing or capacitor charging variations, and outputs up to 6,000 volts at 30 watts. These low ripple, high stability and high efficiency power supplies meet or exceed alternative offerings at a price point that makes them the best value available. The first three series in the UMR collection are the UMR-A, UMR-C, and UMR-AA. The UMR-A series are biasing supplies with 12 or 24 volt input, outputs at 4, 20, or 30 watts from positive or negative 125 to 6,000 volts. This series also has an optional output voltage monitor. The UMR-C series are capacitor charging supplies with 24 volt input, outputs at 20 or 30 watts from positive or negative 125 to 6,000 volts. The series is designed with exceptional capacitor charging capabilities, with limited overshoot and outstanding rise time. The UMR-AA series are biasing supplies with 12 or 24 volt input, outputs at 4, 20, or 30 watts from positive or negative 125 to 6,000 volts. They offer standard voltage monitoring and a minimal footprint. All three series come standard with current monitoring and output voltage control. All models and configurations have UL and CE certification for immediate system integration.

www.deantechnology.com

650 V Gallium Nitride (GaN) Technology

Nexperia has announced a range of GaN FET devices featuring next-gen high-voltage GaN HEMT H2 technology in both TO-247 and the company's proprietary CCPAK surface mount packaging. Devices achieve superior switching FOMs and on-state performance

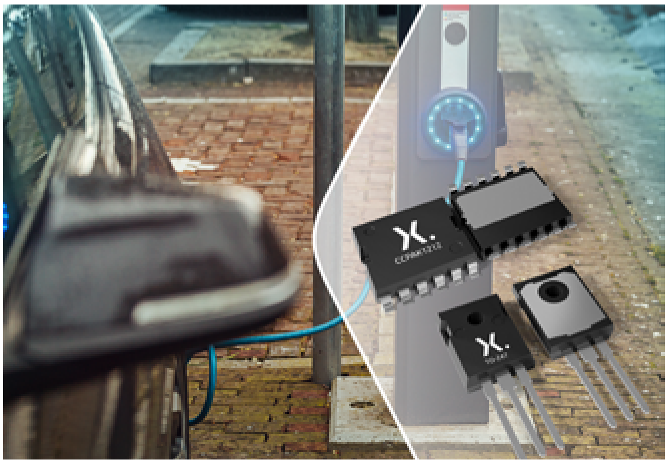

with improved stability and simplify application designs thanks to their cascode configuration which eliminates the need for complicated drivers and controls. The GaN technology employs through-epi vias, reducing defects and shrinking die size by around 24%. RDS(on) is also reduced to just 41 mΩ (max., 35 mΩ typ. at 25 °C) with the initial release in traditional TO-247, with high threshold voltage and low diode forward voltage. The reduction will further increase, to 39 mΩ (max., 33 mΩ typ. At 25 °C) with CCPAK surface-mount versions. Because the parts are configured as cascode devices, they are also simple to drive using standard Si MOSFET drivers. Both versions meet the demands of AEC-Q101 for automotive applications. Dilder Chowdhury, Nexperia's GaN Strategic Marketing Director commented: : "Customers need a highly-efficient, cost-effective solution for high power conversion at 650 V and around the 30-40 mΩ RDS(on), where applications include on-board chargers, DC/DC converters and traction inverters in electric vehicles, and industrial power supplies in the 1.5-5 kW range for titanium-grade rack mounted telecoms, 5G and datacenters."

www.nexperia.com

SiC Diodes Rated for 1700 VDC and 5 Amps

SemiQ Inc. is proud to announce the release of its third generation 1700V 5 Amp SiC Schottky Diode. The GP3D005A170B diode comes in the industry standard TO-247-2 package as well as bare die format.

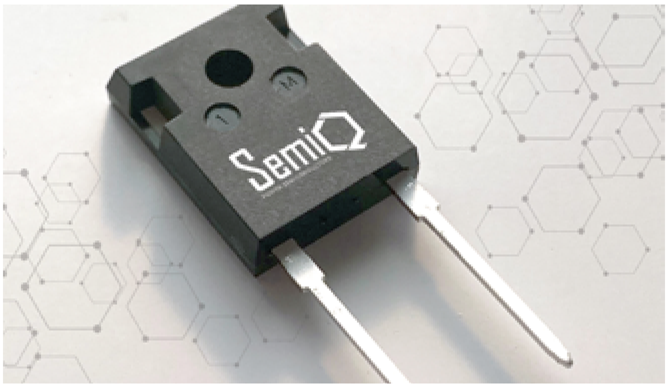

10A and 20A 1700V diodes will follow shortly. Michael T. Robinson, SemiQ President states that, "This 1700V Silicon Carbide Schottky Diode is the latest extension to our Gen 3 product family which was introduced in 2019. This platform was designed and built for reliability and ruggedness. It features dual layer chip passivation with over 12 million device hours of HTRB and H3TRB. Packaged devices are 100% avalanche tested in production ensuring even greater device ruggedness."

SemiQ's 1700V SiC Diodes are optimized for power conversion applications where low losses and high efficiency are critical including: renewable energy, electric vehicle charging, uninterruptable power supplies (UPS), solar power, and fuel cell power systems. Samples are in stock at SemiQ and available through Digikey with manufacturing lead times of 8 weeks.

www.SemiQ.com

Open Frame AC/DC Power Supplies

RECOM announces the launch of its RACM60-K series of 60W AC/DC power supplies. RECOM is adding the RACM60-K series to its range of open-frame AC/DC power supplies. The low-profile 2" x 3" design features 90% efficiency across its load range, enabling full-power operation from -40°C to +55°C without forced cooling, and

up to +85°C with derating or forced air. Input range is universal 80-264VAC and outputs available are 5V, 12V, 15V, 24V, 36V and 48V. The parts are suitable for a wide range of applications with EN 62368-1, IEC 61558-1/-2-16 and IEC/EN 60335-1 certifications for ITE/audio-visual, industrial and household use respectively up to 5000m operating altitude. Medical safety and EMC certifications meet ANSI/AAMI/IEC/CSA 60601-1 for 2x MOPP with an isolation of4kVAC/1 minute suitable for B and BF applications up to 4000m operating altitude. Class B EMC standards are also met in installation class II or class I PELV with grounded output. The RACM60-K series features full protection against short-circuits, output over-voltage, over-current and over-temperature and has line and neutral fusing for medical applications. No-load input current is only 100mW typical at 230VAC. Various mounting options are available: Molex connectors for wired installation, wave-solder pins for direct PCB mount with built-in stand-offs and a 2" x 4" footprint for legacy design compatibility. A cover is available for the 2" x 4" option.

www.recom-power.com

MOSFET for High Voltage Auxiliary Power Supplies

Infineon Technologies complements its CoolSiC™ MOSFET offering with yet another voltage class. Having added 650 V to the portfolio earlier this year, the company is now launching the 1700 V class with its proprietary trench semiconductor technology. Maximizing the strong physical characteristics of silicon carbide (SiC), this ensures that the new 1700 V surface-mounted devices (SMD) offer superior reliability, as well as low switching and conduction losses. The CoolSiC MOSFETs 1700 V are targeting auxiliary power supplies in three-phase conversion systems such as motor drives, renewables, charging infrastructure and HVDC systems. Such low-power applications usually operate below 100 W. In these cases, designers very often prefer a single-ended flyback topology. With the new CoolSiC MOSFETs 1700 V in SMD package, this topology is now even enabled for DC-link connected auxiliary circuits up to 1000 V DC input voltage. High efficiency and high reliability auxiliary converters using a single-ended flyback converter can now be implemented in three-phase power conversion systems. This leads to smallest footprints and a reduced bill-of-materials. "Trench technology of a CoolSiC MOSFET balancing performance and reliability in operation is now available for 1700 V", said Dr. Peter Friedrichs, Senior Director SiC at the Industrial Power Control Division of Infineon. "It combines the best of SiC properties: low losses with small footprint, in a high voltage SMD package. This helps our customers to significantly reduce the complexity in their auxiliary power supplies".

www.infineon.com

Rectifiers with Wettable Flank Contacts

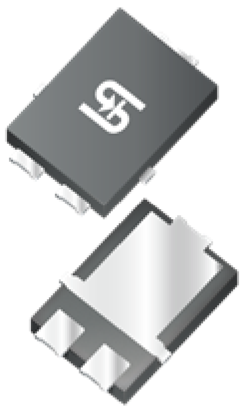

Taiwan Semiconductor announces the introduction of the TUAS8x Series of surface-mount device (SMD) rectifiers, available with voltage ratings from 200V-1000V. The TUAS8x Series device's wettable flank package enables higher power density, increased manufacturing yields and reliability in a wide range of power conversion applications, offering industry-leading 8A maximum current. The industry standard, SMPC4.6U SMD package configured with two anode and one cathode, wettable flank terminations, facilitates automated placement and automated optical inspection (AOI). This package also offers advantages of smaller footprint and height, improved power dissipation and higher resistance to thermal shock. The TUAS8x Series are the only devices available in this space saving, high performance package that offer the combination of high voltage performance (up to 1 KV) at current levels above 5A. Spice models are available online for ease of design.

"Wettable flank packages facilitate lower cost manufacturing (AOI vs X-Ray inspection) and offer higher production yield," reported Sam Wang, Vice President, TSC Products. "These devices offer designers higher power density, improve manufacturability and reliability via resistance to thermal shock and dissipate heat into the PCB faster than alternative package configurations."

Applications include Silicon, GaN or SiC-based power conversion circuits in commercial, industrial, telecom-datacom power systems, freewheeling diodes and anywhere general-purpose rectification is needed.

www.taiwansemi.com

Robust Connection for Power

WR-FAST Fast Connection is the name of a series of THT-configurable male connectors for accommodating single wires with blade receptacles — for example in household appliances. The connectors are available in various blade designs, orientations and dimensions and are intended for current flows up to 16 A and working voltages up to 300 V. Straight or angled contacts in various numbers are available — for the common 6.3 mm blade receptacles but also for the 2.8 mm version. For the latter, the 2863-type WR-FAST connectors are used: the forked blades can accommodate both types of

blade receptacles. WR-FAST is designed for operating temperatures from -30 to +120°C. The connectors have passed glow wire testing according to IEC 60335-1 and meet flammability class UL94 V-0. They also have cULus approval. The WR-FAST connector series is now available from stock without a minimum order quantity. Würth Elektronik also offers a Design Kit Interface with free refill service for this product group.

www.we-online.com

DC/DC Converter with 5kVAC Reinforced Isolation

TRACO Power's 1 Watt, TRV 1M series of High Isolation DC/DC Converter in a compact SIP-9 package provide 5kVAC I/O isolation

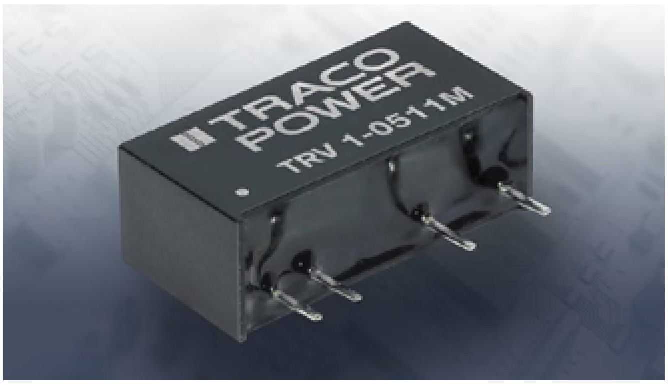

with reinforced insulation for both medical and industrial applications. The series consists of 28 models offering a choice of 4.5-5 / 9.6-14.4 / 12-18 / 19.2-28.8 Vin ranges and single / dual outputs from 3.3V – 15V. With continuous short circuit protection and low leakage current of less than 2 μA, these converters are especially suited to protect any connected interfaces or applied parts to patients. Featuring semi-regulated outputs, -40 to +85°C operating temperature without derating and certifications according to IEC/EN/ES 60601-1 3rd ed. for 2xMOPP and IEC/EN/UL 62368-1, this series is suitable for many different applications where high isolation and reinforced insulation with short circuit protection is critical. Products are in stock and available through distributors around the globe with manufacturing lead times of 12-14 weeks.

www.tracopower.com

Advertising Index


EPE 2020 ECCE Europe
September 7-11, 2020
Lyon, France
The 22nd European Conference on Power Electronics and Applications
http://www.epe2020.com
15 November 2019 : Abstract submission deadline
04 March 2020 : Notification of provisional acceptance
04 June 2020 : Final submission deadline
EPE
ECCE
IEEE ENERGY CONVERSION CONGRESS & EXPO
IEEE
pels
IEEE POWER ELECTRONICS SOCIETY
Powering a Sustainable Future
HOSTED BY:
SuperGrid Institute
Shaping power transmission
IFAC
INTERNATIONAL FEDERATION OF AUTOMATIC CONTROL
le cnam
Ampère
G2Elab
L2S
Focusing on:
• HVDC and MVDC converters for DC grids
• Digital Power Electronics for efficient and reliable operation for DC Grids
» Condition and Health Monitoring
» Advanced control for reliable operation
• e-mobility & interaction with the Grids